Title

The relevance of context in the ecology and evolution of phage interactions with the bacterial plant pathogen Pseudomonas syringae

Author

Hernandez, Catherine A.

Publication Date

2021

Peer reviewed|Thesis/dissertation

The relevance of context in the ecology and evolution of phage interactions with the bacterial plant pathogen *Pseudomonas syringae*

By

Catherine A. Hernandez

A dissertation submitted in partial satisfaction of the

requirements for the degree of

Doctor of Philosophy

in

Integrative Biology

in the

Graduate Division

of the

University of California, Berkeley

Committee in charge:

Professor Britt Koskella, Chair
Professor Michael Boots
Professor Kimberley Seed

Summer 2021

The relevance of context in the ecology and evolution of phage interactions with the bacterial plant pathogen *Pseudomonas syringae*

Abstract

The relevance of context in the ecology and evolution of phage interactions with the bacterial plant pathogen *Pseudomonas syringae*

by

Catherine A. Hernandez

Doctor of Philosophy in Integrative Biology

University of California, Berkeley

Professor Britt Koskella, Chair

Bacteriophages (phages; viruses that infect bacteria) are abundant, diverse, and play important roles in shaping microbial community composition. Phages can structure the composition of bacterial communities by being a direct cause of mortality, altering competitive outcomes, and even providing novel functions to their hosts. Bacteria-phage interactions are highly context-dependent, with environmental variables such as temperature, resource availability, and spatial structure significantly impacting their ecological and (co)evolutionary dynamics. However, while it is known that context is important, relatively little experimental work has explored their interactions in ecologically-relevant conditions. For plant-associated bacteria and phage in particular, there are many open questions about their ecology and evolution in the phyllosphere (aboveground plant tissues). In this dissertation, I explore whether and how context impacts phage interactions with the bacterial plant pathogen *Pseudomonas syringae*, with a focus on the role of the phyllosphere environment. By leveraging the power of experimental evolution, I specifically tested the impacts of coevolution, the foliar environment, and biofilm formation on interactions between *P. syringae* and several obligately lytic phages.

In Chapter 1, I first explored the genotypic and phenotypic consequences of coevolution between *P. syringae* and a single lytic phage. I serially passaged this phage with *P. syringae* under conditions where the bacterium was either allowed to coevolve or was held constant. I then compared the evolved changes in these two groups of phages to determine how coevolution differed from general adaptation to the bacterial host. At the endpoint, individual phages were isolated and genome resequenced to determine identity and frequencies of mutations across populations. Additionally, I quantified the ability of the phages to infect bacterial hosts from their own and alternate populations across time. I found that coevolved phages had more mutations than phages evolved on a constant host, and most mutations were in genes encoding structural proteins. Coevolved phages best reduced growth of past and sympatric hosts, and had a stronger relationship between pairwise genotypic-phenotypic distances than phages evolved on a constant host.

In Chapter 2, I next tested the impact of environmental context on the evolution of bacterial resistance to phage. Specifically, I experimentally evolved replicate populations of *P. syringae* with lytic phages both *in vitro* (in high-nutrient liquid cultures) and *in planta* (syringe-infiltrated into the leaf apoplast) and quantified frequencies of phage-resistant colonies over time. Due to a previously described context-dependent cost of phage resistance *in planta*, we

hypothesized that the spread of evolved resistance and coevolutionary dynamics would be slower in the leaf environment. In two separate experimental evolution projects with high amounts of phage, I found that resistant bacteria were virtually undetectable in the plant environment at the end of each experiment. In contrast, resistance reached high frequencies in liquid culture. A follow up assay determined that low rates of phage replication coupled with a slight cost of phage resistance eliminated the fitness benefit of resistance *in planta*.

In Chapter 3, I tested a seedling-based method for screening phage effectiveness as a biocontrol method for *P. syringae*. In three trials, phages were prophylactically applied to tomato seedlings in sterile conical tubes before flooding with the bacterial pathogen *Pseudomonas syringae* pathovar *tomato* DC3000. I recorded seedling disease progression and quantified endpoint bacteria and phage densities in each trial. Phages replicated in all trials, but reduction of disease symptoms and endpoint *P. syringae* density varied across trials with different application densities. This resource-efficient method rapidly identified an effective phage and application density to mitigate disease on seedlings.

In the final chapter (Chapter 4), I tested how biofilm formation impacts phage interactions on both ecological and evolutionary timescales. Biofilms are multidimensional structures composed of cells and an extracellular matrix that can act as a barrier from external stressors such as antibiotics or phages. I hypothesized that biofilm formation may be one factor that contributed to the low rates of phage replication observed in Chapter 2. To test this, I first completed a series of experiments where I grew *P. syringae* biofilms until a certain time point, applied phage lysates, and then quantified biofilm biomass after phage addition. Across all experiments, phage application never reduced biofilm biomass, and in some cases increased biomass. Next, I experimentally selected for or against *P. syringae* biofilm formation in the absence or presence of phage selection pressure in a fully factorial design. I identified changes in population and individual-level biofilm formation and phage resistance, and found that phage-resistant isolates invested relatively more in biofilm formation than phage-sensitive isolates. In a seedling inoculation assay with a subset of isolates, phage resistance and high investment in biofilm formation were associated with a cost of virulence. In addition, some phage-resistant mutants caused increased disease symptoms in the presence of one phage. These results offer insight into the traits that might impact phage effectiveness in agricultural biocontrol.

Together, this dissertation contributes to a growing body of work exploring context-dependency in bacteria-phage interactions. This work demonstrates that incorporating ecologically-relevant context can yield fundamentally different insights into their ecology and evolution than *in vitro* research using standard culture conditions.

Table of Contents

List of Figures

List of Tables

Acknowledgements

This dissertation would not have been possible without the support of many people. To my advisor, Dr. Britt Koskella, thank you for so many years of guidance and mentorship. Your ability to ask insightful questions and make conceptual connections is truly inspiring, and I can only hope that even a fraction of that has been passed on to me. More importantly, though, is the way that you treat all of us with genuine kindness and respect. It has been a joy to see the lab grow from empty rooms to the bustling space it is today, and I find it a testament to your mentorship. I already miss stopping by your office for a quick chat about data, strange phage plaques, or just casual advice. I am so grateful to have spent my graduate school years working with you, and I hope we continue to cross paths in the future.

Thank you to my committee members, Dr. Mike Boots and Dr. Kim Seed, for supporting me on this often unpredictable path. From early in graduate school, your guidance and feedback have been critical in shaping my work.

Thank you to my collaborators from throughout my time in graduate school. To my collaborators on the phage coevolution project, Dr. Véronique Delesalle and Dr. Greg Krukonis, thank you both for your time and expertise. I am so thankful for your patience through years of virtual meetings while I tried to make sense of data. I hope we can meet in person soon. To Dr. Jeremy Barr, who kindly hosted me for an amazing summer (winter?) experience in his lab at Monash University as part of the Australia-Americas PhD Research Internship Program, I can't thank you enough for such a wonderful experience. I learned so much from you and the rest of the lab, and visiting Melbourne was an experience I will never forget.

I would like to acknowledge the various funding sources that have supported this work: a Berkeley Fellowship from the University of California, Berkeley, a Graduate Research Fellowship from the National Science Foundation, the Australia-Americas PhD Research Internship Program, a Sigma-Xi Grant in Aid of Research (Berkeley chapter), and support from the Integrative Biology department at Berkeley.

Thank you to all of the (past and present) Koskella lab members for friendship and support. You all have enriched my graduate school experience, and I could not think of a better group of people to have worked with. I wish you all the best, including years of functioning autoclaves. To the undergraduates I had the pleasure of working with – (now Koskella lab graduate student) Reena Debray, Kore Lum, Aspen Pastore, Priyanka Ranade, Andrea Salazar, and Sophie Zhai – this work would not have been possible without you, and it was a joy to be a part of your scientific development.

To my friends, you have filled my time here with lots of laughter and good food (both very important). Lisa, thank you infinitely for being a wonderful roommate and friend for all of these years. I am going to miss our wine and cheese nights, and cricket hunting at Sedgwick. I hope your time in Nebraska is all you have dreamed it to be. To Kevin, Andre, and all of the Williams lab, thank you for letting me tag along to so many social events and game nights (and letting me use your pH meter all of the time). Reena and Tristan, thank you both for being so supportive (and great at puns). I am also lucky to have friends from before graduate school who

stuck around throughout this process, and I am thankful for each of you – Nicole, Melissa, Duyen, Ajda, Mylena, Lily, and Jared. And to Jenny, you know I could not have done this without you. There are no words good enough for what you mean to me, and I am so thankful to have you in my life.

To my family, you are the reason I am able to write this dissertation today. Mom, thank you for encouraging a love of science from a young age. Your love and support have kept me going throughout the often difficult experience of being away from home. To my brother Chris, thanks for tolerating my nonsense growing up, and for raising the best nephew with Summer. To Dad, Anna, and the rest of the Hernandez and Cue families, thank you for always making me feel at home even after being away for so long. To my aunt Michelle, you have been such an important role model and source of strength throughout my life, and especially during graduate school. I would not be here without you and Jen supporting me through that transition period as I applied to graduate programs. I also would not be here without my grandparents, who made the difficult decision years ago to leave Cuba with their young families. And to Yoli, te veo pronto y te quiero mucho.

Introduction

The qualitative nature and quantitative strength of a pairwise interaction can differ across populations of interacting species due to genetic or environmental factors. However, despite the general acceptance that genetic and environmental variation can shape species interactions, our current understanding of antagonistic coevolution has largely been limited to studies of single host and single parasite interactions in laboratory environments. This is particularly true for bacteria and bacteriophages (phages; viruses that infect bacteria), where although there is a substantial body of ecological theory on broad patterns of community dynamics with phage (e.g. the "kill-the-winner" and now "piggyback-the-winner" hypotheses), most empirical data results from experimental microcosm studies and we lack a good understanding of the processes that shape the complex patterns we see in natural communities. Given the recent resurgence of interest in phage therapy, efforts at understanding the factors that shape bacteria-phage dynamics in more ecologically-relevant settings will be critical for ultimate translation into clinical or agricultural use. In this dissertation, I build upon this body of work by manipulating the context in which the bacterial plant pathogen *Pseudomonas syringae* interacts with various obligately lytic phages.

Throughout my dissertation chapters, I manipulate context in different ways to study its impacts on bacteria-phage interactions. In my first chapter, I manipulated the biotic context by evolving a single lytic phage on coevolving bacterial hosts or a constant bacterial host. Results from this study demonstrated that host type impacts the genotypic and phenotypic evolution of these viruses. This is important to consider in agricultural biocontrol, where there is little to no control over the hosts that phages encounter once they have been applied on plants. In my next chapter, I directly tested how bacteria-phage coevolution in the plant leaf environment differs from coevolution *in vitro* (in high-nutrient laboratory media) and found that the dynamics are drastically different. Bacteria evolved resistance to phage rapidly *in vitro* but not in the plant environment. While at first this might seem promising for agricultural biocontrol, one major difference between these two environments is that there were much lower rates of phage replication *in planta*. Combined with a slight cost of resistance in the absence of phage, this essentially results in no fitness benefit of resistance, but also means that phages would be unsuccessful at controlling the bacterial infection under these conditions.

In my next two chapters, I explored how a different plant environment (tomato seedlings) and an important trait involved in pathogen virulence (biofilm formation) alter interactions with lytic phages. In the seedling project, I sought to develop and test a method for screening phage effectiveness in a higher-throughput manner than my prior plant-bacteria-phage experiments. I found that tomato seedlings grown in sterile tubes with a water agar base could support high levels of phage replication and phage-mediated reduction of bacterial disease symptoms. This is in contrast to my prior work, in which I found low levels of phage replication on older plants that were inoculated using a different method. Seedling inoculations were done by flooding with phage and bacterial suspensions, while older plant inoculations were done using syringe infiltration directly into the internal spaces of the leaves (the apoplast). Despite both experiments using a "plant" environment, bacterial gene expression and physiology can differ in important ways when growing on the leaf surface or in the apoplast. Some evidence suggests that motility may be more important for *P. syringae* on the leaf surface in order to reach apoplast entry sites and avoid harsh environmental conditions (Haefele and Lindow 1987; Yu et al. 2013). Once within the leaf, the pathogen may switch to a sessile surface-associated stage of growth (i.e. a

biofilm). The outcome of phage interactions with biofilm-associated cells depends on numerous factors such as the structure and age of the biofilm, the type of phage, and the composition of bacterial strains within the biofilm. In my final chapter, I explore how *P. syringae* biofilm formation impacts phage interactions on both ecological and evolutionary timescales. Using a set of lytic phages that were isolated as possible biocontrol candidates, I found that phage application does not seem to reduce biofilm biomass under various conditions. After experimental selection on biofilm formation in the presence and absence of phage, I also found that the evolution of phage resistance in minimal media was associated with higher investment in biofilm formation and reduced virulence in seedlings compared to phage-sensitive strains. Interestingly, in some cases, phage application to phage-resistant strains in seedlings led to increased disease symptoms (relative to that strain in the absence of phage).

While it is well understood that ecology and evolution are context-dependent, the challenge is to determine what aspects of this context-dependency are predictable. When are the results from pairwise *in vitro* bacteria-phage studies more broadly applicable, and when do we need to consider specific features of their environment or genetic backgrounds? For plant-associated bacteria-phage interactions, this dissertation supports the case that context is critical.

Chapter 1. Signatures of genomic and phenotypic change in (co)evolving bacteriophage populations

Introduction

The evolution of an obligate parasite is inseparable from its host. When parasites replicate and acquire mutations within a given host individual, the fate of novel genotypes will depend on transmission between and fitness within available hosts in their local environment. Shifts in available host populations as a result of either ecological or evolutionary change can select for changes in parasite life history traits such as infectivity range, transmission, and virulence (Boots et al. 2004; Bérénos et al. 2009; Best et al. 2014; Gibson et al. 2020). One mechanism by which parasite populations can change is in response to the evolution of host resistance mechanisms. This process of coevolution (reciprocal selection between, in this case, host and parasite) generates a dynamic parasite fitness landscape that can alter evolutionary trajectories compared to adaptation to an unchanging host population (Burmeister et al. 2016; Gupta et al. 2021). Determining the breadth and (un)predictability of coevolutionary trajectories has the potential to improve inference of evolutionary history as well as prediction of evolutionary potential.

The dynamics of host-parasite coevolution fall along a continuum that spans from escalatory arms races to fluctuating selection dynamics, with drastically different expectations for the genotypic and phenotypic evolution of the interacting organisms (Agrawal and Lively 2002). In arms race dynamics, the host and parasite continually increase their resistance and infectivity ranges to adapt to changes in their partner. This ultimately leads to broadly resistant hosts and broadly infectious parasites, although the extent of range expansion can be limited by biological constraints like costs of generalism (Lenski 1984; Frank 1994; Hall et al. 2011b). In contrast, with fluctuating selection dynamics, fitness of a given genotype depends on its frequency in the population. As a host genotype increases in frequency, so does its associated parasite, which will prevent that host genotype from sweeping to fixation. This negative frequency-dependent selection can maintain genetic diversity in and among populations without necessarily impacting host or parasite range.

In natural systems, it can be difficult to disentangle coevolution from single-sided adaptation (of a single interacting partner) or adaptation to shared abiotic conditions. Given this difficulty, much of our knowledge of coevolutionary dynamics has come from systems in which it is possible to experimentally coevolve the organisms of interest (Brockhurst and Koskella 2013). Experimental coevolution allows the researcher to separate the effects of coevolution from single-sided or abiotic adaptation through passaging treatments that (1) keep the interacting partner constant (i.e. not allowed to coevolve), and (2) allow each organism to adapt to abiotic conditions in the absence of the interacting partner. For antagonistic coevolution, this research has often been performed using bacteria and their viral parasitoids (bacteriophages, or phages). Phages infect bacteria by binding to a cell-surface receptor using a receptor-binding protein (for many phages this is often a structure called the tail fiber), making the receptor-binding protein an important component in determining phage host range (Bertozzi Silva et al. 2016; de Jonge et al. 2019). After binding to the receptor, phages then use the bacterial replication and translation machinery to synthesize viral genome copies and structural proteins. Phage host range can also be impacted by bacterial defenses at this intracellular stage, for example through processes that recognize and degrade foreign genetic material (Tock and Dryden 2005; Barrangou et al. 2007;

Ofir et al. 2017) or through processes that prevent completion of the phage infection cycle by prematurely killing the infected cell (Lopatina et al. 2020).

Experimental studies of bacteria-phage systems have demonstrated that coevolution can alter evolutionary trajectories, and that the exact dynamics depend on experimental conditions. Phage coevolution, compared to evolution on an unchanging host population, can lead to higher rates of molecular evolution at both the population and individual-level (Paterson et al. 2010; Scanlan et al. 2011). These molecular changes are accompanied by an increase in coevolved phage host range, as indicative of possible arms race dynamics (Hall et al. 2011a; Kashiwagi and Yomo 2011; Wandro et al. 2019). However, one longer-term coevolutionary study found that these range increases eventually plateau in both host and phage as range expansion becomes costly, and the dynamics can switch to fluctuating selection (Hall et al. 2011b). Changes in resource availability, spatial structure, and microbial community context have also been demonstrated to impact bacteria-phage coevolution (Brockhurst et al. 2003; Lopez-Pascua and Buckling 2008; Blazanin and Turner 2021).

While some patterns have emerged across studies, the generalizability of these results is still limited by the reliance on a few organismal pairs of interest (largely *Pseudomonas fluorescens* strain SBW25 and its phage Φ2), lack of population-level replication and/or single-sided evolution treatments, and inconsistency in choice of resistance and infectivity metrics. To begin addressing some of these gaps, we experimentally coevolved a bacterial plant pathogen (*Pseudomonas syringae* pathovar *tomato* strain PT23) with a non-model lytic phage *in vitro* and compared endpoint phage genotypes and phenotypes to phages that had adapted to a constant bacterial host (ancestral *P. syringae*). We isolated multiple individuals from each of three replicate coevolved and evolved populations, sequenced the whole genomes of these isolates, and measured changes in phage infectivity using a binary individual-level metric (spotting assays) as well as a quantitative population-level metric (reductions in bacterial population growth) on hosts from three time points throughout the experiment (ancestral, midpoint, and endpoint).

Methods

Experimental evolution and coevolution

Experimental lines were generated from a prior experimental evolution project (Hernandez and Koskella 2019). Briefly, a single colony of *Pseudomonas syringae* pv. *tomato* strain PT23 and single plaque of the lytic Podoviridae bacteriophage FRS were isolated to begin the passaging experiment. Ancestral bacteria were initially cultured with ancestral phage at a multiplicity of infection (MOI) of 4:1 (phage:bacteria) in 10 mL high-nutrient liquid media (King's B; KB), and were incubated static at 24°C. We had three replicate cultures (populations) of coevolved and evolved phages. To generate coevolved phages, at each transfer we mixed an amplified filtrate of the entire phage population ($3*10^{-4}$ dilution) along with 100 randomly chosen bacterial colonies from the sympatric population into fresh media. For the single-sided evolution treatment (which we call "evolved" phages throughout the manuscript), we transferred an equivalent volume of phage and added 100 colonies of plated ancestral host at each transfer. Bacteria and phage were cultured together for 72 hours between transfers, and this process was repeated for a total of six transfers.

Bacteria and phage isolation

At the endpoint of passaging, we isolated six individual phage plaques (i.e. strains) from each coevolved and evolved population for whole genome sequencing and phenotypic assays. First, the number of plaque forming units (PFUs) of each population were determined by soft agar overlays on the ancestral bacterial host. We then used the density of phages in each population to determine appropriate dilutions for isolating individual plaques, and plated to isolate these individual plaques on the ancestral host. It is important to note that the choice of isolating phages on the ancestral host biases our isolation towards phages that necessarily have maintained the ability to form plaques on the ancestor. However, we also isolated coevolved phages on colonies from their sympatric endpoint host populations, and found that all phages were still able to infect the ancestor (data not shown). This suggests that our isolation method likely captured a representative set of phages from these populations. Individual plaques were picked randomly with a sterile toothpick and cultured in liquid KB with the ancestral host overnight at 28°C on an orbital shaker.

In addition, we isolated bacterial colonies from the coevolved populations at the midpoint and endpoint of passaging in order to test how phage phenotypes differ across putatively (co)evolved host strains. We randomly isolated individual bacterial colonies from each population at both the mid and endpoint of passaging (12 per population at each time point), grew them individually overnight in liquid KB (shaken at 28°C), and then made -80°C freezer stocks of each culture using 25% glycerol.

Phage sequencing

We sequenced whole genomic DNA of the six phage isolates from each coevolved and evolved population (as well as the ancestor) to identify any variant sites relative to the ancestral phage genome. DNA extractions were performed using the Phage DNA Isolation Kit (Norgen Biotek, Canada). We added DNase I (RNase-free, 20 units) to remove host bacterial DNA and 4 µL of Proteinase K (20 mg/mL) as recommended in the manufacturer protocol, and followed all other steps as listed. Phage DNA was sequenced at the Microbial Genome Sequencing Center (MiGS, Pittsburgh, PA, USA) using Illumina sequencing on the NextSeq 2000 platform.

Genomic analysis

We first assembled the genome of the ancestral phage (FRS; GenBank accession MZ598487) by aligning reads with GS de novo assembler (default settings; Roche Life Science), which were then verified in Consed (Gordon and Green 2013). The FRS genome assembled into a single contig, and we found that the consensus sequence was high quality and did not require further sequencing (Russell 2018). We used PhageTerm to determine genome ends (Garneau et al. 2017). We called putative genes using both Glimmer and GeneMark algorithms (Lukashin and Borodovsky 1998; Delcher et al. 1999), and used protein homology search software (including blastp and HHpred) to predict putative functions of gene products (Söding et al. 2005; Boratyn et al. 2012). To call variants in evolved phages, we followed the pipeline "Finding Variants in Haploid Genomes" on Galaxy (https://galaxyproject.org/tutorials/var_hap/), which culminated in a list of variants that included position in the genome and type of mutation (SNP, insertion, or deletion; Afgan et al. 2018). We determined pipeline accuracy by assembling three genomes of evolved phages using the same methods as the original FRS genome, and compared these sequences using MegaX (Kumar et al. 2018). The same variants were detected using both methods.

Individual-level infectivity metric - spotting assays

Phages were spotted on lawns of each coevolved bacterial isolate and assessed for their ability to form clearance zones ("spots"). All phages were also tested on lawns of the ancestral bacterial host as a positive control (since all phages were isolated on, and could infect, the ancestor). Phages were arranged every other well in a 96 well plate, and spotted (using a flame-sterilized pin replicator that transfers 1 µl of volume) into a single large square petri dish containing a hard agar base and a soft agar top layer mixed with an overnight culture of each colony. After 24 hours of incubation in a 28°C incubator, we recorded whether there was any impact of phage on the lawn. If the phage made any impact on the lawn, we recorded the phage as "infectious" on that host via this assay (with the caveat that spotting assays, while commonly used, are an imperfect metric of phage host range; Hyman and Abedon 2010).

Post-sequencing, we observed that several genetically identical phages had distinct spotting patterns on certain colonies. We repeated the spotting assay twice more for all phages on any colonies with this discrepancy between phages with identical genotypes. For analysis, we averaged the results of all spotting replicates.

Population-level infectivity metric - reduction in bacterial growth (RBG)

In addition to the qualitative spotting assays, we quantified the ability of each phage to reduce bacterial growth of coevolved host populations using a growth curve-based protocol adapted from Turner et al. (Turner et al. 2012). To determine whether the coevolved and evolved phages could reduce bacterial growth from the coevolved populations, we grew fresh overnight cultures of each colony from freezer stocks and combined them at equal density to create a mixed suspension of cells for each population (12 colonies each). We then adjusted the optical density (OD600) of the mixed culture to begin at 0.2 for each growth curve. Stocks of the individual phages were quantified in triplicate using soft agar overlays on the ancestral host, and the average value was used as the density of the stock. We added a total of 100 PFUs per well in a total volume of 200 µL KB broth. The plates were incubated for 18 hours, shaken constantly, at 24°C (the temperature of the passaging experiment), and the OD600 of each well was measured every 5 minutes.

Outer wells were not used in the growth curves to avoid edge effects, and on each growth curve plate we re-randomized the position of the phages. All growth curve plates included the ancestral phage in addition to the coevolved and evolved phages, except for three plates of growth curves on the ancestral host. A single growth curve was done for each coevolved host population, but we replicated the growth curves on the ancestral host (four total growth curves).

Reduction in bacterial growth (RBG) was calculated by smoothing the OD values for each well of the growth curve plates using the smooth.spline function in R with a smoothing parameter value of 0.8 (selected to reduce noise but retain notable features of the curves, based on visual inspection of plots with various parameter values). We subset the data to only include the first 12 hours of growth, as wells across all plates had minimal change in OD values past that point. Next, we calculated the average area under the curve (AUC) for replicate wells with bacteria only (no phage added) on each plate using the auc function from the MESS package in R (Ekstrøm 2020), as well as the area under the curve for each well with bacteria and added phage. For a given growth curve plate, RBG values for each phage were then calculated as:
$(AUC_{\text{bacteria only}} - AUC_{\text{bacteria with phage}}) / AUC_{\text{bacteria only}}$

Statistical analysis and figures

Statistical analysis and figure generation was done in R version 4.0.2. Group means are reported as the mean ± 1 standard deviation. Analysis of variance (ANOVA) was performed on linear models, with significance of fixed effects in mixed models determined using the anova function (Type III with Satterthwaite's method) from the lmerTest package (Kuznetsova et al. 2017). In some analyses, we also tested the significance of fixed effects in mixed models by using likelihood ratio tests that compared the full model to a reduced model excluding the term of interest. Posthoc analyses were performed on significant terms of interest using pairwise comparisons of estimated marginal means (using the emmeans package, Lenth 2020), with a tukey adjustment for multiple comparisons. An alpha level of .05 was used for all tests. Figure panels were compiled and edited in Adobe Illustrator. Individual phages are named according to passaging treatment, population number within that treatment, and individual number within parentheses (e.g. phage C3 (2) is the second phage from the third coevolved population, and phage E1 (4) is the fourth phage from the first evolved population).

Spotting range was treated as a logit-transformed proportion in the temporal and local adaptation models to improve the distribution of model residuals, but raw values were used for the overall range and range vs. RBG analyses. Phage C3 (1) was removed from spotting analyses since it did not appear in the positive control for one set of assays.

Fitness on the ancestral host (RBG)

For comparison of phage fitness on the ancestral host, we compared phage ranks relative to all other phages on the same growth curve plate. Phages were ranked using their RBG values, with low ranks corresponding to high RBG values (i.e. a phage ranked "1" most reduced growth of the bacterial host on that plate). Phages were ranked out of 36 on three replicate plates with the ancestral host (one well per coevolved or evolved phage) or out of 39 on a single plate (one well per coevolved and evolved phage, three wells of ancestral phage). We note that this design does not allow for statistical comparison of the individual average ranks of coevolved/evolved phages to the ancestral phage, which was only ranked on a single plate. We first compared average ranks in a linear mixed model with passaging treatment (coevolved/evolved) as a fixed effect and population as a random effect, followed by a model testing population as a fixed effect.

Overall spotting range

Spotting range was measured on 12 randomly selected colonies from the midpoint and endpoint of the three coevolved populations, which included sympatric and allopatric combinations of hosts and phages. With this design, we may have isolated multiple colonies with the same genotype (especially likely within populations). To compare overall phage breadth, we therefore restricted this analysis to putatively unique genotypes by retaining data from a single colony for any colonies that shared identical spotting patterns across phages. We then statistically compared how many unique colonies each phage could form spots on using a linear model with passaging treatment (coevolved/evolved) as a fixed effect and population as a random effect, followed by a model testing population as a fixed effect.

Temporal and population-specific patterns (spotting and RBG)

For both coevolved and evolved phages, we tested the interaction between host time point, host population, and phage population (with a random effect of phage ID) on spotting

range (logit-transformed proportion) and RBG values using linear mixed models. In this analysis, spotting range included all colonies tested within each population. For coevolved phages, we were also specifically interested in how range and RBG values changed for the three populations across sympatric hosts from different time points. To test this, we generated a linear mixed model testing the interaction between host time point and phage population (with a random effect of phage ID) on sympatric spotting range (again as a logit-transformed proportion) and sympatric RBG values. The RBG analysis included the ancestral host, while spotting did not (as it only contains a single value - all phages infect the ancestor in this binary assay).

Local adaptation of coevolved phages (spotting and RBG)

To test whether the coevolved phages were locally adapted to their sympatric host populations, we generated a linear mixed model that included a term which specified whether a given phage was tested on its sympatric host population, as well as a host population by time (midpoint/endpoint) interaction, phage population fixed effect, and random effect of phage ID (to account for non-independence of data points in the experimental design). Note that in this model we did not allow phage population to interact with the other terms. Instead, we specifically tested how sympatric/allopatric combinations impact spotting (logit-transformed proportion) and RBG values given (1) average differences in resistance of host populations across time and (2) average differences in how well the three populations infect across all hosts from both time points. We then tested the significance of the term using ANOVA and a likelihood ratio test with a reduced model excluding the term of interest.

Relationship between individual (spotting) and population-level (RBG) infectivity metrics

To test whether phages from the coevolved and evolved groups differed in their relative ability to reduce bacterial growth, we generated a model that included an interaction between a second-degree polynomial of within-population spotting range (as an average value out of 12 total colonies) with phage passaging treatment (coevolved/evolved), and included a separate interaction term between host population, host time point, and phage population (with phage ID as a random effect) to account for non-independence in the design of the experiment. We then tested the significance of the interaction term between passaging treatment and range using both ANOVA and likelihood ratio tests.

Number of observed mutations

We tested whether phages from the coevolved and evolved treatments differed in mutation numbers per individual phages, counting each instance of a SNP, insertion, or deletion as a single change from the ancestor. We then generated a linear model with passaging treatment as a fixed effect and phage population as a random effect.

Relationship between genotypes and phenotypes

Finally, we explored the relationship between genotype and phenotype by quantifying pairwise distances between phages and performing Mantel tests on the resulting distance matrices (using the mantel function from the vegan package). We calculated pairwise distances between phages in genotype (presence/absence of mutations at each variable site) and phenotype (spotting pattern), and the Mantel tests on these matrices then indicate whether phages that are more similar in genotype are also more similar in phenotype. For this analysis, we chose to focus on binary host range (i.e. spotting pattern) as the phenotype of interest. Genetic distances were

calculated using Euclidean distances on a matrix indicating presence/absence of a mutation relative to the ancestral phage, and phenotypic distances were calculated using Manhattan distance on the averaged spotting matrix. For partial Mantel tests, we also calculated a third distance matrix that indicated whether phages were from the same population or different populations (a distance of 0 or 1, respectively). We ran both Mantel and partial Mantel tests (with the population distance matrix) on the spotting data with either (1) all variable sites across the genome, (2) tail fiber sites only, or (3) tubular protein B sites only, for the coevolved and evolved phages separately. For bacterial colonies with identical spotting patterns across phages, we retained only a single representative isolate. Additionally, only the variable sites of each data subset were included in each analysis.

Results

Fitness on the ancestral host (RBG)

We first tested whether the coevolved and evolved phages differed in their ability to reduce bacterial growth of the ancestor in the 96-well plate assay. The RBG rank average of individual phages (the average of how well the phage reduced bacterial growth relative to others on that same plate) did not differ across the coevolved and evolved passaging treatments ($F_{1,4}$=2.38, p=0.20; Fig. 1A). The mean rank for coevolved and evolved phages were similar (mean ± 1 S.D. for coevolved = 23.17 ± 8.87; evolved = 14.64 ± 5.28), and the RBG values (mean ± 1 S.D. for coevolved = 0.80 ± 0.024; evolved = 0.81 ± 0.043) were also similar and relatively high (compared to the RBG values on coevolved hosts), as expected given that these phages were isolated and amplified on the ancestral host. However, phages from one coevolved population (C1: mean ± 1 S.D. = 34 ± 1.47) consistently ranked lower than phages from all other populations (comparing estimated marginal means in a model with significant fixed effect of population on rank average; C1 compared to all other populations, p<0.001; Fig. 1C).

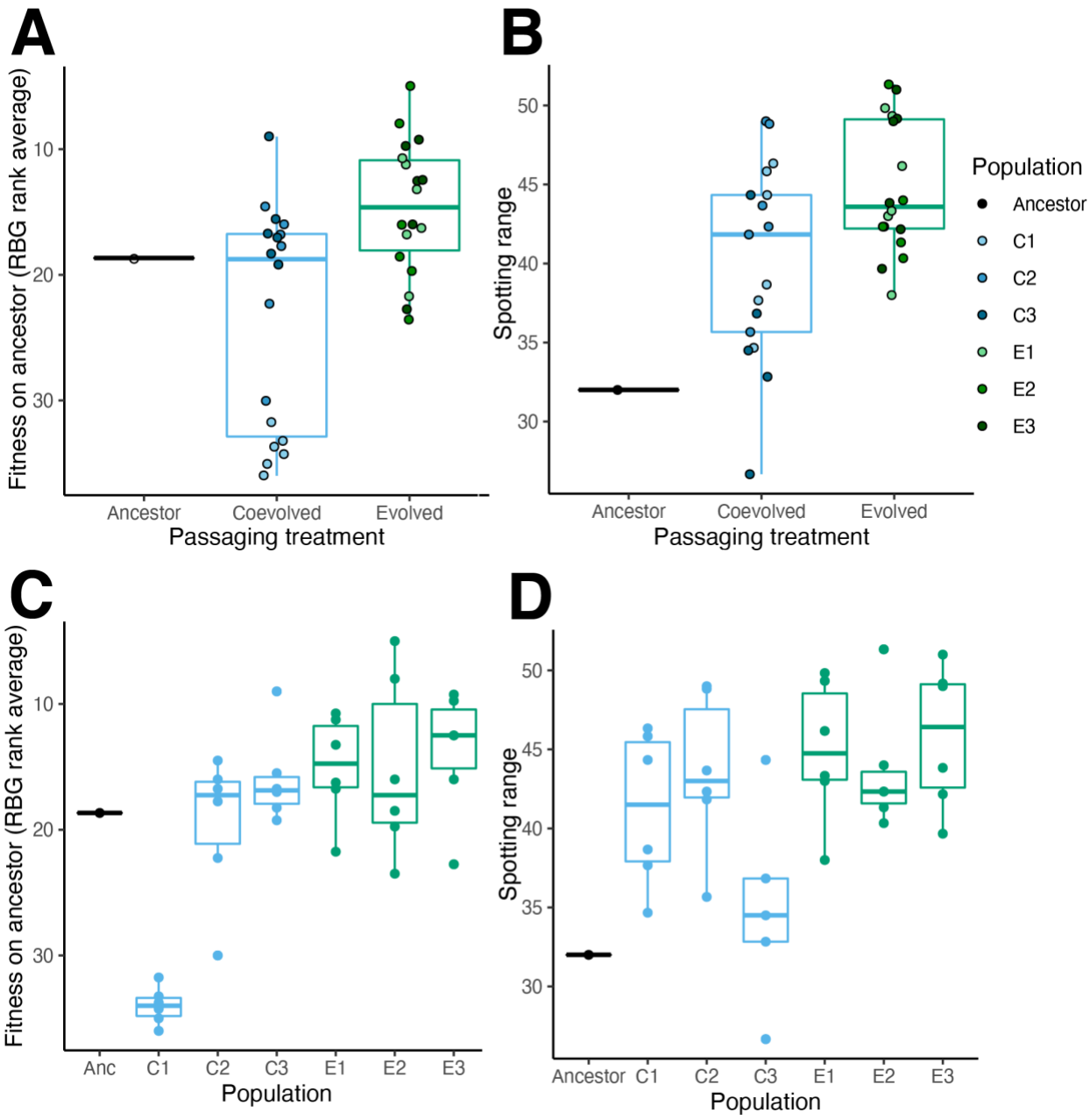

Figure 1. Fitness on the ancestor and overall infectivity range did not differ between coevolved and evolved phages. (**A**) Boxplots of average rank of phage RBG values across replicate growth curve plates of the ancestral host for the coevolved and evolved phages. (**B**) Spotting range on putatively unique coevolved colonies. Note that the y-axis has been reversed in panel A to represent phages with the highest ranks/fitness towards the top of the plot. Each point is an individual phage, with phage population indicated by point color (note legend to the left of panel B applies to both panels). (**C**) and (**D**) depict the same values as (**A**) and (**B**), respectively, but split by population.

Overall spotting range

Almost all individual phages from each population (both coevolved and evolved) increased their spotting range relative to the ancestor (out of 58 putatively unique coevolved colonies, from a total of 72 initially tested: ancestor range = 32; mean ± 1 S.D. for coevolved = 40.24 ± 6.20; evolved = 44.79 ± 4.17; Fig. 1B). However, range did not differ between phages from the coevolved and evolved treatments ($F_{1,3.73}$=3.45, p=0.14). Individual populations did differ ($F_{5,29}$=3.39, p=0.0156), with population C3 having a lower spotting range than E1 and E3 (p=0.0245 and p=0.0120, respectively; Fig. 1D).

Temporal and population-specific patterns in coevolved phages (spotting and RBG)

To determine the factors that predict spotting and RBG patterns on the coevolved hosts, we tested for a three-way interaction between host time point, host population, and phage population in a linear mixed model that included a random effect of phage ID. For spotting ranges of coevolved phages, the three-way interaction was not significant ($F_{4,70}$=0.71, p=0.5904), only the two-way interaction between host population and host time point was significant ($F_{2,70}$=41.07, p<0.001; phage pop*host pop: $F_{4,70}$=1.59, p=0.1864; phage pop*host time point: $F_{2,70}$=1.11, p=0.3339), and all main effects were significant (all p<0.05; Fig. 2A). For RBG values of coevolved phages, again the three-way interaction was not significant ($F_{4,75}$=1.75, p=0.1476), but all two-way interactions and main effects were significant (all p<0.002; Fig. 2B). Posthoc analysis of the host population by host time point interaction (averaged over the individual phage populations) identified that host populations C1 and C3 had lower spotting and RBG values at the endpoint (all p<0.001), while host population C2 had mixed findings (spotting ranges were lower at the endpoint but not a significant difference, p=0.0560; RBG values were higher at the endpoint but also not significantly different, p=0.0846).

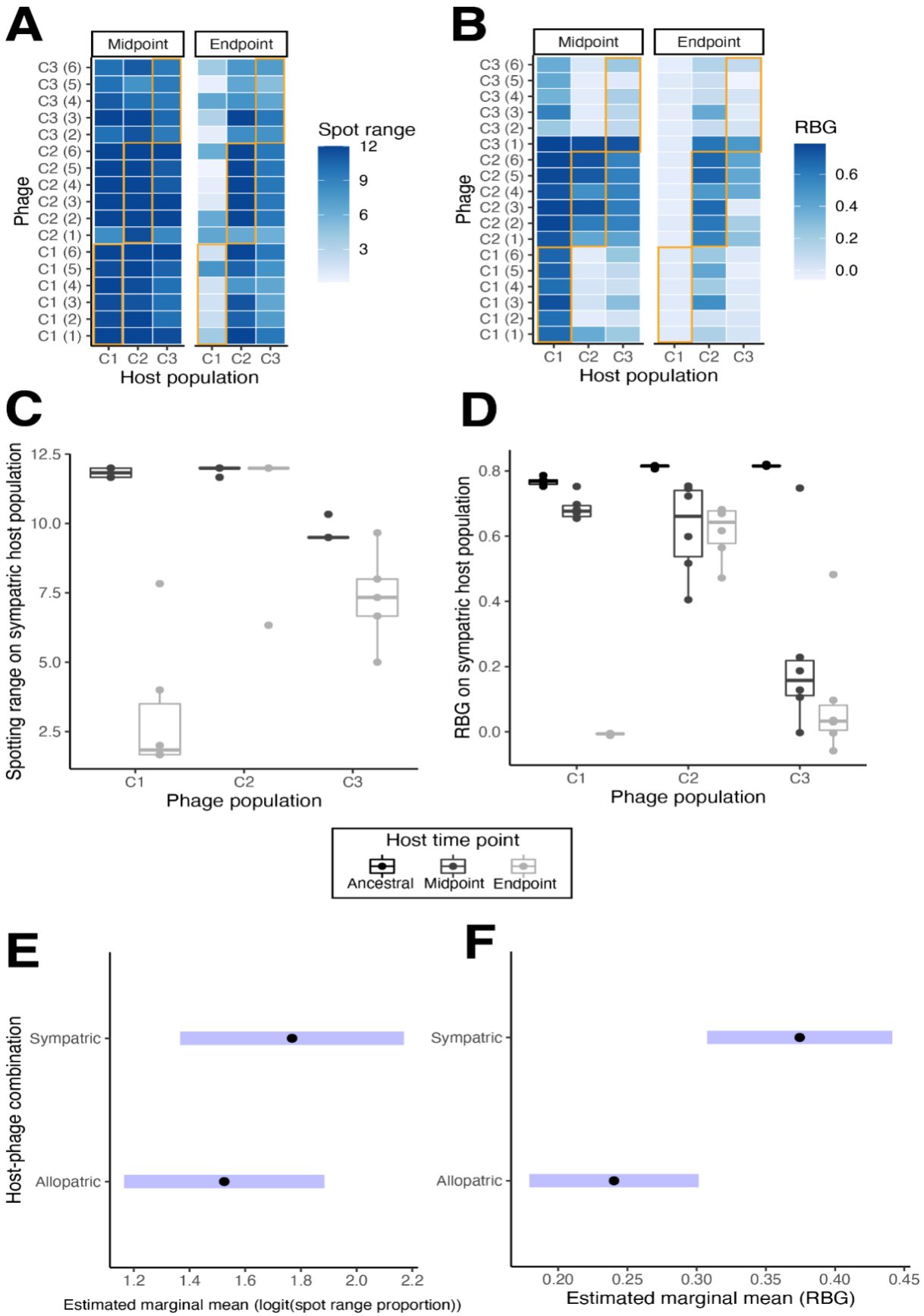
A
Midpoint
Endpoint
Phage
C3 (6)
C3 (5)
C3 (4)
C3 (3)
C3 (2)
C2 (6)
C2 (5)
C2 (4)
C2 (3)
C2 (2)
C2 (1)
C1 (6)
C1 (5)
C1 (4)
C1 (3)
C1 (2)
C1 (1)
C1 C2 C3
C1 C2 C3
Host population
Spot range
12
9
6
3
B
Midpoint
Endpoint
Phage
C3 (6)
C3 (5)
C3 (4)
C3 (3)
C3 (2)
C3 (1)
C2 (6)
C2 (5)
C2 (4)
C2 (3)
C2 (2)
C2 (1)
C1 (6)
C1 (5)
C1 (4)
C1 (3)
C1 (2)
C1 (1)
C1 C2 C3
C1 C2 C3
Host population
RBG
0.6
0.4
0.2
0.0
C
Spotting range on sympatric host population
12.5
10.0
7.5
5.0
2.5
C1
C2
C3
Phage population
D
RBG on sympatric host population
0.8
0.6
0.4
0.2
0.0
C1
C2
C3
Phage population
Host time point
Ancestral
Midpoint
Endpoint
E
Host-phage combination
Sympatric
Allopatric
1.2
1.4
1.6
1.8
2.0
2.2
Estimated marginal mean (logit(spot range proportion))
F
Sympatric
Allopatric
0.20
0.25
0.30
0.35
0.40
0.45
Estimated marginal mean (RBG)

Figure 2. Coevolved phages best reduce growth of past and sympatric host populations. Heatmaps of the spotting range (**A**) and RBG values (**B**) of coevolved phages on the three coevolved host populations from the midpoint and endpoint of passaging. Darker colors in the cells indicate greater values, and the orange boxes indicate sympatric combinations of hosts and phages. (**C**) and (**D**) depict boxplots of the spotting range and RBG values, respectively, of phages from each population on sympatric hosts from each time point. Each point is an individual phage. Note that (**C**) only includes the midpoint and endpoint populations, while (**D**) also includes values from the ancestral host. Panels (**E**) and (**F**) indicate the estimated marginal means (emms) of the sympatric/allopatric term in linear mixed models that also included a host population by host time point interaction, phage population fixed effect, and random effect of phage ID. (**E**) plots the emms for sympatric and allopatric combinations with the dependent variable being logit-transformed proportional spotting range. (**F**) plots the equivalent emms for a model with RBG values as the dependent variable.

We were then specifically interested in how spotting and RBG values differed across time on only the sympatric host populations (including the ancestral host for the RBG analysis) and whether the effect of time differed across the three coevolved phage populations. There was a significant interaction between host time point and phage population on spotting ranges ($F_{2,14}$=28.11, p<0.001; Fig. 2C) and RBG values ($F_{4,30}$=35.88, p<0.001; Fig. 2D). Spotting ranges were lower for C1 phages on endpoint hosts than midpoint hosts (p<.001), but did not differ for C2 or C3 phages at these time points (p=.8464 and p=0.3972, respectively). The RBG values of C1 phages were lower on endpoint than midpoint and the ancestor (p<0.001), of C2 phages were lower on midpoint and endpoint than the ancestor (p=0.0281 and p=0.0178 respectively), and of C3 phages were lower on midpoint and endpoint than the ancestor (p<0.001).

Local adaptation of coevolved phages (spotting and RBG)

Next, we tested whether there was a signature of local adaptation in the coevolved phages (whether phages from sympatric populations as the tested host infected more colonies than expected, or reduced bacterial growth more than expected). Sympatric combinations did not impact within-population spotting range ($F_{1,79}$=0.08, p=0.7795; Fig. 2E), but resulted in a significant increase in RBG values ($F_{1,84}$=27.79, p<0.001; Fig. 2F). By comparing estimated marginal means of the sympatric/allopatric term, sympatric combinations led to an estimated 0.134 increase in RBG values compared to allopatric combinations. As a secondary test, we also determined the significance of the sympatric/allopatric term by generating a reduced mixed model that excluded the term, and compared the full and reduced models using a likelihood ratio test. Again, this term was not significant for spotting range (X^2(1)=2.24, p=0.1346), but significantly impacted RBG values (X^2(1)=25.72, p<0.001).

Temporal and population-specific patterns in evolved phages (spotting and RBG)

For evolved phages, we tested how the interaction between host population, host time point, and phage population (with a random effect of phage ID) impacted spotting ranges and RBG values. The three-way interaction was significant for both spotting range and RBG values (spotting: $F_{4,75}$=3.10, p=0.0205; RBG: $F_{4,75}$=5.17, p<0.001; Fig. 3A and 3B, respectively). The host population by host time point interaction was also significant in both datasets (spotting:

$F_{2,75}$=116.21, p<0.001; RBG: $F_{2,75}$=72.20, p<0.001), while the host population by phage population interaction was only significant for the spotting data (spotting: $F_{4,75}$=4.16, p=.00043; RBG: $F_{4,75}$=1.40, p=0.2437), and the host time point by phage population interaction was not significant in either dataset (spotting: $F_{2,75}$=2.99, p=0.0564; RBG: $F_{2,75}$=2.35, p=0.1022). All main effects were significant for RBG (all p<0.03), but only host population and host time point were significant for the spotting data (host population and host time point p<0.001, phage population p=0.8098). Posthoc analysis of the host population by host time point interaction (averaged across the phage populations) found that spotting ranges and RBG values on C1 and C3 hosts were lower at the endpoint (all p<0.04), while C2 spotting ranges did not differ across time points (p=0.6216), but C2 RBG values were higher at the endpoint (p<0.001).

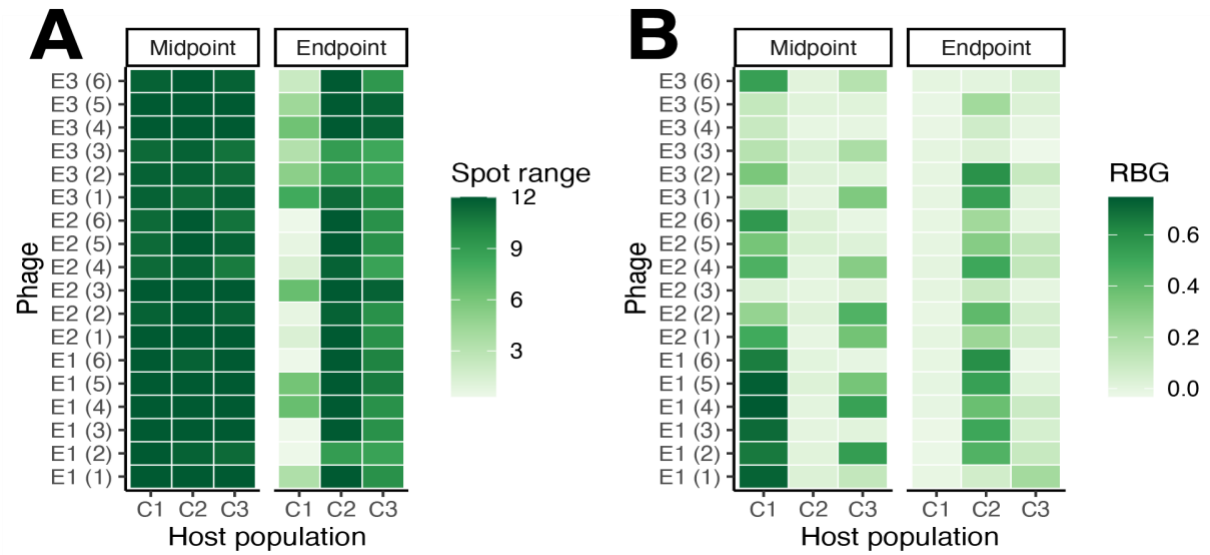

Figure 3. Spotting and RBG patterns of evolved phages differ across populations and time points. Heatmaps of the spotting range (**A**) and RBG values (**B**) of evolved phages on the three coevolved host populations from the midpoint and endpoint of passaging. Darker colors in the cells indicate greater values.

Relationship between individual (spotting) and population-level (RBG) infectivity metrics

We were next interested in the quantitative relationship between the individual-level spotting metric and the population-level reduction in bacterial growth metric. In particular, we tested whether the relationship between the spotting range and RBG values of each phage on each host population differed between the coevolved and evolved passaging treatments. We hypothesized that even though overall spotting ranges did not differ between coevolved and evolved phages, their relative quantitative impacts on the host populations might differ. The interaction of range and passaging treatment was significant ($F_{2,136.64}$=4.94, p=0.0085; Fig. 4). A likelihood ratio test comparing the full model to a reduced model excluding the interaction term between spotting range and passaging treatment, but including those terms as fixed effects, validated this finding and rejected the null (reduced) model (X^2(2)=10.74, p=0.0047).

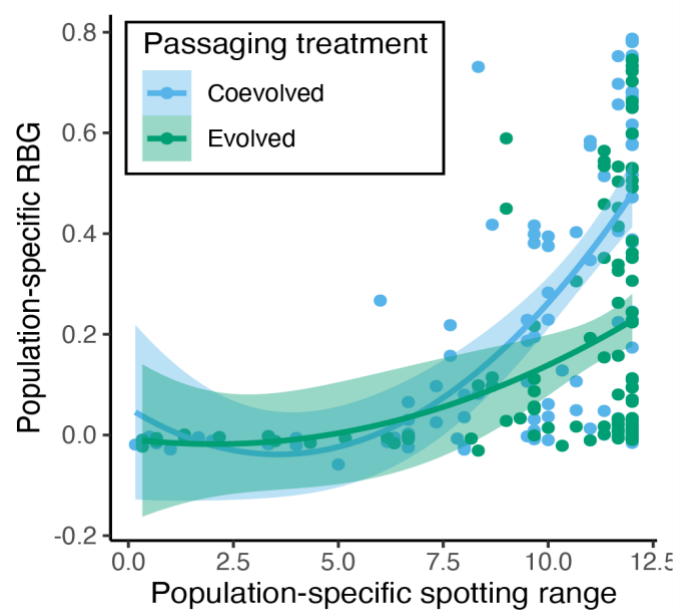

Figure 4. Relative population-level reduction of bacterial growth is greater in coevolved phages, particularly when the phages infect many isolates from that population. The relationship between spotting range and RBG values on individual populations for coevolved (light blue) and evolved (dark green) phages. Each point represents the spotting range (out of 12) and RBG value of an individual phage on an individual host population. The relationship between range and RBG was plotted as a second-degree polynomial of spotting range, with the shaded region around the line indicating the 95% confidence interval of the predictions.

Identity and frequency of observed mutations

We observed a total of 44 unique mutations across all phages, with 39 different single nucleotide polymorphisms (SNPs), 3 insertions, and 2 deletions (Fig. 5A). The gene with the most observed mutations was the tail fiber (15 different SNPs), followed by the tail tubular protein B (12 different SNPs). All mutations besides one (at position 39686) were located within coding sequences, and the majority of mutations (32 out of 44) were found within the coding sequences of phage structural proteins. Most SNPs (except for the mutations at positions 5015 and 34638) led to nonsynonymous amino acid changes.

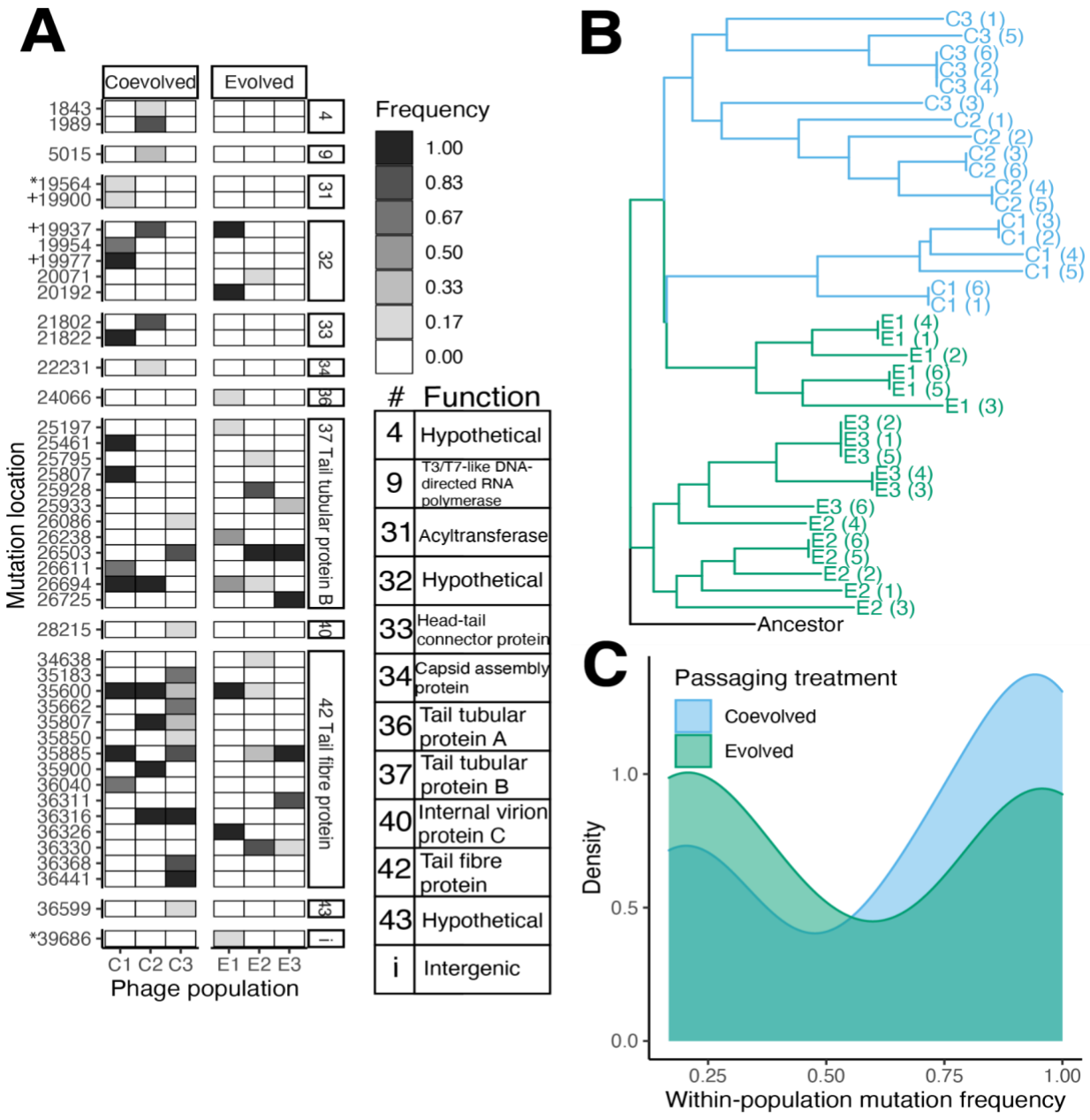

Figure 5. Coevolution selected for increased numbers of mutations in structural genes. (A) Heatmap of all observed mutations in the coevolved and evolved phages. Location numbers correspond to position in the genome. Most mutations are SNPs, except for rows marked + (insertions) and rows marked * (deletions). Cells of the heatmap are shaded based on the frequency of each mutation in the population. The table at the bottom right indicates the function of each gene (gene numbers are also specified at the right side of the heatmap). **(B)** Neighbor-joining tree of the coevolved and evolved phages with the ancestral phage set as the outgroup of the tree. Genetic distances were calculated as Euclidean distances on a matrix that indicated which SNPs and indels (each instance of an insertion or deletion counted as a single change) were present in each phage. Branch lengths represent evolutionary distances. Tips and branches

are colored according to the clades present within them, with light blue representing coevolved phages and dark green representing evolved phages. **(C)** Density plots of mutation frequencies within each population for each passaging treatment.

We found that coevolved and evolved phages differed in mutation numbers per individual (while including a random effect of phage population; $F_{1,4}$=37.07, p=0.0037; as indicated by the longer branch lengths in Fig. 5B), with individual coevolved phages having more mutations than evolved phages (mean ± 1 S.D. for coevolved = 8.50 ± 1.38, evolved = 4.56 ± 0.98). The distribution of mutations was bimodal for both coevolved and evolved phages, but the heights of the peaks differed (Fig. 5C). Evolved populations had similar amounts of rare and common mutations, while coevolved populations had more common than rare mutations.

Relationship between genotypes and phenotypes

We compared the relationship between genetic and phenotypic (spotting pattern) similarity using Mantel and partial Mantel tests of pairwise distance between coevolved and evolved phages (separately for each passaging treatment). We used genetic distance values for all variable sites across the genome, variable sites in the tail fiber only, or variable sites in the tail tubular protein B. All Mantel and partial Mantel tests of the coevolved phages were significant (p<0.01; Table 1). In contrast, only the Mantel tests of the tail fiber and tubular protein B variable sites were significant in the evolved phages (p<0.05; Table 1), and none of the partial Mantel tests were significant. We display correlations of pairwise whole genome distances and pairwise spotting distances as a representative visual (Fig. 6).

Table 1. Results of Mantel and partial Mantel tests on genotype and spotting phenotype distances. The Mantel test statistic (r) and significance values (p) are reported for each test. Stars indicate significance level (*<0.05, **<0.01, ***<0.001).

	Coevolved		**Evolved**	
	Mantel	**Partial Mantel**	**Mantel**	**Partial Mantel**
Whole genome	r=0.4592, p=1e-04***	r=0.508, p=1e-04***	r=0.1257, p=0.0792	r=-0.03958, p=0.6568
Tail fiber	r=0.4702, p=4e-04***	r=0.5137, p=3e-04***	r=0.2249, p=0.0052**	r=0.1299, p=0.0506
Tail tubular protein B	r=0.3798, p=0.0017**	r=0.2949, p=0.0052**	r=0.1636, p=0.0483*	r=0.04, p=0.3117

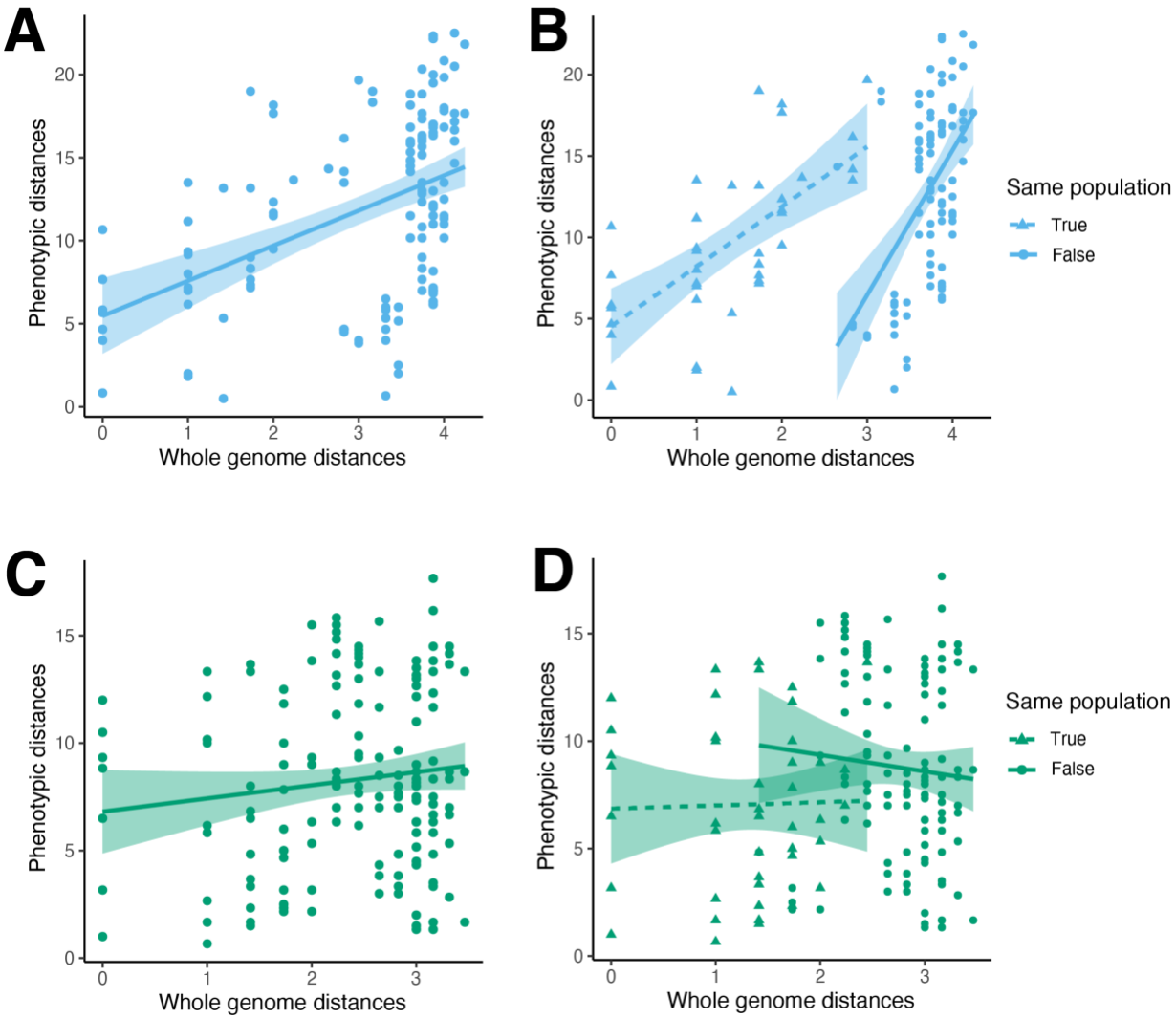

Figure 6. Coevolution, but not evolution, led to a significant relationship between pairwise genotypic and phenotypic distances. Panels (**A**) and (**B**) illustrate the correlation between pairwise whole genome distances and spotting matrix distances in coevolved phages, while panels (**C**) and (**D**) illustrate the same for evolved phages. Each point represents the value of genetic distance (x-axis) and phenotypic distance (y-axis) between a pair of phages. Linear regression lines are surrounded by shaded regions that indicate 95% confidence intervals. Panels (**B**) and (**D**) split the correlations based on whether the pairwise comparison was between phages in the same population (triangle points, dashed line) or different populations (circle points, solid line).

Discussion

We experimentally coevolved and evolved a lytic phage with the bacterial plant pathogen *P. syringae* to determine how the hosts in their environment shape patterns of genotypic and phenotypic evolution. We found that coevolved phages expanded their infectivity ranges and most dramatically reduced growth of sympatric hosts from past time points, which is indicative

of early arms race dynamics. Phages from the three coevolved populations also specialized in reducing sympatric population-level bacterial growth, suggesting that they were locally adapted. Interestingly, range expansion also occurred in the evolved phages, but coevolved phages were relatively more efficient at reducing bacterial population growth. Whole genome resequencing identified that individual coevolved phages had more mutations on average than evolved phages, but in both treatments there were numerous mutations in structural genes. Additionally, genetic similarity was more predictive of spotting pattern similarity for coevolved than evolved phages. In summary, coevolution led to strong selection for changes to phage structural proteins that expanded phage host range and increased efficiency in reducing coevolved bacterial population growth.

Phenotypic changes in coevolved phages are indicative of directional, yet diverging, selection

The temporal and spatial (across population) phenotypic patterns in the coevolved phages provide some insight into the coevolutionary dynamics of this system. All but one coevolved phage had increased spotting ranges relative to the ancestral phage, as expected in arms race dynamics (Fig. 1B, 1D). When comparing the phenotypic temporal patterns on their sympatric host populations, only one population had a reduced spotting range at the endpoint compared to the midpoint (Fig. 2C). In contrast, two populations had lower RBG values at the endpoint than the midpoint, and all endpoint values were lower than RBG on the ancestral host (Fig. 2D). Together, this suggests that the ability to infect novel coevolved hosts was not associated with a loss in the ability to infect or reduce growth of past hosts, as expected in an early coevolutionary arms race. Additionally, across all phages (coevolved and evolved) spotting ranges and RBG values were lower on endpoint hosts from populations C1 and C3, while host population C2 had mixed findings (Fig. 2A, 2B, 3A, 3B). This indicates that for two of the three populations, hosts became overall more resistant to phage. However, the coevolved phages did specialize in reducing bacterial growth of their sympatric populations, suggesting that the populations were diverging despite selection for increased range in all populations (Fig. 2F). This directional yet diverging selection across replicate bacteria-phage communities has been observed previously, although with contrasting findings regarding which partner is locally adapted (Buckling and Rainey 2002; Gurney et al. 2017).

Coevolved phages are relatively more efficient at reducing bacterial growth, but do not differ from evolved phages in overall range or fitness on the ancestral host

Our experimental design allowed us to determine the unique impacts of coevolution on viral phenotypic evolution. Although all coevolved phage populations increased in spotting range relative to the ancestral phage, the same was true for phages evolved on an unchanging host population (Fig. 1B, 1D). Additionally, average ranks of RBG values on the ancestral host did not differ between treatments (Fig. 1A, 1C). This is despite the expectation that coevolved phages would have greater spotting ranges compared to evolved phages, as seen in some (but not all) prior studies (Poullain et al. 2008; Paterson et al. 2010; Hall et al. 2011a; Scanlan et al. 2011), and that evolved phages would have higher RBG ranks on the ancestral host compared to the coevolved phages. One possible explanation is that adaptation to the ancestral host led to the acquisition of mutations that also conferred the ability to infect novel resistant strains, and conversely that coevolution did not impact the ability to reduce growth of the ancestor. Alternatively, similarities between these treatments may be a result of our relatively long passage length, which allowed for some resistant bacteria to arise throughout the course of the

experiment in the evolved phage lines (Hernandez and Koskella 2019). The coevolved and evolved phages did differ, however, in their relative impacts on bacterial population growth (Fig. 4). For a given number of isolates that a phage can spot on in each bacterial population, coevolved phages reduce bacterial population growth more than evolved phages. This is only evident when the phages infect more than half of the isolates in the population, as below that point the phages have minimal to no impact on growth in this assay. Thus, while both coevolution and evolution led to increases in spotting range, coevolved phages became relatively more efficient at reducing population growth.

Patterns of molecular evolution suggest selection on phage structural genes in both treatments, with coevolved phages having a greater number of mutations

Whole genome resequencing of our phage isolates also revealed passaging treatment-specific patterns. Coevolved phages had more mutations per individual (SNPs and indels) than evolved phages, which is consistent with prior work (Paterson et al. 2010; Scanlan et al. 2011; Fig. 5A, 5B). Additionally, the distribution of mutation frequencies within populations differed across treatments, with coevolved populations having relatively more fixed mutations (in our small sample of individuals) than evolved populations (Fig. 5C). The observed mutations were largely in structural genes, and almost all were nonsynonymous changes, suggesting strong selection for changes to phage structural proteins. The two genes with the most unique observed mutations across all phages were the tail fiber (11 in coevolved, 6 in evolved) and the tail tubular protein B (5 in coevolved, 8 in evolved). Mutations in these genes were found in all populations, and included some identical mutations that arose independently across populations within a passaging treatment, as well as across passaging treatments. Mutations found in both coevolved and evolved populations are likely involved in adaptation to abiotic conditions or to general host association, while mutations unique to a passaging treatment are more likely specific to adaptation to that host type (coevolving or ancestral). Changes in the tail fiber are unsurprising, as it is involved in binding to the cell surface receptor on the bacterial host and has been observed to evolve in other phage coevolution studies (Paterson et al. 2010; Hall et al. 2011b; Scanlan et al. 2011, 2017; Perry et al. 2015; Wandro et al. 2019). The tail tubular protein B also forms part of the tail structure, and while its exact role in the infection process for this phage is undefined, in other phages it has been shown to impact thermal tolerance and acquire different mutations in coevolved and evolved phages (Paterson et al. 2010; Kering et al. 2020).

Genotypic similarity predicts phenotypic similarity in coevolved phages

Finally, we tested for a link between genotype and spotting patterns on the coevolved hosts. We were interested in whether there was an additive effect of increasing similarity in phage genotypes on similarity in phage phenotypes, which we tested using Mantel and partial Mantel tests on pairwise distance matrices. For coevolved phages, there was a significant relationship between these distances for all genetic subsets we looked at (all variant positions, tail fiber sites, tail tubular protein B sites) in both types of tests (Table 1, Fig. 6A, 6B). Thus, for coevolved phages on coevolved hosts, genetic similarity can be used to predict similarity in infectivity patterns both within and across populations. In contrast, for the evolved phages, only the Mantel tests of the tail fiber and tail tubular protein B were significant (the whole genome tests and all partial Mantel tests were non-significant; Table 1, Fig. 6C, 6D). This suggests that similarity in the tail fiber and tail tubular protein B are likely associated with spotting phenotypes, but that the pattern is driven by divergence between populations. The lack of a

significant relationship across all variant sites could be due to epistasis (interactions between mutations) or due to the accumulation of many mutations with no effect on infectivity.

Agricultural relevance

In addition to extending our understanding of bacteria-phage coevolutionary dynamics, our work also has implications for the use of phages in agricultural biocontrol. When phages are applied agriculturally to control bacterial infections, there is no (or minimal) control over the subsequent hosts that those phages encounter. Our coevolved treatment is analogous to a scenario in which phages replicate and select for resistant bacteria on an individual host plant, coevolve with the local bacterial population, and do not disperse much between plants. In contrast, our evolved treatment is similar to what might be expected if phages experience an initial period of replication on bacteria on a single plant, and then repeatedly disperse to new plants that share the same phage-susceptible bacterial strain as the initial plant. While the extent of phage dispersal across plants in nature or agriculture is relatively unknown, some evidence suggests that the scale of phage local adaptation is at the level of an individual plant, suggesting that dispersal across plants may be limited (Koskella et al. 2011). Dispersal is also likely to depend on environmental conditions that impact phage persistence, such as UV, temperature, and humidity (Iriarte et al. 2007). However, agricultural phage evolution may not be straightforward to predict from *in vitro* experiments, due to drastic differences in factors such as resource availability, spatial structure, and competition with other microbes.

Transition

These results have demonstrated that biotic context is important in *P. syringae* and phage interactions. The genotypic and phenotypic evolution of the phage depends on the hosts that they encounter in their environment. Determining how viral evolution differs depending on the host context is critical for predicting the possible impacts of agricultural biocontrol using phages, since there is limited to no control over the fate of the phages post-application. However, this work was done exclusively under high-nutrient laboratory conditions, which is unlikely to be a relevant model for the plant-associated environment. In my next chapter, I build upon this work by explicitly testing how bacteria and phages coevolve (or evolve with an unchanging partner) in both laboratory conditions and within plant leaves. Prior work in this system found that the cost of phage resistance was context-dependent, with a higher fitness cost for phage resistance *in planta*. From this, I hypothesized that the pace of (co)evolutionary change would be slower within plant leaves, which I tested using two different experimental evolution projects in both environments.

Chapter 2. Phage resistance evolution *in vitro* is not reflective of *in vivo* outcome in a plant-bacteria-phage system

This work has been reproduced from the following, with permission from the Graduate Division and all coauthors:
Hernandez, C.A. and Koskella, B., 2019. Phage resistance evolution *in vitro* is not reflective of *in vivo* outcome in a plant-bacteria-phage system. Evolution, 73(12): 2461-2475.

Introduction

Parasites and pathogens can have substantial negative fitness effects on their hosts, which imposes strong selection pressure on the host to evolve a protective strategy such as resistance to infection. Determining the conditions under which resistance will evolve and persist has been the focus of much theoretical and empirical work due to implications for virulence evolution and treatment of disease (Anderson and May 1982; Gandon and Michalakis 2000; Mackinnon et al. 2008; Schneider and Ayres 2008; Brown 2015). While parasite resistance intuitively seems the best strategy for a host, the prevalence of parasitism as a lifestyle necessarily indicates the continued presence of susceptible hosts (Dobson et al. 2008; Koskella 2018). One mechanism for the maintenance of susceptibility in natural populations is the existence of a fitness cost of resistance (Sheldon and Verhulst 1996; Kraaijeveld and Godfray 1997; Moret and Schmid-Hempel 2000). Whether or not there are costs of parasite resistance can have important impacts on host evolution. Theory predicts that when hosts pay no fitness cost, high levels of resistance are likely to sweep through a host population (Agrawal and Lively 2002; empirically demonstrated in Buckling and Rainey 2002). With costs, there may be an optimal intermediate resistance value that predominates in the population, or there may be splitting of the population into subpopulations with different resistance values (Boots and Haraguchi 1999).

Costs of resistance have been found across many systems; for example, in plants due to tradeoffs in growth and defense pathways (Tian et al. 2003), in animals due to metabolic costs of upregulating immune responses (reviewed in Lochmiller and Deerenberg 2000), and in bacteria due to phage receptor cell-surface protein mutations which impact nutrient uptake abilities (Thirion and Hofnung 1972; Bohannan et al. 1999). However, while costs of resistance could explain the observed polymorphism in resistance traits for many host species (Antonovics and Thrall 1994; Stahl et al. 1999; Vale et al. 2015), studies that assay for these costs have also often not detected any (reviewed in Bergelson and Purrington 1996; Ferrari et al. 2001; Lennon et al. 2007). It is unclear whether costs are simply absent in these systems or whether they would be revealed under different experimental conditions. Nutrient availability, temperature, and water availability have all been demonstrated to impact measured costs of resistance (respectively, Lopez-Pascua and Buckling 2008; Luong and Polak 2007; Dietrich et al. 2005). Assays for costs of resistance are typically designed for laboratory tractability and do not replicate the natural environment of the host-parasite interaction.

In addition to context-dependent costs of resistance, the strength of parasite-mediated selection (e.g. through increased host-parasite contact rate or parasite virulence) will impact the evolutionary trajectory of resistance in a host population. If there is a tradeoff between resistance to the parasite and other fitness-impacting traits, the strength of selection will be important in determining whether resistant mutants can spread throughout a population, with even very costly resistance being initially selected for when the risk of infection is high (Boots and Haraguchi 1999; Brockhurst et al. 2003). In contrast, without fitness tradeoffs, resistant mutants will be

expected to increase in frequency at a rate that depends only on the strength of parasite-mediated selection.

In bacteria-phage systems, most research has been performed either *in vitro* or by tracking dynamics in natural populations and communities. It is unclear, however, when the ecological and evolutionary processes that have been experimentally measured *in vitro* can explain the correlational patterns observed in natural bacteria-phage interactions. For host-associated bacteria in particular, the *in vivo* environment differs in numerous ways from *in vitro* experiments. Bacteria and phage found in or on a living host (e.g. as part of a microbiome) interact in a more stressful environment than that of laboratory media, often including low resource availability, microbial competition, pH and osmotic stress, and contending with host immune responses. These conditions can impact bacterial physiology and ultimately the ability of phages to access and replicate in their hosts (Hadas et al. 1997; Lindow and Brandl 2003; Louis and O'Byrne 2010; Lebeis et al. 2015; Bryan et al. 2016). It is therefore unclear if and how the wealth of existing knowledge about bacteria-phage interactions *in vitro* can be used to predict how phages will shape the evolution of host-associated bacterial populations.

Few studies have examined bacteria-phage (co)evolution *in vivo* (Capparelli et al. 2006; Meaden and Koskella 2017; Wang et al. 2017; De Sordi et al. 2018), and none have directly compared the outcome of serially-passaged bacteria and phage *in vitro* and *in vivo*. However, a growing body of work has focused on understanding bacteria and phage dynamics in ecologically-relevant conditions (Gómez and Buckling 2011; Laanto et al. 2017; Scanlan et al. 2019). For example, recent work investigating *Vibrio cholerae* phage replication in aquatic environments found that two of three clinically-isolated phages had some level of replication in estuarine water, but none were able to replicate in fresh water (Silva-Valenzuela and Camilli 2019). This finding suggests that the long-held speculation that bacterial dynamics in this system are controlled by phage-mediated lysis in aquatic environments may not be accurate (Faruque et al. 2005). Similarly, previous work in a plant pathogenic bacteria-phage system found that costs of resistance were context-dependent, where phage-resistant bacterial mutants reached lower densities in the natural plant host, but grew comparably to phage-sensitive cells *in vitro* (Meaden et al. 2015). However, it is unknown whether this context-dependent cost of resistance would impact frequency of *de novo* phage-resistant mutants in these two environments, particularly given that the strength of phage-mediated selection *in planta* is unknown. Thus, we tested how the environmental context of bacteria-phage interactions influences the frequency of resistance evolution in two serial passaging experiments using plant pathogenic *Pseudomonas syringae* and lytic phages *in vivo* (in tomato leaves) and *in vitro* (in high-nutrient media). The first serial passaging experiment included coevolution and single-sided evolution treatments using a single phage, and the second tested the impact of higher phage pressure and a "phage cocktail" treatment.

Study System

Pseudomonas syringae is a gram-negative bacterial plant pathogen and model system for studying plant-pathogen interactions (Xin and He 2013). Across pathovars, it infects a wide variety of species including tomato, kiwifruit, and soybean (Sarkar and Guttman 2004). After arriving on a suitable host by wind or rain-mediated dispersal, it begins as an epiphyte on leaf surfaces (Lindemann et al. 1982; Constantinidou et al. 1990). Once reaching a sufficiently high density as determined via quorum sensing, the bacterium enters the apoplast (internal intercellular space) of the leaf through stomata or wounds (Quiñones et al. 2005; Misas-Villamil

et al. 2013). In the apoplast, the pathogen expresses effector proteins that suppress plant defense responses and cause disease symptoms (Guttman et al. 2002; Hauck et al. 2003; Kim et al. 2005; Zhang et al. 2007). *Pseudomonas syringae* pathovar *tomato* strain PT23 (draft genome in Meaden and Koskella 2017) causes the disease bacterial speck on tomato and is virulent on multiple tomato genotypes including Moneymaker, the plant host used in our experiments.

Phages of Pseudomonads have commonly been used to investigate bacteria-phage interactions, with studies spanning topics such as evolutionary diversification, coevolutionary dynamics, and local adaptation (reviewed in Brockhurst et al. 2007). The lytic phage replication cycle begins with attachment to a cell-surface receptor, and proceeds with injection of genetic material, genome replication, phage gene expression and protein assembly, packaging of completed phage particles, and ultimately a burst of the host cell. Bacterial hosts can rapidly evolve resistance to phage through cell-surface receptor modifications (Lenski and Levin 1985; Meaden et al. 2015), production of extracellular compounds that can prevent phage access to host cells (Doolittle et al. 1996; Hammad 1998; Scanlan and Buckling 2012), or acquisition of novel CRISPR spacers targeting previously-encountered phages (Barrangou et al. 2007), among other mechanisms (Labrie et al. 2010). We investigated the evolution of *P. syringae* under phage selection from the Podoviridae lytic phage "FRS" and Myoviridae lytic phage "SHL", both of which have been previously shown to select for cell-surface receptor-based resistance mutations *in vitro* that have context-dependent fitness costs, with their likely receptor being the Gram-negative bacteria outer membrane molecule lipopolysaccharide (LPS; Meaden et al. 2015).

Methods

Six-passage experimental co(evolution) in planta *and* in vitro

A single colony of *Pseudomonas syringae* pv. *tomato* PT23 (obtained from Gail Preston, University of Oxford) was isolated to begin the evolution experiment. After washing and resuspending a liquid culture of this strain in 1 mM $MgCl_2$, density of cells was determined via dilution plating. The Podoviridae lytic phage FRS (obtained in 2008 from OmniLytics Inc.) was co-cultured with PT23 in KB liquid media shaken at 28°C, and cell-free lysate was obtained by filtration (0.45 μm) after 24 hours. Enumeration of phage stock was obtained by dilution plating on soft agar overlays.

Initial inoculation of plants and *in vitro* tubes was done at 4:1 (phage:bacteria) multiplicity of infection (MOI), with starting bacterial density of $7x10^6$ colony forming units (CFU) per mL and starting phage density of $2.5x10^7$ plaque forming units (PFU) per mL. The experiment included three replicate lines (separate plants and *in vitro* tubes) each of: (i) bacteria without phage ("B only"); (ii) phage without bacteria ("P only"); (iii) co-passaged bacteria and phage ("Coevolved"); (iv) evolving bacteria with ancestral phage ("B evolved"); and (v) evolving phage with ancestral bacteria ("P evolved"). Additionally, we included a control magnesium chloride-inoculated plant each week, which was interspersed among treatment plants in the growth chamber.

Four-to-five-week-old Moneymaker plants grown from surface-sterilized seeds were randomly assigned to a treatment, with six randomly chosen leaves inoculated per plant. Inoculation was done by blunt-end syringe injection into the abaxial side of the right half of each leaf (approximately 300 μL). While syringe inoculation bypasses the epiphytic growth phase of this pathogen, previous work using this method has demonstrated the context-dependent tradeoff in phage resistance and growth that motivated our study (Meaden et al. 2015). *In vitro* tubes were similarly "inoculated" with 300 μL of prepared inoculum in 10 mL of KB liquid media. Plants

and *in vitro* tubes were statically incubated in a single growth chamber set to 24°C, 15h day:9h night light cycle, with darkness beginning right after inoculation (to reduce possibility of phage decay due to UV; Iriarte et al. 2007).

After 72 hours, plants were sampled by taking a single hole punch (6 mm diameter) from each of the inoculated leaves and homogenized in a single tube with 1 mM $MgCl_2$ and two sterile ceramic beads. *In vitro* tubes were sampled by mixing 700 µL of 1 mM $MgCl_2$ and 300 µL of culture. Bacterial density was obtained by dilution plating, and 100 random colonies were then picked for passaging (as in Meaden and Koskella 2017). This ensured an equal bottleneck of host populations at each passage across treatments. We found that filtration of homogenized plant tissue led to substantial loss of phage titers relative to estimates of pre-filtration phage concentration (evident as serially-diluted plaques in CFU dilution plates; see supplement and data on Dryad) that would have led to complete loss of phage before the planned end of experiment. In order to ensure phage pressure on bacteria would persist throughout the experiment (though we recognize that this method may not reflect natural dynamics of this system) we added an "amplification" step where samples were incubated in media for six hours (incubation duration was selected to correspond with previously determined time-to-detectable-increases in FRS titer during co-culture; Morella et al. 2018). To do this, 50 µL of sample (e.g. leaf homogenate or *in vitro* culture) was added to 2 mL KB broth and incubated at 28°C, shaken, for six hours. These samples were then filtered and plated on soft agar overlays with ancestral PT23 to quantify amplified PFUs (Fig. S1). This process added a short phage replication step outside of the plant environment but only in the presence of bacteria from plant homogenate, and resulted in similar amplified PFUs across treatments (Fig. S1). Amplified phage filtrate and the 100 mixed colonies were then diluted 1:100 in 1 mM $MgCl_2$ for subsequent passages, and this process was repeated for a total of six passages through each environment. Bacteria and/or phage spent 432 total hours in each environment (estimates of generations are infeasible given the heterogeneity of the plant environment).

Phage resistance assay in vitro

Bacterial colonies from passage three (12 colonies each line) and passage six (approximately 96 colonies each line) were isolated from homogenized plant tissue and *in vitro* samples as described above, grown in 1 mL liquid KB, and incubated shaken at 28°C for 48 hours. Each bacterial clone was then streaked across a line of high titer ancestral or contemporary phage (i.e. isolated from that evolution line at the same time point as the assayed bacteria) on hard agar plates (Miller 1998). After incubation, each colony's streak "phenotype" was recorded as one of three categories: sensitive (no growth over phage – the ancestral state), moderately resistant (growth over phage, but reduced), or fully resistant (no reduction of growth over phage). An overnight culture of ancestral PT23 was streaked against all phages to confirm that phage titer was sufficient to identify sensitive hosts.

Phage resistance assay in planta

We hypothesized that the streak assay may not accurately represent phage resistance in the plant environment, so we assayed for resistance in plant-passaged lines by growing the experimentally-evolved bacteria in the presence and absence of phage *in planta*. Approximately 96 bacterial colonies isolated from the final passage for each line were re-streaked to separate them from phage contamination, then mixed (to yield a single population for each line) and suspended in 1 mM $MgCl_2$. Plants were randomly assigned to a treatment and inoculated with

bacteria in the presence or absence of 100:1 MOI ancestral phage (*in planta* evolution lines used: three "B only", two "Coevolved" (one line could not be separated from phage), and three "B evolved"). Starting bacterial density was approximately $8x10^6$ CFU/mL, with $8x10^8$ PFU/mL of phage. This high MOI (100:1) was selected in order to maximize our chance of detecting any subtle resistance mechanisms. Nine leaves were inoculated per plant, with a single hole punch taken from three of the leaves at each time point (0, 24, and 72 hours post-inoculation). Tissue samples were snap-frozen in dry ice and ethanol until homogenization and dilution plating to measure bacterial densities.

Additional modified in planta *resistance assay using ddPCR*

We performed a second *in planta* resistance assay to quantify phage replication in addition to bacterial growth over time using droplet digital PCR (ddPCR), which allows for absolute and simultaneous culture-independent quantification of bacteria and phage using fluorescent probes (Morella et al. 2018). For this assay, we prepared passage six bacterial colonies from the "B only" and "B evolved" lines (which we hypothesized might be the treatment most likely to show evidence of ancestral phage resistance) using the same methods as above. We inoculated nine leaves of four-week-old Moneymaker plants with a starting bacterial density of $2.5x10^6$ CFU/mL, and a 100:1 MOI of ancestral FRS phage in 1 mM $MgCl_2$. The colony mixtures from each line were inoculated onto separate plants in the absence or presence of phage. Three hole punches were taken from each of three leaves at three time points (0, 24, and 72 hours post-inoculation), and each leaf's hole punches were snap-frozen in dry ice and ethanol until homogenization.

For bacteria and phage enumeration, we homogenized two randomly chosen leaf samples per plant per time point in 1 mL water and quantified densities using the Bio-Rad QX200™ Droplet Digital™ PCR system. ddPCR has been previously used to simultaneously track *P. syringae* and FRS densities *in planta*, and we used the same probes and methods in this assay (Morella et al. 2018). The averages of the copy number values (sample concentration as measured by ddPCR) were used for analysis. Detailed ddPCR methods are available in the supplement.

Phage cocktail serial passaging experiment

We followed up on our initial passaging experiment with a second experiment involving stronger selection pressure (a higher MOI), an additional phage (Myoviridae phage "SHL", provided in 2008 by Omnilytics Inc.), and a "phage cocktail" treatment. In this experiment, we evolved bacteria but applied ancestral phage each week at a higher MOI (20:1) than the previous experiment. Ancestral bacteria and phage were prepared as described for the first passaging experiment. We selected a lower initial starting bacterial density for this experiment, to allow for a longer period of active bacterial replication. Initial bacterial concentration was $3.5x10^4$ CFU/mL and total phage concentration each passage was $7x10^5$ PFU/mL. Experimental lines included three each of: (i) bacteria only lines ("B only"); (ii) bacteria with FRS lines ("B+FRS"); (iii) bacteria with SHL lines ("B+SHL"); and (iv) bacteria with FRS and SHL lines (the phage cocktail, "P cocktail"). Sampling and passaging were performed as in the previous passaging experiment, except that when plating for bacterial densities each week, we added two additional dilution plates spread with high titers of FRS or SHL to assay the entire population for phage resistance by comparing CFUs on plates with and without phage ("phage agar" as used in Lederberg and Lederberg 1952; method tested for antibiotic resistance in Vieira et al. 2008). This

allowed us to identify any bacterial cell that can grow in the presence of phage, rather than screening a subset of the population.

***Benefits of resistance assay* in planta *and* in vitro**

Our final experiment sought to compare the growth of resistant and sensitive bacterial colonies (evolved *in vitro)* in the presence and absence of phage across the two environments, to determine whether there is a fitness benefit of resistance under the different conditions. To generate resistant and sensitive colonies, we grew a single colony of ancestral PT23 in independent liquid cultures in the presence or absence of high titer ancestral FRS (four cultures each). Colonies from each population were isolated after shaken incubation at 28°C, and were streaked across a line of high titer ancestral FRS to determine resistance status. Overnight cultures of four confirmed resistant and four sensitive colonies (one per independent culture) were then spun, washed, and resuspended in 1 mM $MgCl_2$, and were plated to verify lack of phage contamination. Plants and *in vitro* tubes were then inoculated using the same conditions as the "phage cocktail" passaging experiment (same starting densities and MOI), except that resistant and sensitive clones were paired such that each clone was inoculated onto three leaves of a shared plant. A single hole punch from each leaf per clone was sampled and combined in a single tube for each time point (1, 24, and 72 hours post-inoculation) prior to homogenization. 300 µL of each *in vitro* culture was mixed with 700 µL 1 mM $MgCl_2$. Bacterial densities at each time point were determined via CFU plating and ddPCR. 72 hour samples were additionally plated for density of resistant CFUs using the "phage agar" method. We focus our interpretation on the ddPCR results due to its precision, and provide statistical analysis of CFU results and a correlation between densities from each method in the supplement (Fig. 6, Figs. S2 and S3).

Statistical analysis and figures

All statistics were run in R version 3.4.0. For all analyses, values below the limit of detection were treated as if they were at that limit (as a conservative estimate). Bacteria and phage densities were $\log_{10}$ transformed prior to statistical analysis, and a significance level of 0.05 was used in all tests. Posthoc analyses were run when appropriate, comparing estimated marginal means (R package *emmeans*) for significant interactions or main effects using a Bonferroni correction for multiple testing.

Bacteria and phage densities over time in the six-passage experiment were analyzed as repeated measures models using the aov_car function from the *afex* package, testing for a two-way interaction between passage number and evolution treatment on $\log_{10}$ CFU or PFU per ml culture/1 mm^2 leaf tissue in each environment.

For resistance assays from the six-passage experiment, we analyzed results from *in vitro* lines only (as plant lines had no evidence of resistance), and fit models for each bacterial time point separately. We tested for effects on the number of sensitive and resistant colonies with bias-reduced binomial generalized linear models, using the *brglm* package as recommended for separated data (Heinze and Schemper 2002). We first fit a model for a phage type (ancestral/contemporary) by evolution treatment interaction for each time point, and tested significance of terms by sequential dropping and determined change in fit with likelihood ratio tests. We then subset the resistance results for ancestral phage only (due to "B only" having no contemporary phage) and tested for a treatment effect. For passage six, we ran the model without the "P evolved" treatment due to phage-mediated extinction of two bacterial lines, and for

comparison we ran the passage three models both with and without the "P evolved" treatment for that time point.

For resistance *in planta* assays (and the paired *in vitro* assay in Fig. 6 and Fig. S2), we analyzed bacteria and phage growth over time using a repeated measures model testing for a time by phage by evolution treatment interaction on density (log_{10} bacteria/phage copies from ddPCR or log_{10} CFU). In the ddPCR resistance *in planta* assay, we also tested for an effect of time on background phage density in plants that were inoculated with bacteria but without phage.

In the phage cocktail experiment, proportion resistant was calculated from the number of colonies on the "phage agar" plate divided by the number of colonies on the plate without phage. We then subtracted the small proportion of ancestral PT23 colonies (plated as a control) that were able to grow on the phage agar plates from the proportions for all experimental samples. Due to missing values after the first passage *in vitro* (all bacteria from "phage cocktail" lines and two "B+SHL" lines went extinct), we analyzed the effect of treatment on bacterial density at all passages separately using linear models. *In planta*, we ran a repeated measures model testing for a time by treatment interaction. No statistical tests were run on the resistance results for this experiment due to many missing values from extinct lines (but a description of results is presented).

For the benefits of resistance experiment, the one-hour time point was excluded from the ddPCR and CFU analyses due to many values being near or below the limit of detection. We ran linear mixed effects models (using the lmer function from *lme4* package) testing for a time by resistance category by phage interaction on bacterial density, including a random effect of colony within time and plant within phage. To parse results further, we generated separate models for the two time points and tested for a resistance category by phage interaction including a random effect of colony, and ran planned contrasts on estimated marginal means (planned contrasts: resistant v. sensitive in the absence of phage, resistant v. sensitive in the presence of phage, resistant with and without phage, sensitive with and without phage) with a Bonferroni correction for multiple testing. Interestingly but not unexpectedly, ddPCR results differ slightly from the number of CFUs in some conditions (CFU results and correlation with ddPCR results available in supplement). Phage copy number ddPCR values from this experiment were not presented due to a technical issue of low amplification.

Figures for all experiments were made using the *ggplot2*, *scales*, *cowplot*, *ggpubr*, and *Cairo* packages, and subsequently edited in Adobe Illustrator. All data, code for statistical analysis, and code for figures are available on Dryad.

Results

Six-passage experiment

Bacterial densities after each passage

We tested for an effect of experimental evolution treatment and passage number on bacterial densities observed during passaging in each environment. *In planta*, there was an interaction between treatment and passage number that impacted bacterial densities ($F_{7.25,\ 19.35} = 4.42$, $p = 0.0042$; Fig. 1), and an effect of passage number ($F_{2.42,\ 19.35} = 51.12$, $p < 0.001$), but no main effect of treatment ($F_{3,\ 8} = 0.057$, $p = 0.9807$). After passage one *in planta*, bacterial densities from the "P evolved" treatment were significantly higher than "B only" ($p = 0.0187$), but after the last passage "P evolved" bacterial densities were lower than all other treatments (all $p < 0.002$). *In vitro*, bacterial densities were also impacted by an interaction of treatment and passage number ($F_{8.83,\ 23.55} = 2.85$, $p = 0.0203$), as well as both main effects (both $p < 0.005$; Fig.

1). After the first passage, all treatments with phage were significantly lower than "B only" (all $p < 0.05$), but not significantly different from each other. After the last passage, the "P evolved" densities were lower than all other treatments ($p < 0.0001$), but no other comparisons were significantly different.

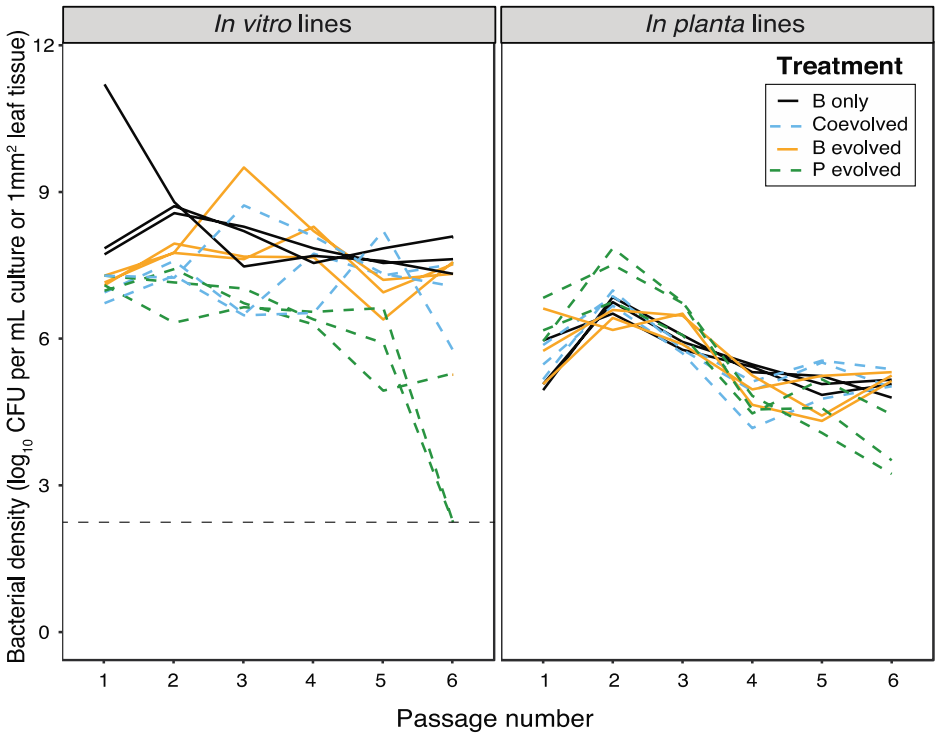

Figure 1. Bacterial densities after 72 hours of growth at each passage *in vitro* and *in planta*. Bacterial density (in $\log_{10}$ CFU per mL culture for *in vitro* lines, and $\log_{10}$ CFU per 1 mm^2 leaf tissue for *in planta* lines) after each passage in the six-passage coevolution and one-sided evolution experiment *in vitro* and *in planta*. Individual lines represent the densities for a specific evolution line measured over time. Different evolution treatments ("B only" bacteria were evolved in the absence of phage, "Coevolved" bacteria were co-passaged with phage, "B evolved" bacteria evolved against the ancestral phage, and "P evolved" was ancestral bacteria exposed to evolving phage) are grouped by line type and color as indicated in the legend. The dashed line represents the limit of detection for our assay, and points on this line were at or below this limit.

Resistance to phage, in vitro *assay*

We streaked our passage three and six *in vitro* and *in planta*-evolved bacteria across both ancestral and contemporary phage to determine proportion of resistant colonies to phage from both time points. For *in vitro*-evolved bacteria after passage three, we found that evolution treatment impacted the proportion of resistant colonies both when the "P evolved" treatment was included or excluded ($X^2_3 = -68.39$, $p < 0.0001$, and $X^2_2 = -15.45$, $p = 0.0004$, respectively), and this did not depend on phage time point ($p = 0.9843$ with, and $p = 0.8728$ without "P evolved"; Fig. 2A). Analyzing only ancestral phage results, we again found an effect of treatment ($X^2_3 = -45.91$, $p < 0.0001$) when the "P evolved" treatment was included, which had higher resistance

than all other treatments (all $p < 0.006$). Once that treatment was removed, there were no significant pairwise comparisons (although there remained an overall effect of treatment, $X^2_2 = -14.07$, $p = 0.0009$). Unlike the third passage results, the proportion of resistant colonies after passage six depended on both treatment and phage time point ($X^2_1 = -6.93$, $p = 0.0085$), with bacteria from lines passaged with phage being more resistant than "B only" (all $p < 0.05$), and having a higher proportion of resistance to ancestral phage compared to contemporary phage ($p < 0.0001$; suggesting phage coevolution in response to bacterial resistance evolution). Analyzing just ancestral phage results, there again was a treatment effect ($X^2_2 = -802.38$, $p < 0.0001$), with all pairwise comparisons of treatment groups being significantly different (all $p < 0.0001$). No statistics were performed on *in planta* results due to many samples having 0 or nearly 0 resistant colonies (at passage three all samples had 0; and at passage six, five lines were found to have very low proportions of resistance, including one "B only" line (0.031), two "Coevolved" lines (both 0.011), one "B evolved" line (0.010), and two "P evolved" lines (0.0263 and 0.0105; Fig. 2B).

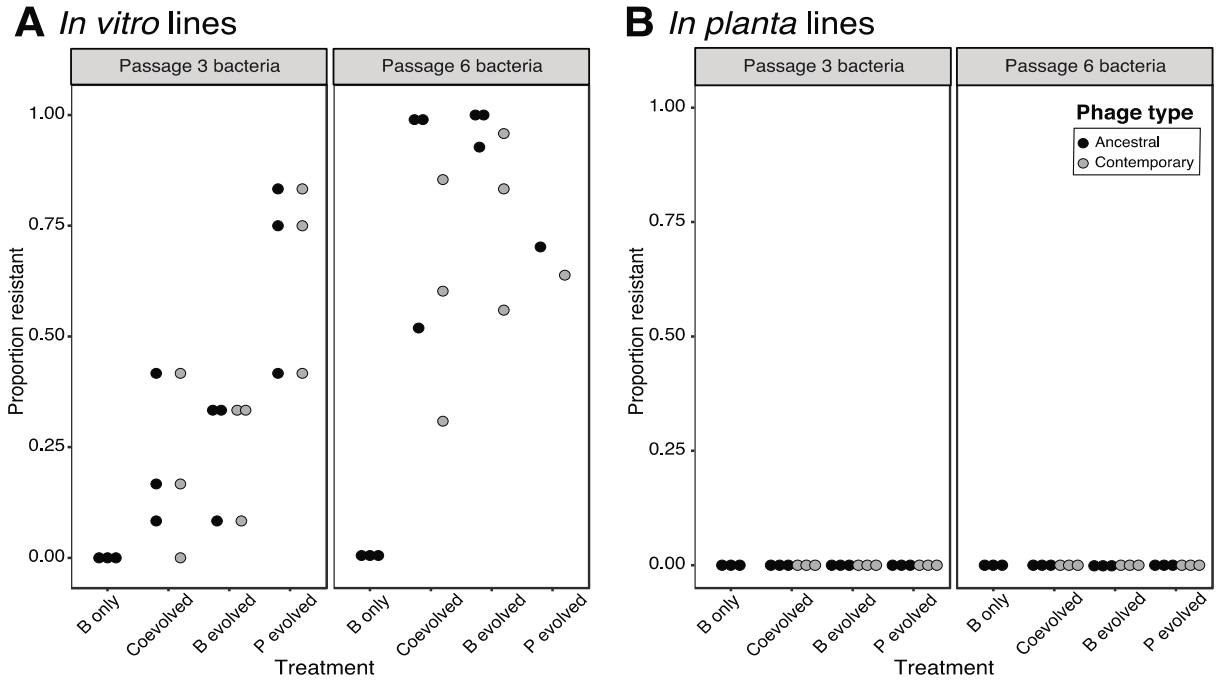

Figure 2. Proportion of passage three and passage six colonies that were resistant to ancestral and/or contemporary phage *in vitro* and *in planta*.
Proportion of resistant colonies (complete or slightly reduced growth over the phage line) in the streak assay for resistance after passage three and passage six for the *in vitro* (A) and *in planta* (B) evolved bacteria from the six-passage coevolution and one-sided evolution experiment. Bacterial evolution treatment ("B only" bacteria were evolved in the absence of phage, "Coevolved" bacteria were co-passaged with phage, "B evolved" bacteria evolved against the ancestral phage, and "P evolved" was ancestral bacteria exposed to evolving phage) is plotted against the proportion, with separate points for phage type used in the streaking assay (black for ancestral, and gray for contemporary).

Resistance to phage, in planta *assay (CFU)*

When the *in planta*-evolved lines were grown in the presence and absence of phage *in planta*, we found no interaction between treatment (bacterial evolutionary origin; "B only", "Coevolved", and "B evolved"), presence/absence of phage, and time post-inoculation on bacterial density ($F_{2, 5} = 0.80$, $p = 0.5007$; Fig. 3). However, there was an effect of phage that depended on time ($F_{1, 5} = 20.16$, $p = 0.0065$), and main effect of both time ($F_{1, 5} = 123.64$, $p = 0.0001$) and phage presence ($F_{1, 5} = 21.95$, $p = 0.0054$) on bacterial density. Phage presence decreased bacterial densities after 24 hours post-inoculation ($p = 0.0001$) but not after 72 hours ($p = 0.8805$).

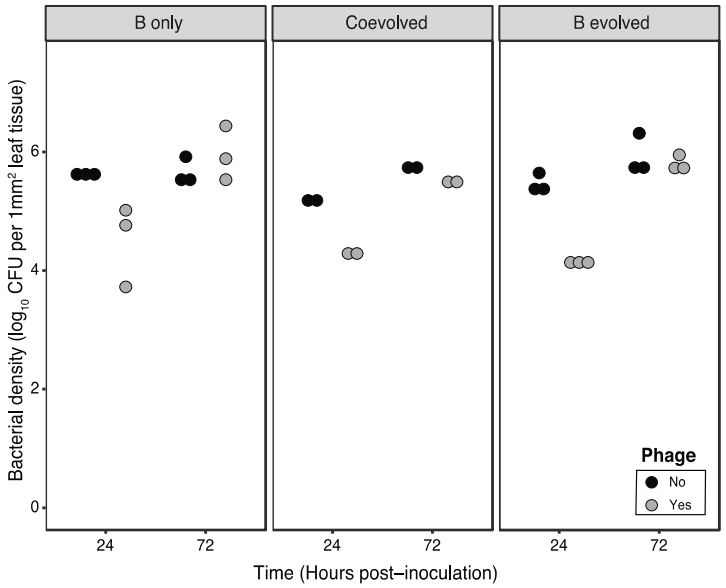

Figure 3. Bacterial densities over time in the *in planta* resistance assay for *in planta*-evolved bacteria.

Bacterial density (in $\log_{10}$ CFU per 1 mm^2 leaf tissue) at 24 and 72 hours post-inoculation in the *in planta* resistance assay of mixed bacterial colonies from the plant-evolved endpoint populations of the six-passage coevolution and one-sided evolution experiment. The ancestral phage from the passaging experiment was used as the phage applied in this assay (in the plant inoculum). The plots are split by bacterial evolution treatment during passaging ("B only" bacteria were evolved in the absence of phage, "Coevolved" bacteria were co-passaged with phage, and "B evolved" bacteria evolved against the ancestral phage), and points are shaded according to whether phage was absent (black) or present (gray) in the plant inoculum for this assay.

Resistance to phage, in planta *assay (ddPCR)*

We again tested for the impacts of treatment ("B only" and "B evolved"), phage presence/absence, and time on bacterial densities *in planta*, but used ddPCR to measure bacterial densities. Again, no three-way interaction was observed ($F_{1.51, 12.09} = 0.40$, $p = 0.6207$), but there was a significant effect of treatment that depended on time ($F_{1.51, 12.09} = 5.55$, $p = 0.0259$) and a main effect of time ($F_{1.51, 12.09} = 1322.78$, $p < 0.0001$; Fig. 4A). Bacterial densities from both treatments increased over time ($p < 0.02$ for all comparisons), but unlike the previous experiment in which we quantified CFUs, there was no measurable effect of phage on bacterial densities

from either treatment at any time point. “B evolved” densities were slightly higher than “B only” at the start ($p = 0.0124$), but lower than “B only” at 24 hours ($p = 0.0309$) and not significantly different at 72 hours ($p = 0.3822$).

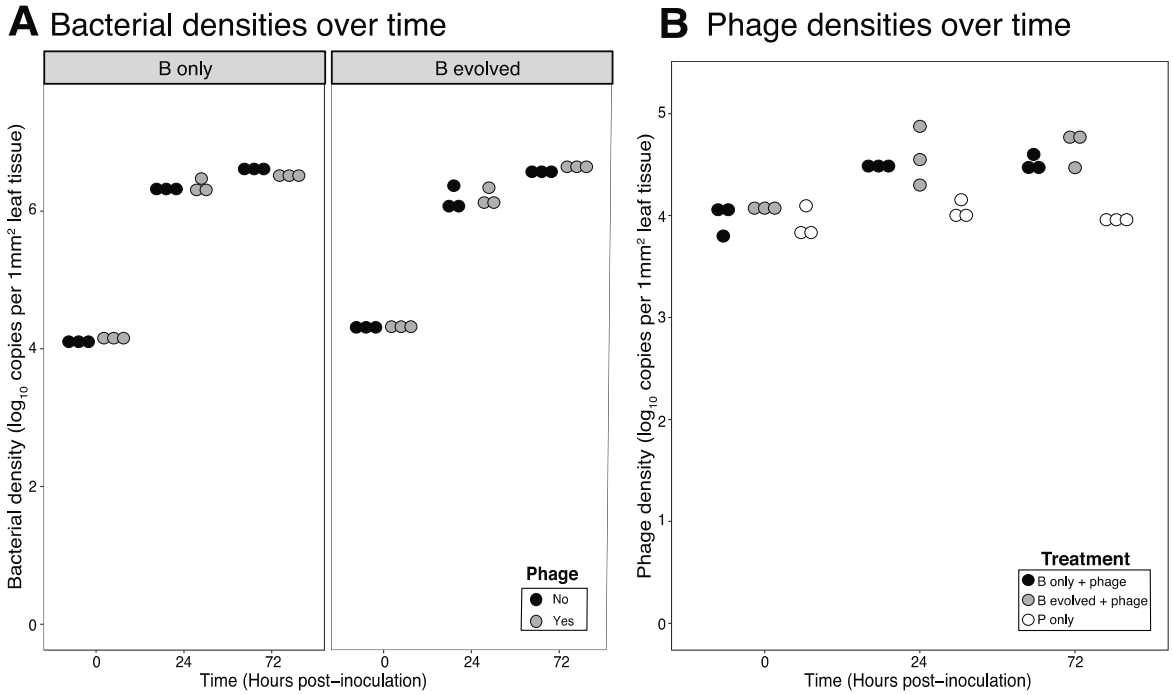

Figure 4. Bacteria and phage densities over time in the *in planta* resistance assay using ddPCR.

Bacteria (A) and phage (B) densities over time (hours post-inoculation) in $\log_{10}$ ddPCR copies per 1 mm^2 leaf tissue. Bacteria in this assay consisted of mixed colonies from the plant-evolved endpoint populations of the six-passage coevolution and one-sided evolution experiment, and the applied phage in the plant inoculum was the ancestral phage from the passaging experiment. In panel A, plot is split by bacterial evolution treatments (“B only” bacteria were evolved in the absence of phage, and “B evolved” bacteria evolved against the ancestral phage), with points shaded according to whether phage was absent (black) or present (gray) in that plant inoculum. In panel B, points are shaded as follows: black represents bacteria from the “B only” evolution lines that had phage applied, gray represents bacteria from the “B evolved” evolution lines that had phage applied, and white represents plants that were inoculated with the ancestral phage but without any bacteria.

For phage densities, we also tested whether there were effects of treatment and/or time in samples inoculated with phage (both with and without bacteria), and found a marginally significant interaction effect ($F_{2.36,\ 7.08} = 4.16$, $p = 0.0597$; Fig. 4B), while both time and treatment had significant effects on phage density (time: $F_{1.18,\ 7.08} = 24.04$, $p = 0.0014$; treatment: $F_{2,\ 6} = 19.03$, $p = 0.0025$; Fig. 4B). Both “B only” and “B evolved” bacteria supported significant increases in phage density from 0 to 24 hours ($p < 0.003$ for both) but not between 24 and 72 hours, while there were no changes in phage density in the “P only” treatment ($p = 0.7990$ between 0 and 24 hours, $p = 1$ between 24 and 72 hours).

Phage cocktail experiment

In vitro, there was a significant effect of evolution treatment on bacterial densities at passage one ($F_{3, 8}$ = 8.48, p = 0.0073), with the "phage cocktail" densities being significantly lower than "B only" (p = 0.0133) and "B+FRS" (p < 0.0330; Fig. 5A). All other pairwise comparisons were not significant, and there was no effect of treatment after passage two ($F_{2, 4}$ = 1.90, p = 0.2626) or three ($F_{2, 4}$ = 1.08, p = 0.4222). *In planta*, we found no interaction between treatment and time on bacterial density ($F_{4.77, 12.73}$ = 0.63, p = 0.6749), and no significant main effects (passage number: $F_{1.60, 12.73}$ = 0.36, p = 0.6556; treatment: $F_{3, 8}$ = 2.67, p = 0.1184; Fig. 5A).

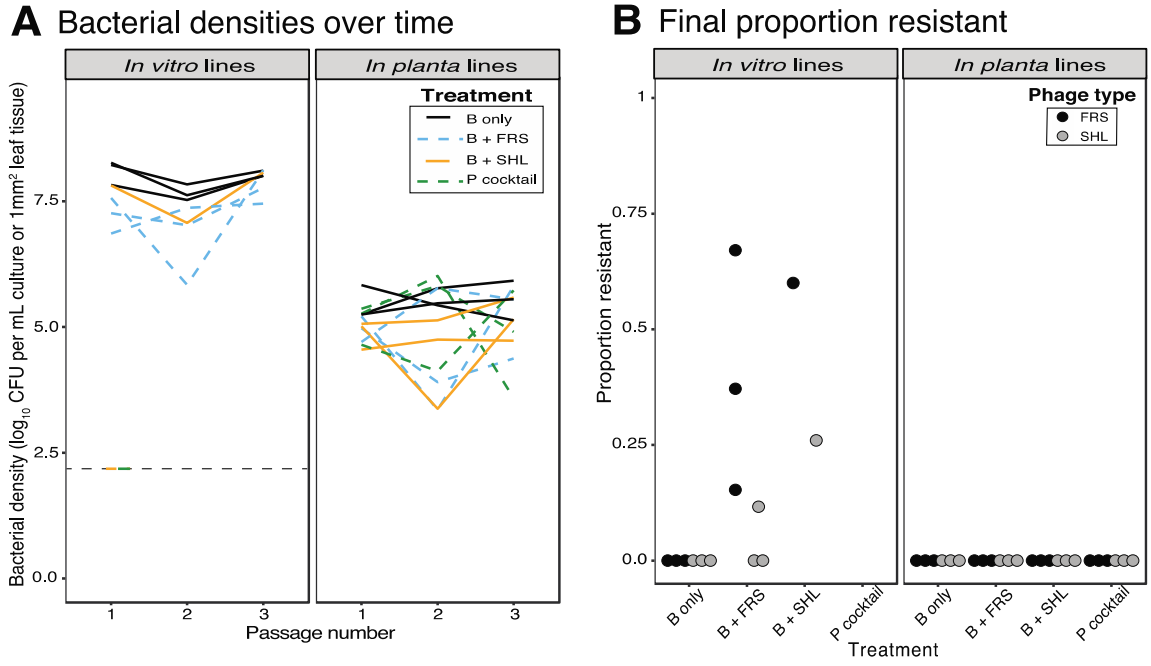

Figure 5. Bacterial densities at each passage *in vitro* and *in planta* in the phage cocktail experiment, and proportion of resistance at the endpoint.
In panel A, bacterial densities (in $\log_{10}$ CFU per mL culture for *in vitro* lines, or $\log_{10}$ CFU per 1 mm^2 leaf tissue for *in planta* lines) are plotted over time (after each passage) for the phage cocktail passaging experiment *in vitro* and *in planta*. Individual lines represent the values for a specific evolution line measured over time. Different evolution treatments ("B only" bacteria were passaged in the absence of phage, "B+FRS" bacteria were passaged in the presence of ancestral FRS, "B+SHL" bacteria were passaged in the presence of ancestral SHL, and "P cocktail" bacteria were passaged in the presence of both phages) are grouped by line type and color as indicated in the legend. The dashed line represents the limit of detection for our assay, and points on this line were below this limit. After the first passage, all three "P cocktail" and two "B + SHL" lines had no detectable bacteria, and have no plotted values in passages two and three. Proportion of resistant colonies over total colonies using the "phage agar" resistance assay is plotted in panel B, with bacterial evolution treatment on the x-axis, and phage type (for which we were assaying for resistance) on the plate indicated by the different color points (black for FRS, gray for SHL). Note that missing points indicate lines for which all bacteria had been eliminated by phage.

When we quantified resistance proportions using the "phage agar" method for the *in vitro* lines, we found that "B only" lines had either no resistant colonies or extremely low proportions of resistance after the last passage (two lines for FRS: $6.76x10^{-05}$, $8.77x10^{-06}$, one line for SHL: $7.3x10^{-05}$; Fig. 5B). In contrast, "B+FRS" lines had higher proportions of resistant colonies to FRS (0.37, 0.60, and 0.15), and extremely low or a small proportion of resistant colonies to SHL ($2.99x10^{-06}$, $1.79x10^{-05}$, and 0.12, respectively). Only one "B+SHL" line persisted (the rest were lost to phage-mediated extinction), and this line had some resistance to SHL (0.26) and, interestingly, relatively high cross-resistance to FRS (0.6). *In planta*, all lines had either 0 or extremely low proportions of resistance to either phage (all below 0.0002; Fig. 5B).

Benefits of resistance experiment

To determine the relative benefit of phage resistance in both environments, we next measured whether there was an impact of bacterial resistance category (resistant/sensitive) and phage pressure on bacterial growth over time. *In vitro*, we found that the interaction of these factors shaped density over time ($F_{1, 12} = 24.71$, $p = 0.0003$; Fig. 6A). When the time points were analyzed individually, there was an interaction between resistance category and phage presence at both times ($F_{1, 12} = 59.29$ at 24 hours, $F_{1, 6} = 19.99$ at 72 hours, both $p < 0.005$). Phages decreased sensitive bacterial densities at both time points (both $p < 0.005$), and resistant bacterial densities were higher than sensitive bacterial densities in the presence of phage at both time points (both $p < 0.008$).

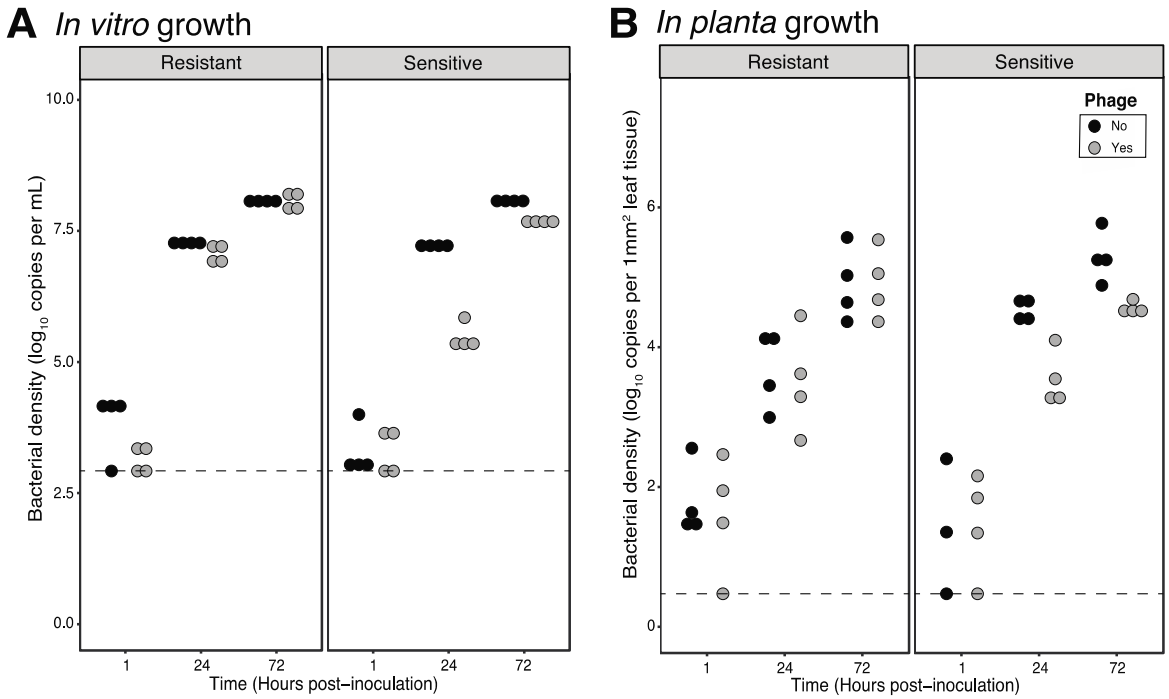

Figure 6. Bacterial densities over time *in vitro* and *in planta* in the context-dependent benefit of resistance experiment.

Bacterial density (in $\log_{10}$ ddPCR copies per mL culture for the *in vitro* samples, and $\log_{10}$ ddPCR copies per 1 mm^2 leaf tissue for the *in planta* samples) is shown over time (hours post-inoculation) *in vitro* (A) and *in planta* (B) for colonies resistant or sensitive to ancestral phage (indicated as different sections of each plot). Bacteria evolved resistance *in vitro*, and were grown (in addition to sensitive colonies) in the presence and absence of ancestral phage in both

environments. The dashed line represents the limit of detection for our assay, and points on this line were at or below this limit. Dot color indicates whether phage was absent (black) or present (gray) in the applied inoculum. Note that the y-axes across panels span different ranges.

In contrast to our *in vitro* results, we did not find an interaction effect of resistance category, phage presence, and time on bacterial densities *in planta* ($F_{1, 8.84} = 0.08$, $p = 0.7812$), but there was a resistance category by phage interaction ($F_{1, 8.84} = 43.50$, $p = 0.0001$) and two observed main effects (phage: $F_{1, 3.41} = 26.00$, $p = 0.0106$; time: $F_{1, 11.68} = 24.21$, $p = 0.0004$; Fig. 6B). There was also an interaction effect of resistance category and phage presence on bacterial density when the data were split by time point, as well as an overall effect of phage at both times (all $p < 0.03$). At both time points, the only significant planned comparison was between sensitive colonies in the absence and presence of phage ($p < 0.007$ for both). This indicates that only sensitive bacterial densities were decreased by phage, and that resistant bacteria did not reach higher densities than sensitive bacteria in either the absence or presence of phage.

Additionally, after 72 hours of growth *in vitro*, initially sensitive clones that were exposed to phage had evolved resistance (average proportion resistant = 0.689). Sensitive clones grown in the absence of phage remained sensitive, and resistant clones remained resistant both in the absence and presence of phage. *In planta*, bacteria that were classified as resistant or sensitive prior to inoculation retained their status post-sampling in both the presence and absence of phage (data not shown but available on Dryad).

Discussion

In light of the growing interest in understanding the role phages play in host-associated microbiomes, it is imperative that we study the impact of phages on bacterial ecology and evolution within their natural environments. There is reason to predict that knowledge gained from laboratory studies will not clearly translate to natural patterns, as *in vitro* studies that aim to incorporate more ecological realism consistently find that increasing complexity critically changes bacteria-phage interactions (Gómez and Buckling 2011; Jończyk et al. 2011; Gómez et al. 2015; De Sordi et al. 2017; Laanto et al. 2017; Wang et al. 2017). We set out to test the impact of phages on evolution of an agriculturally-relevant bacterial pathogen, *P. syringae*, based in part on expanding industry interest in using phages as biocontrol in this system. Using multiple experimental approaches, in which both the MOI and number of phages used were varied, we found that phages did not select for resistance within the tomato leaf despite rapid evolution *in vitro* (Figs. 2, 5B), evidence of phage persistence and replication *in planta* (Fig. 4B), and successful growth of resistant mutants (evolved *in vitro*) within leaves (Fig. 6B). Overall, our results suggest that the benefit of resistance is not great enough to spread within bacterial populations in the apoplast.

No evidence for evolution of phage-selected resistance in planta

In resistance assays from both passaging experiments, we found that the frequency of phage resistance *in planta* was significantly lower (in most cases non-existent) than that *in vitro* (Figs. 2, 5B). In the *in planta* resistance assay of the six-passage experimental lines, where we sought to test for resistance mechanisms that may not be observable on agar plates, bacterial densities from all treatments were significantly reduced by phage at 24 hours, but not at 72 hours post-inoculation (Fig. 3). If phage-passaged bacteria were resistant *in planta*, we would have expected those densities to be less impacted by phage than bacteria passaged without phage. Our

lack of a treatment effect adds support to our conclusion that phage-selected resistance is absent or negligible for our experimentally-evolved bacteria in the apoplast.

In the phage cocktail experiment, the evolution of resistance to phage again occurred rapidly *in vitro*, and we detected no phage-selected resistance in the *in planta* lines (Fig. 5B). This is despite high MOIs that significantly decreased bacterial densities, and the use of two taxonomically distinct phages that led to high levels of resistance *in vitro*. Thus, the evolution of resistance to phages in plant-associated bacteria may be less common than *in vitro* studies of the same bacteria-phage pair would predict. For agricultural phage therapy, this suggests that the evolution of resistance may be a less problematic concern than the relatively low rate of phage replication on bacteria in the apoplast.

While our experiments only allow us to draw conclusions about bacteria-phage interactions post-invasion of the leaf interior, prior work has investigated the epiphytic fitness impacts of *P. syringae* resistance to phages that use pili as receptors (such as ø6). In this system, phage resistance can incur fitness costs via traits specifically relevant to the epiphytic lifestyle (through loss of pili), but bacteria can also become phage resistant without evident costs (e.g. through becoming superpiliated; Romantschuk and Bamford 1986; Romantschuk et al. 1993). However, some evidence suggests that phage-mediated selection pressure is likely greater in the leaf interior. First, UV and desiccation on the leaf surface are expected to decrease bacteria-phage contact rates, while the interior is largely protected from UV and is modified by *P. syringae* to be more aqueous (Iriarte et al. 2007; Xin et al. 2016). Second, previous work found higher levels of, and more locally-adapted, infective *P. syringae* phages within leaves relative to on the leaf surface (Koskella et al. 2011). Our results are relevant to the scenario in which *P. syringae* experiences phage contact after apoplast invasion, or if phages were applied therapeutically on plants already showing disease symptoms.

Interestingly, the few studies that have experimentally evolved bacteria with phages in plant and animal systems have also often found limited or no evidence of resistance evolution (Maura et al. 2012; Meaden and Koskella 2017; De Sordi et al. 2018). Bacteria grown *in vivo* are in a different physiological state from those grown in high nutrient media, and it is possible that these cells may be transiently protected from phage through expression of products that prevent phage access to bacterial cells. The idea of transient phenotypic resistance (in which bacteria remain genotypically sensitive but can reduce phage adsorption rate) has been recently discussed in the literature as a mechanism for continued coexistence of phages and suitable bacterial hosts, and may act as a bet-hedging strategy for phages to replicate without the risk of eliminating all hosts (Bull et al. 2014; Cenens et al. 2015). While bacterial resistance to phage is often assayed *in vitro* for technical reasons, the numerous environmental and physiological differences of eukaryotic-associated bacteria compared to those *in vitro* indicates that these *in vitro* assays are unlikely to recapitulate the relevant interaction conditions and may misrepresent the *in vivo* resistance status.

Decreased levels of phage-mediated bacterial lysis in planta

Our results suggest that the impact of phage on bacterial densities, and consequently selection pressure on bacterial populations, was lower *in planta* than *in vitro*. At week one of the six-passage experiment, experimental lines with phage *in vitro* had significantly lower densities than bacteria only lines, but lines both with and without phage *in planta* often overlap in bacterial densities (Fig. 1). Additionally, in the phage cocktail experiment, all lines inoculated with the phage cocktail and two lines inoculated with SHL had no bacteria after the first passage

in vitro, while bacteria from all experimental lines *in planta* persisted throughout the experiment (Fig. 5A). The limited impact of phage on bacterial densities *in planta* in our experiments led us to question whether phage replication was occurring at detectable levels. Thus, we simultaneously measured bacteria and phage signal over time in an *in planta* resistance assay, and found a modest (but significant) level of phage replication despite a lack of measurable impact on bacterial densities during this time (approximately tripling, Fig. 4B). A previous study using the using the same inoculation concentrations and bacteria-phage pairs as our phage cocktail experiment also found a modest increase (on average, a doubling) in phage DNA copies over time *in planta* (Morella et al. 2018). In order to rule out that ddPCR phage signal may have decayed over time *in planta*, we also measured phage signal over time in plants inoculated with phage only, and found no significant change in signal over 72 hours (Fig. 4B). These results suggest that phages are replicating at much lower rates *in planta* than *in vitro*, often with no measurable impact on bacterial densities (Fig. 4).

One additional explanation for the lack of phage impact on bacterial densities in our passaging experiments *in planta* may be that phage replication only occurs early after inoculation. Our results suggest that phage replication (and impact on bacterial density) is greatest in the first 24 hours while bacteria are also actively replicating (Figs. 3, 4B). By 72 hours post-inoculation, bacterial densities in phage-applied treatments may have had time to rebound and reach comparable densities to phage-free treatments. Leaf heterogeneity may allow for bacteria to reach high densities in spatial refuges free from phage, even if phage actively replicated in certain areas. Further work must be done to determine which environmental factors are responsible for the decreased impact of phage *in planta*, especially if phage treatments can be designed to overcome these barriers to infection in this agriculturally-important environment.

Resistance is beneficial in vitro *but not* in planta

As previous work in this system identified a context-dependent cost of phage resistance for *P. syringae in planta* and *in vitro* (Meaden et al. 2015), we sought to determine whether resistant mutants would be selected for or against in the presence and absence of phage in both environments. We found that both *in planta* and *in vitro*, sensitive bacterial densities are significantly reduced in the presence of phage, while resistant bacteria reach comparable densities in the absence and presence of phage (Fig. 6). Thus, our *in vitro*-selected phage-resistant mutants were effectively resistant in both environments. *In vitro*, resistant mutants reach higher densities than sensitive clones in the presence of phage (Fig. 6A), suggesting that there is a fitness benefit of resistance in this environment. *In planta*, however, both resistant and sensitive colonies reach similar densities in the presence of phage (Fig. 6B). These results suggest that, while there is phage-mediated lysis of bacteria both *in planta* and *in vitro*, phage-resistant mutants only experience a significant fitness benefit in high nutrient laboratory media and not in the apoplast. The frequency of *de novo* resistant mutants that arise in a population of entirely sensitive cells *in planta* would therefore only be expected to change through drift, and would be unlikely to reach high and detectable frequencies.

Conclusions

We have demonstrated that *de novo* evolution of phage resistance in *P. syringae* is context-dependent, with resistance evolving rapidly and reaching high frequencies *in vitro* but not *in planta* due to differences in the benefit of resistance. We have ruled out various alternative hypotheses for the lack of resistance *in planta*, including phage decaying over time, lack of

phage replication, phage-resistant cells dying or reverting to sensitivity within our sampling period, and phage becoming inactive. Instead, it appears that despite standardized inoculation MOI, phage replication and subsequent decreases in bacterial densities *in planta* occur at a lower rate than *in vitro*. Further, the slight benefit of being a phage-resistant cell in the presence of phage *in planta* is likely offset by a slight cost, leading to similar growth of resistant and sensitive cells in this environment. Thus, *de novo* phage-resistant mutants from an initially sensitive population are unlikely to reach high frequencies *in planta*. These results suggest that effectiveness of agricultural phage therapy may be limited more by low phage replication rather than high rates of resistance evolution.

Future work exploring eukaryotic host-associated bacteria-phage interactions and evolution should therefore aim to run experiments in the host of interest when possible, but minimally should attempt to identify the relevant environmental factors that can impact that interaction (e.g. spatial structure, nutrient availability, water content) and incorporate them *in vitro* to uphold applicability in the natural system. However, one factor that can only be incorporated with *in vivo* experiments and is likely to impact bacteria-phage interactions is the eukaryotic host immune system, which may respond to bacterial lysis products or even directly to phage presence (Abramovitch et al. 2006; Hodyra-Stefaniak et al. 2015; Krut and Bekeredjian-Ding 2018). In our case, resistance to phage is often associated with changes in lipopolysaccharide (LPS) (Meaden et al. 2015), and LPS is a known pathogen-associated molecular pattern that induces plant defenses. It is therefore possible that evolving resistance to phage could alter the pathogen's interactions with host defenses.

Our experimental results are an interesting contrast to previously described evidence for phage-mediated selection in natural phyllosphere communities (Koskella 2013; Koskella and Parr 2015). The likely explanation for this difference is that experimental evolution relies on the spread of *de novo* resistance mutations, while natural populations might be more responsive to phage-mediated selection due to standing variation and migration. Overall, our results suggest that strength of phage-mediated selection can vary quite significantly *in vitro* and *in vivo* despite standardized inoculation conditions, leading to drastic differences in the rate of resistance evolution to parasites. This highlights the impact of environmental conditions in shaping host-parasite interactions and the need for research in the environments of interest.

Supplementary Materials

Detailed methods

Six passage experimental co(evolution) in planta *and* in vitro

A single colony of *Pseudomonas syringae* pv. *tomato* PT23 (obtained from Gail Preston, University of Oxford) was randomly selected from a culture spread on a King's B (KB) hard agar plate to begin the evolution experiment. After 24 hours of growth in KB liquid media, the culture was then centrifuged, washed three times, and resuspended in sterile 1 mM $MgCl_2$. Density of the resuspended cells was determined via dilution plating. The Podoviridae lytic phage "FRS" (obtained from OmniLytics Inc.) was co-cultured with PT23 in KB liquid media at 28°C (shaken at 150 rpm, VWR advanced digital shaker), and cell-free lysate was obtained by filtration (0.45 µm; Millipore Sigma) after 24 hours. Concentration of phage stock was obtained by dilution plating on soft agar overlays, with plaques counted after 24 hours of incubation at 28°C.

Initial inoculation of plants and *in vitro* tubes with bacteria and/or phage was done at approximately 4:1 (phage:bacteria) multiplicity of infection (MOI), with a starting bacterial density of $7x10^6$ colony forming units (CFU) per mL and starting phage density of $2.5x10^7$ plaque forming units (PFU) per mL. This MOI was chosen because in our pilot experiments it did not lead to extinction of our static bacterial populations *in vitro* but still provided a relatively high ratio of phage to bacteria (data not shown). Experimental lines included three replicates (lines) of: bacteria without phage ("B only"), phage without bacteria ("P only"), co-passaged bacteria and phage ("Coevolved"), evolving bacteria with ancestral phage ("B evolved"), and evolving phage with ancestral bacteria ("P evolved"). Additionally, there was a negative control magnesium chloride-inoculated plant each week, which was interspersed in the growth chamber with the treatment plants.

Four-to-five week old Moneymaker tomato plants grown from surface-sterilized seeds (70% ethanol for one minute, 33% concentrated commercial bleach diluted in sterile 0.2% Tween 20 solution for 20 minutes, six washes in sterile MilliQ water) were randomly assigned to a treatment, with six randomly chosen leaves inoculated per plant. Inoculation was done by blunt-end syringe injection into the abaxial side of the right half of each leaf (approximately 300 µL). Syringe inoculation directly forces the inoculum into the apoplast, which bypasses the natural infection steps prior to entering the stomata (Katagiri et al. 2002) but allows for far more consistent population densities across replicates. *In vitro* tubes were similarly "inoculated" with 300 µL of prepared inoculum in 10 mL of KB liquid media. Plants and *in vitro* tubes were statically incubated in a single growth chamber set to 24°C, 15h day:9h night light cycle, with darkness beginning right after inoculation (to decrease the amount of phage decay due to UV sensitivity).

After 72 hours, plants were sampled by taking a single hole punch (6 mm diameter) from each of the six inoculated leaves using a flame-sterilized hole puncher, and combining these into 1 mL of 1 mM $MgCl_2$ buffer and two sterile ceramic beads (1/4" spherical). Samples were homogenized in a FastPrep-24 5G (MP Biomedicals) set to 4.0 m./second for 40 seconds. Each tube was sampled by mixing 700 µL of 1 mM $MgCl_2$ and 300 µL of culture from that tube. Dilution series of homogenized plant tissue and *in vitro* samples were plated in duplicate on KB hard agar to obtain bacterial densities (all bacterial incubation on hard agar was done for 48 hours at 28°C). We then spread 100 µL of an appropriate dilution of each sample, as well as ancestral PT23 for "P evolved" lines, on agar plates to obtain 100 single colonies for passaging

(as in Meaden and Koskella 2017). 100 colonies of bacteria were picked from each experimental line using sterile toothpicks and swirled into 1 mL of 1 mM MgCl2. We found that filtration of the homogenized plant tissue did not yield sufficient titers of phage for inoculation (the recovered concentrations would have led to extinction of phage before the end of the experiment), despite evidence of infective phage (plaques) at dilute concentrations of the homogenized tissue used in CFU plating. To estimate the amount of infective phage recovered from our passaged samples, we recorded the last dilution in the series in which we saw visible plaques (for all samples and weeks except for the *in vitro* samples after the first passage; details available on Dryad). After the first passage, we saw plaques in all dilution series of samples that came from plants inoculated with phage, often at 10^{-3} and 10^{-4}. At the end of the experiment, we again saw plaques in all phage-inoculated plant samples (except for one of the "P evolved" lines), with most at 10^{-2} and 10^{-3}. *In vitro*, we saw plaques in only a few samples at the end of the experiment, but we caution interpretation of these results given that there are numerous reasons we would not observe phage in this assay (for example, heterogeneous bacterial populations would not support plaque formation, and bacteria have evolved resistance in many lines).
In order to ensure phage pressure on bacteria would persist throughout the experiment (though we recognize that this method may not reflect natural dynamics of this system) we added an "amplification" step where samples were incubated in media for six hours, to generate phage for subsequent passaging (incubation duration was selected to correspond with previously determined time-to-detectable-increases in FRS titer during co-culture, Morella et al. 2018). To do this, 50 µL of sample from the *in vitro* tubes or plant homogenates was added to 2 mL KB broth and incubated at 28°C, shaken, for 6 hours. These were then filtered using 0.45 µm filters, and plated on soft agar overlays with ancestral PT23 to quantify the amplified PFUs. The filtered samples were then used as the phage portion in subsequent inoculations. Amplified phage filtrate and the 100 mixed colonies were each diluted 1:100 in 1 mM $MgCl_2$ for subsequent passages, and this process was repeated for a total of six passages through plants and tubes. Six passages were done simultaneously and side-by-side in the growth chamber *in vitro* and *in planta*.

Phage resistance assay in planta

We assayed for resistance and potential costs of resistance in plant-passaged lines by growing the "evolved" bacteria in the presence and absence of phage *in planta*. Bacterial clones isolated from the sixth (final) passage were grown in KB liquid media for 24 hours at 28°C and then streaked on an agar plate to separate cells from any possible phage in the cultures. Colonies were re-picked after 48 hours of incubation from the end of each streak and grown in KB liquid media for another 24 hours. Colonies from each line were then mixed, washed, and resuspended in 1 mM $MgCl_2$. A co-culture of ancestral FRS was prepared with ancestral PT23, and filtered after 24 hours to obtain phage for inoculations. Plants were randomly assigned to a treatment and inoculated with suspensions of approx. 96 mixed colonies from each of the lines in the presence or absence of 100:1 MOI ancestral phage (*in planta* evolution lines used: three "B only", two "Coevolved" (one line could not be separated from phage), and three "B evolved"). Starting bacterial density was approximately $8x10^6$ CFU/mL, with $8x10^8$ PFU/mL of phage. This high MOI (100:1) was selected in order to maximize our chance of detecting any subtle resistance mechanisms. There were two control plants – one inoculated with the phage suspension without bacteria and one inoculated with magnesium chloride. Nine leaves were inoculated per plant, with a single hole punch taken from three of the leaves at each time point (0, 24, and 72 hours post-inoculation). Tissue samples were snap-frozen in dry ice and ethanol

until homogenization (using same conditions as previously described, with 1 mL 1 mM $MgCl_2$) and dilution plating for CFUs.

Additional modified in planta *resistance assay using ddPCR*

We performed a second *in planta* resistance assay using modified methods to quantify phage replication in addition to bacterial densities over time. For this assay, we prepared the bacterial clones from passage six from the "B only" and "B evolved" lines (which we hypothesized might be most likely to show evidence of resistance to ancestral phage out of all treatments) using the same methods as the previous section. We inoculated 9 leaves of 4 week old Moneymaker plants with a starting bacterial density of $2.5x10^6$ CFU/mL, and a 100:1 MOI of ancestral FRS phage diluted in 1 mM $MgCl_2$. The bacterial colony mixtures from each line were inoculated onto separate plants in the absence or presence of phage, in addition to three phage-only plants and a single negative control plant inoculated with sterile 1 mM $MgCl_2$. Three hole punches were taken from each of three leaves at three time points (0, 24, and 72 hours post-inoculation), and each leaf's hole punches were snap-frozen in dry ice and ethanol until homogenization.

For bacteria and phage enumeration, we homogenized two randomly chosen leaf samples per plant per time point in 1 mL sterile water and quantified densities using the Bio-Rad QX200™ Droplet Digital™ PCR system. ddPCR has been previously used to simultaneously track *P. syringae* and FRS densities *in planta*, and we have used the same probes and reaction preparation methods for this experiment (reference in main text). Reaction mixtures were prepared with the following: 11 µL Bio-Rad ddPCR™ Supermix for Probes (no dUTP), 1.1 µL *P. syringae* probe, 1.1 µL FRS probe, 6.8 µL molecular grade water, and 2 µL homogenate as template. Samples were randomized on the ddPCR plate, and a no template control (with 2 µL molecular grade water instead of homogenate) was run in the last well of each column. Droplet generation was performed according to manufacturer instructions, and PCR was run with the following conditions: 95°C for 10 minutes, 94°C for 30 seconds, 60°C for 1 minute, 72°C for 1 minute, 40 cycles of steps 2-4, and 98°C for 10 minutes. Droplet fluorescence was quantified on a Bio-Rad QX200™ Droplet Reader. The positive-negative thresholds were set by column, with droplet fluorescence values within the range of the no template control (NTC) well median classified as negative. For all ddPCR results, any NTC signal post-threshold was considered contamination from reaction preparation, and we subtracted the average of the NTCs across a plate from the raw data values. Total target copies within a well is representative of the number of copies in 2 µL of original sample. The averages of the two leaves from each plant per time point were used as the datapoints for analysis.

Costs and benefits of resistance assay in planta and in vitro

To generate resistant and sensitive colonies for growth comparisons *in planta* and *in vitro*, we chose a single colony of ancestral PT23 and grew it in independent liquid cultures in the presence or absence of high titer ancestral FRS (four cultures of each). Cultures were incubated on an orbital shaker at 28°C and streaked on a hard agar plate after 24 hours growth (no phage cultures) or 48 hours (co-cultures with phage, to allow time for resistant colonies to arise). Multiple colonies from each plate (which came from a single tube) were stabbed individually with a sterile toothpick, swirled into liquid KB for 24 hour growth, and streaked across a line of high titer FRS to determine resistance status. Liquid cultures of colonies that were appropriately resistant or sensitive were then streaked on hard agar to separate the bacterial

cultures from phage. A single colony from the end of each of the independent streak plates was then grown in 4 mL KB broth for 24 hours and streaked to confirm that the resistance status had not changed. Overnight cultures were then spun, washed, and resuspended in 2 mL 1 mM $MgCl_2$, and were plated on soft agar mixed with bacteria to verify lack of phage contamination.

Plants and *in vitro* tubes were then inoculated using the same conditions as the "phage cocktail" passaging experiment (same starting densities and MOI), except that resistant and sensitive clones were randomly paired and each clone was inoculated onto three leaves of a shared plant (for a total of six inoculated leaves per plant). A single hole punch was taken from each of the three leaves for each clone after 1, 24, and 72 hours of growth, and tissue was homogenized using the same conditions as previously described. *In vitro* tubes were sampled at the same time points by taking 300 µL of sample and mixing with 700 µL 1 mM $MgCl_2$. Dilution series of all samples were plated in duplicate on KB hard agar, and colony counts were recorded after 48 hours of incubation at 28°C. 72 hour samples were also plated for density of resistant CFUs using the "phage agar" plating method as described above. ddPCR was also performed for all samples in this experiment using the same conditions as previously described, using 2 µL of homogenate as template. A few *in vitro* samples with high densities were diluted 1:10 or 1:100 in sterile water due to positive droplet saturation of the ddPCR system, which precludes quantification of the targets. We focus our interpretation on the ddPCR results in the main text with statistical analysis of CFU results and a correlation between the two methods present in the supplement (Fig. 6, Fig. S2 and S3).

Additional results

Statistical analysis of amplified PFU results

A model testing for a three-way interaction between environment, treatment, and passage number was produced for the log-transformed amplified phage densities. There was no significant three-way interaction ($F_{4, 23.99} = 2.42$, $p = 0.0761$), but there was a significant interaction between environment and passage number ($F_{2, 23.99} = 9.86$, $p = 0.0008$), and there were significant main effects of passage number ($F_{2, 23.99} = 35.71$, $p < 0.0001$) and environment ($F_{1, 12} = 256.68$, $p < 0.0001$). After splitting by environment and testing for a two-way interaction between treatment and passage number, only passage number was significant *in planta* ($F_{1.17, 7.01} = 17.92$, $p = 0.0032$), but both the interaction ($F_{4.65, 13.96} = 5.53$, $p = 0.0057$) and main effect of passage number ($F_{2.33, 13.96} = 33.76$, $p < 0.0001$) were significant *in vitro*.

Resistance to phage, in planta *assay (ddPCR)*

Plants inoculated with bacteria and no phage in this experiment had on average three orders of magnitude lower background signal from the phage probe, which did not significantly change over time ($F_{1.49, 7.46} = 1.37$, $p = 0.2986$).

Bacterial densities over time (CFU) in the costs and benefits of resistance experiment

In the three-way model testing for a resistance category by phage by time interaction for the *in planta* results, there was a significant time by phage interaction ($F_{1, 8.55} = 9.61$, $p = 0.0135$) and main effect of time ($F_{1, 11.52} = 22.70$, $p = 0.0005$). For the models testing a resistance category by phage interaction at each time point, there was only a significant main effect of phage at 24 hours ($F_{1, 6} = 10.45$, $p = 0.0178$) but no other significant terms. *In vitro,* all terms were significant in the three-way model (all $p < 0.003$), all terms were significant in the two-way model at 24 hours (all $p < 0.0007$), but only phage was significant in the 72 hour two-way model

($F_{1,\ 12}$ = 5.38, p = 0.0388). At 24 hours, posthoc analysis revealed a significant difference between sensitive bacteria in the absence and presence of phage ($p < 0.0001$) and between resistant and sensitive bacteria in the presence of phage ($p < 0.0001$).

Correlation between ddPCR and CFU values in the costs and benefits of resistance experiment

To analyze the relationship between the CFU and ddPCR results, we generated a linear model of the correlation between $\log_{10}$ CFU values and their corresponding $\log_{10}$ ddPCR values (Pearson's correlation). We excluded any values at or below the limit of detection for either variable. ddPCR and CFU values were highly correlated (estimated slope = 0.76, r = 0.94, $p <$ 0.0001), and adding presence of phage into the model was not significant (p = 0.134). Notably, the slope lower than one suggests that ddPCR values overestimate the corresponding CFUs in the lower range, and underpredict values in the upper range.

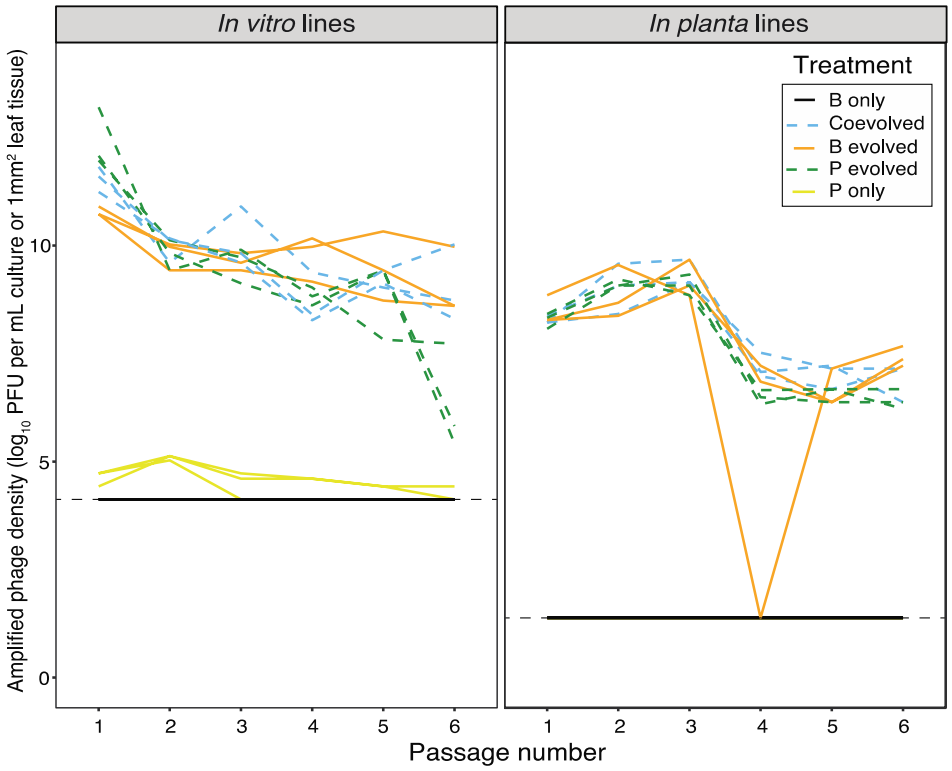

Figure S1. Amplified phage density at each passage *in vitro* and *in planta*.
Amplified phage density (in $\log_{10}$ PFU per mL culture for *in vitro* lines, and $\log_{10}$ PFU per 1 mm^2 leaf tissue for *in planta* lines) after each passage in the six-passage coevolution and one-sided evolution experiment *in vitro* and *in planta*. Individual lines represent the densities for a specific evolution line measured over time. Different evolution treatments ("B only" bacteria were evolved in the absence of phage, "Coevolved" bacteria were co-passaged with phage, "B evolved" bacteria evolved against the ancestral phage, and "P evolved" was ancestral bacteria exposed to evolving phage) are grouped by line type and color as indicated in the legend. The dashed line represents the limit of detection for our assay, and points on this line were at or below this limit.

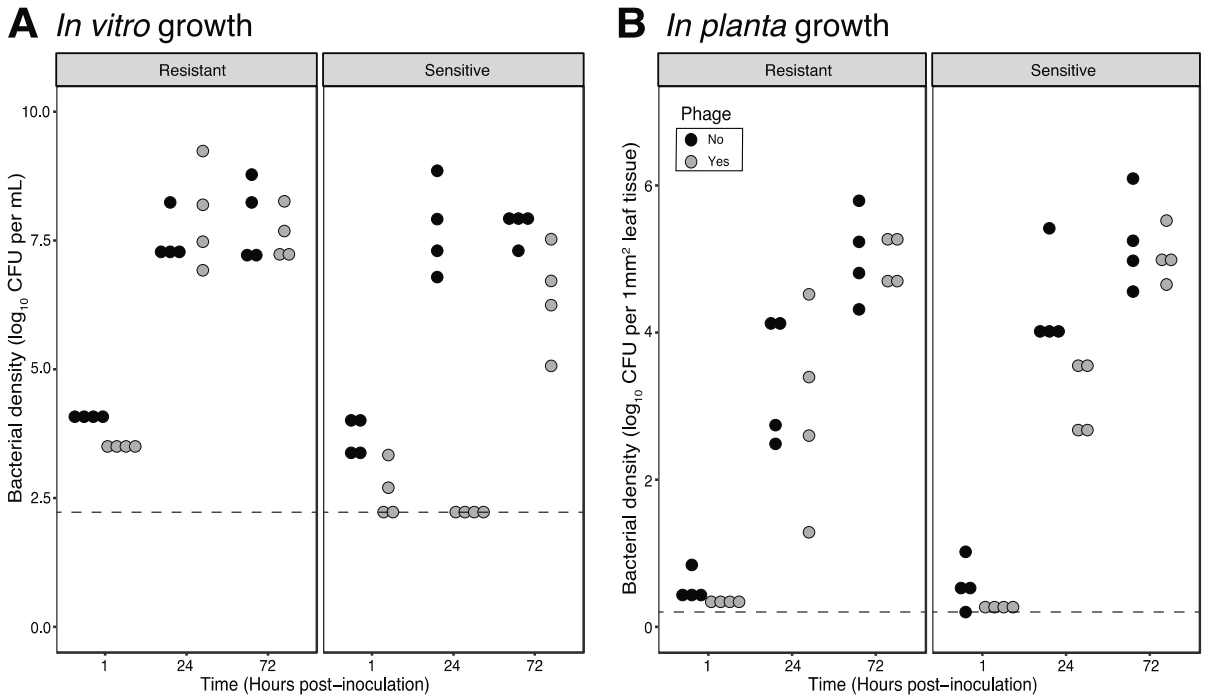

Figure S2. CFU results in the context-dependent benefit of resistance assay.
Bacterial density (in $\log_{10}$ CFU per mL culture for the *in vitro* samples, and $\log_{10}$ CFU per 1 mm^2 leaf tissue for the *in planta* samples) is shown over time (hours post-inoculation) *in vitro* (A) and *in planta* (B) for colonies resistant or sensitive to ancestral phage (indicated as different sections of each plot). Bacteria evolved resistance *in vitro*, and were grown (in addition to sensitive colonies) in the presence and absence of ancestral phage in both environments. The dashed line represents the limit of detection for our assay, and points on this line were at or below this limit. Dot color indicates whether phage was absent (black) or present (gray) in the applied inoculum. Note that the y-axes across panels span different ranges.

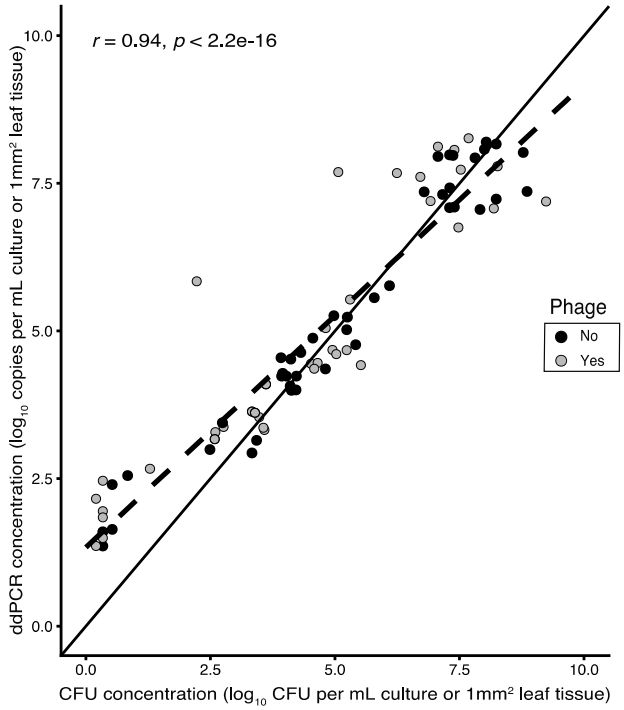

Figure S3. Correlation between CFU and ddPCR results in the context-dependent benefit of resistance assay.

Bacterial CFU (in $\log_{10}$ CFU per mL culture or 1 mm^2 leaf tissue) and ddPCR values (in $\log_{10}$ copies per mL culture or 1 mm^2 leaf tissue) are plotted for resistant and sensitive bacterial clones grown in the absence and presence of phage *in vitro* and *in planta*. The dashed line represents the correlation between CFU and ddPCR values for samples above the limit of detection. The solid black line indicates a theoretical perfect correlation between the values, with an intercept of 0 and slope of 1. The *r* and *p*-value were calculated using a Pearson correlation. Points are shaded according to whether there was phage absent (black) or present (gray) in the sample.

Transition

With this work, I have demonstrated that the dynamics of phage resistance evolution differ between laboratory and ecologically-relevant conditions. As hypothesized, the pace of (co)evolutionary change was certainly slower within plant leaves, but the difference was even greater than I had initially expected. I found that there appeared to be no fitness benefit of phage resistance even in the presence of phage *in planta*, due to low phage replication rates and a slight cost of resistance. This led to the hypothesis that the formation of bacterial biofilms in the apoplast could be one factor limiting bacteria-phage contact rates, which if true would result in low phage replication and low phage-mediated selection. I also hypothesized that bacteria-phage contact rates might be different on the leaf surface compared to the apoplast, which could be tested by inoculating plants using a different method. In this chapter (Chapter 2), I inoculated four-to-five week old tomato leaves using the syringe infiltration method, which bypasses the initial stage of pathogen growth on the leaf surface. Therefore, in my next chapter, I sought to determine whether applying bacteria with phage directly on the leaf surface would lead to increased phage replication rates. In addition, I hoped to develop a higher-throughput method for studying plant-bacteria-phage interactions in this system. This led me to trial a seedling-based method in my next chapter.

Chapter 3. Bacteriophage-mediated reduction of bacterial speck on tomato seedlings

This work has been reproduced from the following, with permission from the Graduate Division and all coauthors:
Hernandez, C.A., Salazar, A.J. and Koskella, B., 2020. Bacteriophage-Mediated Reduction of Bacterial Speck on Tomato Seedlings. PHAGE, 1(4): 205-212.

Introduction

Agricultural yields are threatened by declining soil health, climate change, insect pests, and microbial pathogens (Funk and Brown 2009; Gornall et al. 2010; Lal 2015; Deutsch et al. 2018; Savary et al. 2019). Although global yield of major crops has increased for decades, the current rate of increase is predicted to be insufficient to meet nutritional needs by 2050 (Tilman et al. 2011; Ray et al. 2013). Bacterial pathogens can impact yield through both destructive epidemics and more subtle losses like fruit quality reduction (Coates and Johnson 1997; Gottwald et al. 2002; Hopkins and Purcell 2002; Bassanezi et al. 2009; Haapalainen 2014). Current control methods include breeding for genetic resistance, chemical application, antibiotics, and modifications of growing practices to reduce transmission (Sundin et al. 2016). However, the rise of antimicrobial resistance has increasingly challenged the effectiveness of many management strategies. Bacteria have evolved resistance to both chemical treatments and antibiotics, and have evolved counteradaptations that allow them to overcome host genetic resistance (Kearney et al. 1988; Cooksey 1994; Sundin and Wang 2018).

The *Pseudomonas syringae* species complex has been a particularly difficult management challenge and was responsible for several recent disease outbreaks, notably including kiwifruit bacterial canker (Everett et al. 2011; Lamichhane et al. 2014, 2015). The species complex as a whole infects a wide range of agriculturally-important hosts, and the host range of individual strains varies from specialized to generalized (Morris et al. 2019). The pathovar *P. syringae* pv. *tomato* infects tomato (*Solanum lycopersicum*) and causes bacterial speck disease, which produces lesions on leaf and fruit surfaces (Goode and Sasser 1980). Infection by this pathogen can reduce yield by impacting host photosynthetic ability and fruit quality (Goode and Sasser 1980; Ishiga et al. 2009). *P. syringae* can transmit vertically via seeds, horizontally through water droplets to nearby plants, and even long-distance through aerosolization, making it difficult to completely prevent infection (McCarter et al. 1983; Morris et al. 2008). Disease control strategies have included breeding for genetic resistance and long-term application of copper compounds, both of which have suffered from reduced efficacy due to pathogen evolution (Pitblado and Kerr 1979; Pitblado and MacNeill 1983; Bender and Cooksey 1986; Cooksey 1987; Jacobsen 1997; Pedley and Martin 2003; Kunkeaw et al. 2010; Lamichhane et al. 2015). More recently, growers and researchers have turned to exploring biocontrol methods such as bacteriophage (phage) therapy as an option for *P. syringae* management (Buttimer et al. 2017; Omnilytics, Inc. 2018).

Lytic phages have been underexplored for treating plant diseases, but interest has been reinvigorated with recent successes in clinical phage therapy and the spread of antibiotic resistance (Buttimer et al. 2017; Gordillo Altamirano and Barr 2019). To infect a cell, phages first bind to a receptor on the cell surface, inject their genomic material, use host resources to synthesize proteins and new copies of their genome, and ultimately burst the cell to release viral particles. Phages are a promising treatment due to their ability to replicate, coevolve with

bacteria, and their limited impact on the resident microbial community (due to their narrow host ranges; Loc-Carrillo and Abedon 2011). However, their narrow host ranges also make it challenging to rapidly characterize phages that infect novel outbreak-causing bacterial strains (Nilsson 2014). Additionally, *in vivo* effectiveness of phage therapy candidates has often been unpredictable from results *in vitro* (Balogh 2006; Balogh et al. 2018; Hernandez and Koskella 2019), but *in vivo* trials can be time-consuming and resource intensive (Sabouri et al. 2017). Success of agricultural phage therapy trials has been mixed, with some understanding of the environmental factors that can impact phage persistence (such as UV, temperature, and desiccation) and effective methods for reducing phage decay (using protective formulations and evening applications), but with little mechanistic understanding of the variation across studies and systems (Iriarte et al. 2007; Frampton et al. 2012; Jones et al. 2012).

We sought to develop a seedling-based method for measuring phage-mediated reduction of bacterial speck disease on tomato. We performed three trials where we assessed the effectiveness of phage pre-treatment at reducing disease symptoms and endpoint bacterial densities. One of the two tested phages successfully replicated in all trials, and reduced disease symptoms and pathogen density in two of three trials. This method is rapid (can identify effective phages in under two weeks) and space-efficient (each seedling requires the space of a single conical tube), allowing researchers to identify suitable candidate phages *in vivo* using minimal time and resources.

Materials and Methods

Seed sterilization and germination

Tomato seeds (*Solanum lycopersicum* cultivar Moneymaker) were sterilized in 70% ethanol for 1 minute, followed by a 20 minute soak in sterilization solution (1 part 8.25% bleach, 3 parts 0.2% Tween 20 in water). Seeds were then washed in an excess of autoclaved MilliQ water, and placed in loosely capped sterile 15 ml tubes with 7 mL water agar (one seed per tube). Tube racks were covered in aluminum foil and placed in a 21°C chamber and checked daily for signs of germination. Post-shoot emergence, tubes were moved to a 28°C chamber with a 15 hour day:9 hour night cycle.

Bacteria and phage preparation

Bacterial cultures were grown from a freezer stock of *P. syringae* pv. *tomato* DC3000 that originated from a single colony. Cultures were shaken in King's B (KB) liquid media at 28°C until stationary phase. Cells were then pelleted and washed in sterile 10 mM $MgCl_2$ to remove culture media. Bacterial suspensions were then adjusted to the desired optical density (OD600 of 0.0002 in the first trial, and 0.002 in the others) with 0.015% filter sterile Silwet.

Two phages were used for this study, *Podoviridae* phage FRS (hereafter P1) and *Myoviridae* phage SHL (hereafter P2), both of which were isolated from water by OmniLytics, Inc. (USA) as candidate biocontrol agents and were characterized using microscopy and whole genome sequencing by the Koskella lab. In the first trial, phages were prepared using a "webby plate" of each phage stock on a lawn of DC3000. Phages were recovered by swirling 10 mM $MgCl_2$ on each plate. The recovered volume was filtered (0.45 μm) and quantified by dilution series on double agar overlay plates to determine plaque forming units (PFU). This method yielded low concentration phage stocks that contained visible amounts of plating media (yellow color). Therefore, in subsequent trials, phages were prepared by co-culturing with DC3000 in liquid KB. Co-cultures were shaken overnight at 28°C, filtered, and quantified by PFU. Lysates

were then diluted in a large volume of 10 mM $MgCl_2$ to the desired concentration for seedling inoculations. In the third trial, we included an "inactivated" phage treatment as an additional control. A lysate of P1 was autoclaved for 30 minutes at 121°C with 15 psi pressure, which completely eliminated infectious phage particles (as determined by PFU), and this solution was used as the inactivated phage treatment.

Throughout the text and figures, we use the following abbreviations for treatment names: DC3000 only is "B only", DC3000 with FRS phage is "B+P1", DC3000 with SHL phage is "B+P2", DC3000 with autoclaved FRS phage is "B+inactivated P1", FRS phage only is "P1 only", SHL phage only is "P2 only", autoclaved FRS phage only is "Inactivated P1 only", and the magnesium chloride control is "$MgCl_2$ control".

Inoculation and seedling incubation

In each trial there were two inoculation rounds, with all steps performed aseptically. First, either active phage, inactivated phage, or 10 mM $MgCl_2$ was added to each seedling (depending on the randomly assigned treatment). Seven to twelve-day-old seedlings were flooded with 7 mL of the appropriate solution and placed on an orbital shaker at room temperature for 4 minutes. We then removed the solution and dried each tube in a biosafety cabinet. In the next round of inoculations, 7 mL of either the prepared bacterial suspension or 10 mM $MgCl_2$ was added to each tube as appropriate for the treatment. Tubes were shaken for 4 minutes before liquid removal and drying. This inoculation method minimizes the possibility of bacteria-phage interactions occurring in residual liquid on the tube walls or water agar surface. Seedlings were then placed in a 28°C chamber with a 15 hour day:9 hour night cycle. Disease symptoms were scored blindly and approximately daily, following the protocol of Morella et al. (Morella et al. 2019). Trials differed in their tested treatments and applied bacteria and phage densities (Table 1).

Table 1. Treatment and inoculation details for each trial.

Trial number	Seedling age	Treatments (n)	Bacterial density (OD600[d])	Applied MOI[e] (phage:bacteria)
1	12 days	$MgCl_2$ control(3), P1[a] only (3), P2[b] only (3), B[c] only (8), B+P1 (8), B+P2 (8)	0.002	0.015:1
2	7 days	$MgCl_2$ control (3), P1 only (6), B only (6), B+P1 (6)	0.0002	8.15:1
3	11 days	$MgCl_2$ control (3), P1 only (7), Inactivated P1 only (7), B only (7), B+P1 (7), B+inactivated P1 (7)	0.0002	455:1

[a]Phage 1 (FRS); [b]Phage 2 (SHL); [c]Bacteria (*P. syringae* pv. *tomato* DC3000);[d]Optical density at 600 nm; [e]Multiplicity of infection

Endpoint bacteria and phage quantification

At the endpoint of each trial, each whole seedling was individually weighed and homogenized in 10 mM $MgCl_2$ with two sterile ceramic beads in a FastPrep-24™ 5G (MP Biomedicals, CA, USA) set to 4 m/sec for 60 seconds. We quantified bacterial densities by dilution plating and counted colony forming units (CFU) after 48 hours of incubation at 28°C. Additionally, we quantified bacteria and P1 densities using droplet digital™ PCR (ddPCR; Bio-Rad, CA, USA), a DNA-based quantification technique. For each reaction, we used 3 µl of 1:10 homogenate diluted in water as template, and included fluorescent probes specific to Pseudomonads and phage P1 (as in Morella et al. 2018, and using the same setup and reaction conditions). After the third trial, we performed a small-scale phage resistance assay by isolating 8 colonies from five of the replicate B+P1 samples, and 4 colonies from the sixth. We streaked overnight cultures of each colony across a high titer line of P1 on a hard agar plate (cross-streak method), and incubated for 48 hours at 28°C. Colonies that could grow over the phage line were recorded as resistant, and those that could not were recorded as sensitive.

Statistics and figures

Figure 1 is an overview of our experimental methods and was made using BioRender. Generation of plots for all other figures and statistical analysis was done in R version 3.6.2 using packages lme4, emmeans, PMCMR, and dunn.test (Bates et al. 2015; Dinno 2017; R Core Team 2017; Pohlert 2018; Lenth 2020). Figure panels were compiled in Adobe Illustrator. The effect of treatment on disease progression over time in each trial was analyzed as a mixed model testing for a treatment by day interaction, with a random effect for each seedling. We then tested for the effect of treatment on the area under disease progress curve (AUDPC), endpoint bacterial densities (CFU and ddPCR), and endpoint phage densities in each trial separately using either linear models or Kruskal-Wallis tests (for models with poor fit, as determined by visual inspection of residuals). A linear model of the relationship between CFU and ddPCR copies per milligram seedling was generated for all bacteria-inoculated samples, while controlling for the effects of treatment and trial. Similarly, we quantified the relationship between endpoint bacteria and phage densities in a single treatment of interest (B+P1) using a linear model controlling for the effect of trial. Posthoc analysis for linear models was done comparing estimated marginal means, with a Tukey adjustment for multiple testing. For the non-parametric Kruskal-Wallis tests, posthoc analysis was done using Dunn's tests with a Bonferroni correction for multiple testing of planned comparisons. An alpha level of 0.05 was used in all statistical tests. All data files are available in the Dryad data repository (DOI: 10.6078/D15T4M).

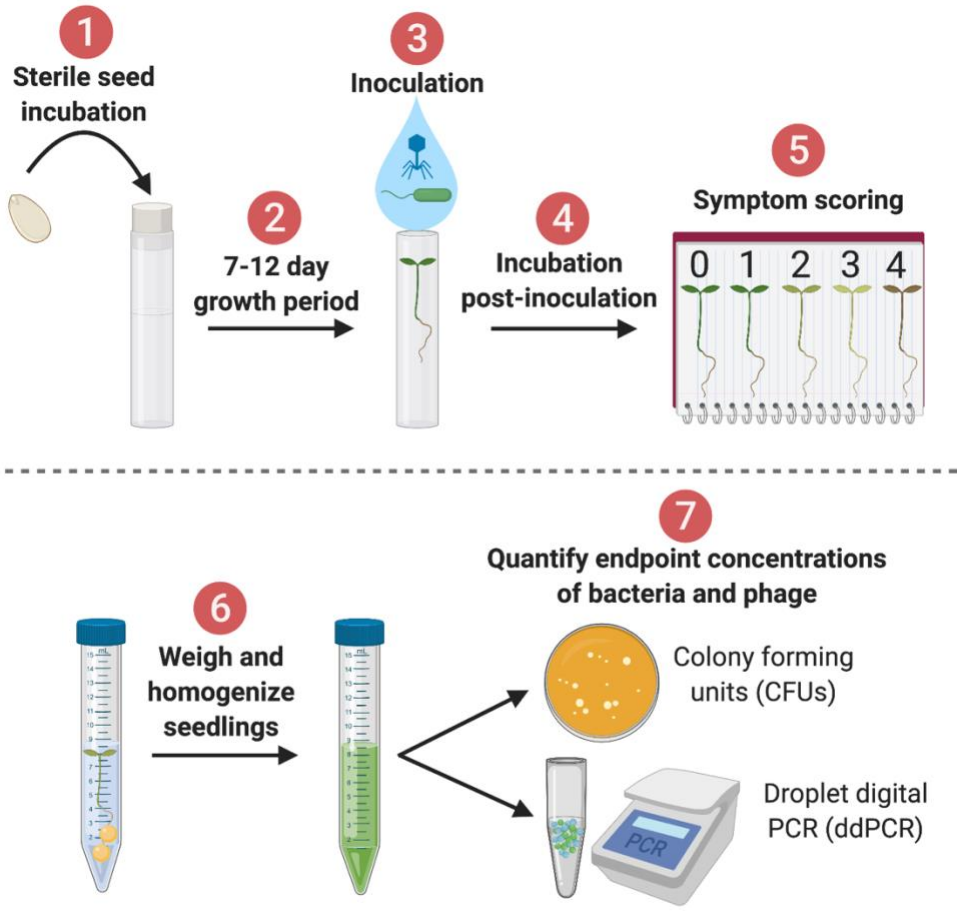

Figure 1. Diagram of seedling inoculation and sampling methods, created with BioRender.com. Note that representative images of seedling symptoms associated with each disease score can be found in Morella et al. 2019.

Results

Phage-mediated reduction of disease symptoms

In all trials, the effect of inoculum treatment on disease score depended on day post-inoculation (trial 1: $F(20, 102.36)=6.47$, $p<0.001$; trial 2: $F(12, 68)=2.04$, $p=0.0338$; trial 3: $F(30, 192)=8.07$, $p<0.001$; Figure 2A). In the first trial, no treatments differed in their starting disease scores (all $p>0.98$), but all bacteria-inoculated treatments had higher final disease scores than those inoculated without bacteria (all $p<0.005$). Phage treatment did not reduce disease symptoms on the final day (B+P1 and B+P2 each compared to B only, $p>0.8133$), but on the second to last day B+P1 disease scores were significantly lower than B only ($p=0.0209$). With this preliminary result, we chose to move forward testing only P1 at a higher dose in subsequent experiments. In trials 2 and 3, phage P1 significantly reduced final disease symptoms compared to bacteria inoculated without phage (in both trials $p<0.001$). Additionally, B+P1 symptoms were not significantly different from controls (magnesium chloride and phage only) in both trials ($p>0.74$). Autoclaved phage did not significantly reduce final disease symptoms compared to bacteria alone ($p=0.99$).

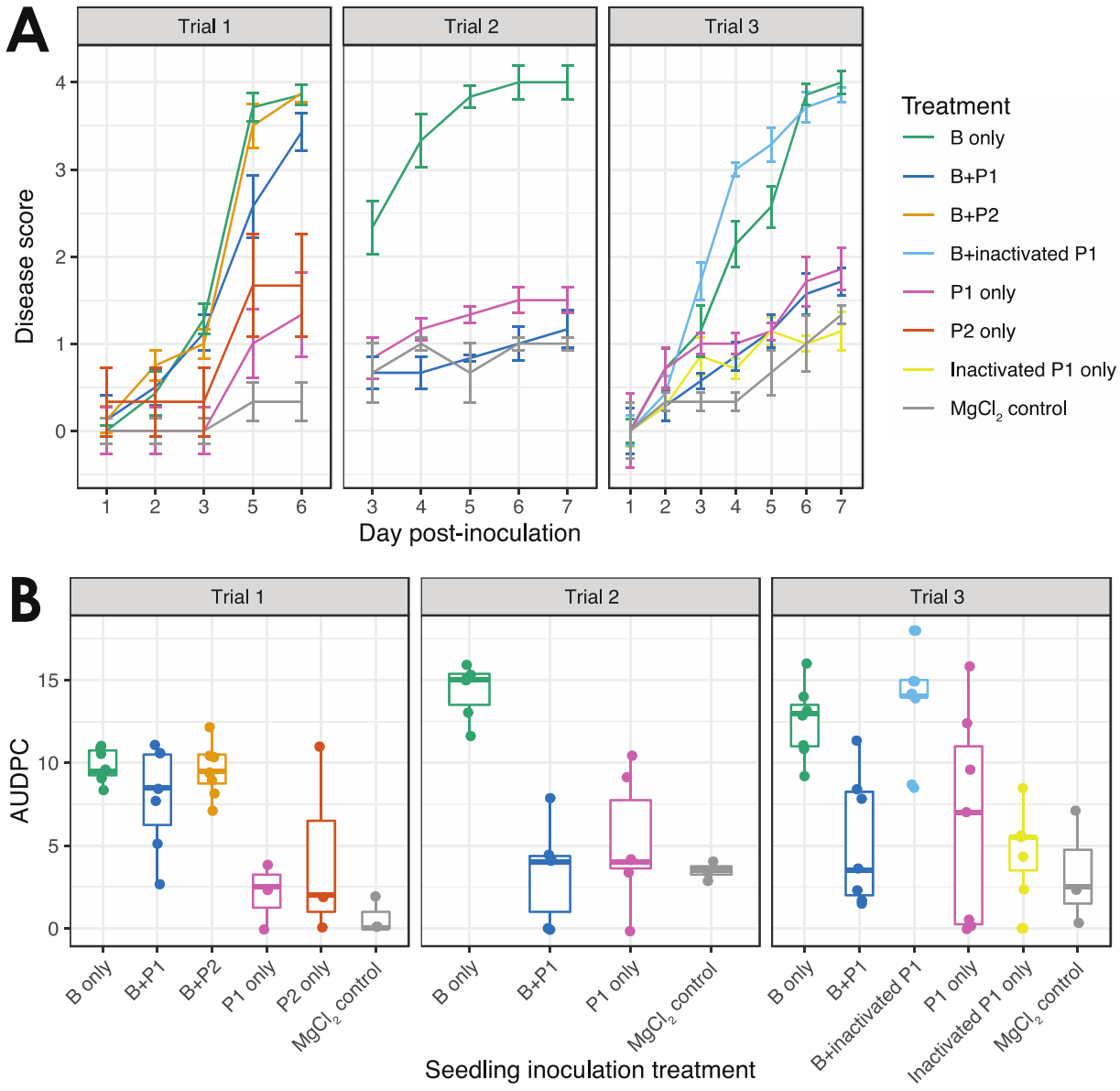

Figure 2. Disease progression curves and area under the disease progress curve (AUDPC) in all trials. Treatment abbreviations are as follows: DC3000 only is "B only", DC3000 with phage FRS is "B+P1", DC3000 with phage SHL is "B+P2", DC3000 with autoclaved phage FRS is "B+inactivated P1", phage FRS only is "P1 only", phage SHL only is "P2 only", autoclaved phage FRS only is "Inactivated P1 only", and the magnesium chloride control is "$MgCl_2$ control". (A) Seedling disease scores by day post-inoculation for the tested treatments in each trial. The line represents the mean score for the treatment, and error bars are ± 1 SE, corrected for the within-subjects design. (B) Boxplots of AUDPC values for each treatment in each trial. The horizontal line within the box displays the median value, the box displays the interquartile range, and the whiskers represent ± 1.5 times the interquartile range. Points outside the whiskers are possible outliers.

Analysis of the AUDPC results suggested the same qualitative findings as the mixed model analysis of disease scores over time (Figure 2B). In all trials and comparing across all treatments (including controls), treatment significantly impacted AUDPC (trial 1: $F(5, 25)=9.91$, $p<0.001$; trial 2: $H(3)=12.94$, $p=0.0048$; trial 3: $F(5, 32)=7.84$, $p<0.001$). In trial 1, neither phage P1 nor P2 had an impact on disease symptoms compared to bacteria only (P1: $p=0.7205$; P2: $p=0.99$), but disease scores were reduced by phage P1 in trials 2 and 3 (trial 2: $p=0.016$; trial 3: $p=0.0211$). Autoclaved phage did not reduce AUDPC ($p=0.97$).

Active phages replicate on seedlings and reduce bacterial densities

We analyzed endpoint densities in two ways, first using droplet digital™ PCR (ddPCR) to quantify the absolute number of DNA copies that match our bacteria and phage probes, and then quantifying colony forming units (CFUs) of bacteria. For ddPCR results, we included all samples in the initial test of a treatment effect on endpoint bacteria and phage densities (Figure 3A). Treatment significantly impacted densities of bacteria and phage in all trials (all $p<0.002$). Compared to bacteria-inoculated seedlings without phage, phage P1 reduced bacterial densities in trials 2 and 3 (trial 2: $p=0.0039$; trial 3: $p=0.015$), but autoclaved phage had no effect ($p=1.00$). We tested whether phage replication occurred by comparing P1 densities in B+P1 and P1 only treatments, and found that B+P1 phage densities were significantly higher in all trials (trial 1: $p=0.0167$; trial 2: $p=0.0050$; trial 3: $p=0.0014$). We then hypothesized that samples with the highest phage densities may have the lowest bacterial densities, which we tested using densities from the B+P1 treatment across all trials. Interestingly, we instead observed a significant positive correlation between endpoint bacteria and phage densities ($b=0.64$, $t(16)=5.37$, $p<0.001$; Figure 3C), suggesting that phage replication may be limited by bacterial density.

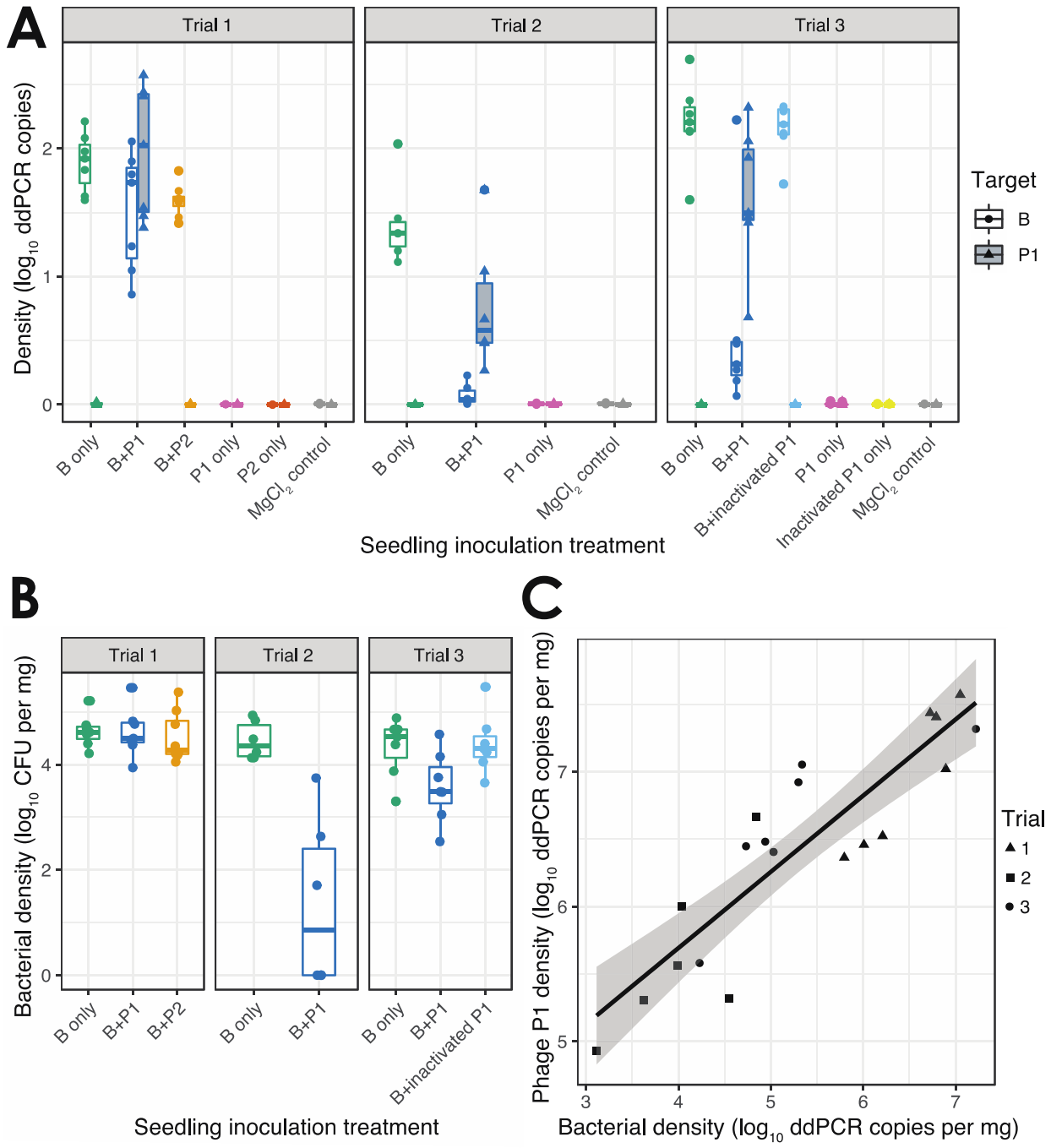

Figure 3. Endpoint bacteria and phage densities quantified by colony forming units (CFUs) and target DNA copies (by droplet digital PCR, ddPCR). Treatment abbreviations are as follows: DC3000 only is "B only", DC3000 with phage FRS is "B+P1", DC3000 with phage SHL is "B+P2", DC3000 with autoclaved phage FRS is "B+inactivated P1", phage FRS only is "P1 only", SHL phage only is "P2 only", autoclaved phage FRS only is "Inactivated P1 only", and the magnesium chloride control is "$MgCl_2$ control". (A) Copies per µL of DNA target (either bacteria or phage) in the ddPCR reactions, normalized by weight of each seedling and $\log_{10}$

transformed. The left box in each treatment (circular points, white box) represents the bacterial density ("B"), and the right box (triangular points, gray shaded box) represents the phage P1 density ("P1"). Note that the bacteria and phage P1 probes were used for all samples, and phage P2 was not quantified using ddPCR. Also note that to avoid artificially inflating low value samples near the limit of detection, the y-axis in panel A differs from that of panel C (which is presenting a subset of relatively high concentration samples). The horizontal line within the box displays the median value, the box displays the interquartile range, and the whiskers represent ± 1.5 times the interquartile range. Points outside the whiskers are possible outliers. (B) Bacterial density (in $\log_{10}$ CFU per milligram seedling) for treatments that had been inoculated with bacteria in each trial. (C) Correlation between bacterial density (in $\log_{10}$ ddPCR copies per milligram seedling) and phage P1 density (also in $\log_{10}$ ddPCR copies per milligram seedling) in each trial, exclusively for samples that had been inoculated with B and P1. The solid black line represents the correlation of AUDPC and density across all samples, and the gray shaded region represents ± 1 SE. Point shape corresponds to trial number.

CFU results led to similar qualitative conclusions and were positively correlated with ddPCR data (b=0.22, t(46)=2.33, p=0.0241; Figure S1). In the case of CFUs, statistical analysis only included treatments inoculated with bacteria (both in the presence and absence of phage), as all others were zero except for a single contaminated sample. In trial 1 there was no effect of phage on bacterial densities (F(2, 19)=0.16, p=0.8563), as observed above, but phage P1 reduced bacterial densities in trial 2 (F(1, 10)=21.33, p=0.0010; Figure 3B). In trial 3, there was an overall main effect of treatment on bacterial densities (F(2, 18)=4.02, p=0.0361). B+P1 bacterial densities were lower than that of B+autoclaved P1 (p=0.0497), but were not significantly lower than B only samples (although marginally significant, p=0.0755).

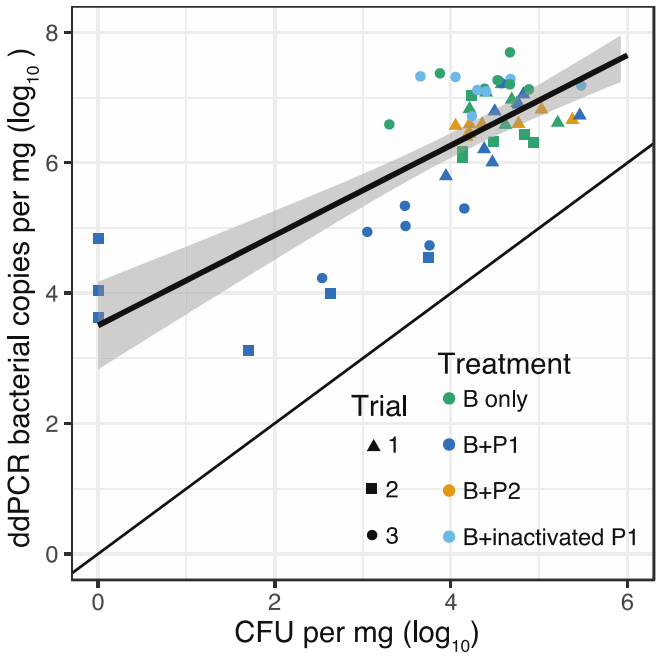

Figure S1. Correlation between bacterial quantification methods. The thick black line in the gray shaded area represents the correlation of bacterial density in colony forming units (CFU)

per milligram seedling and ddPCR bacterial copies per milligram seedling for samples that had been inoculated with bacteria. The gray shaded region represents ± 1 SE. Treatment abbreviations are as follows: DC3000 only is "B only", DC3000 with phage FRS is "B+P1", DC3000 with phage SHL is "B+P2", and DC3000 with autoclaved phage FRS is "B+inactivated P1". The thinner black line that crosses at the origin shows a hypothetical 1:1 correlation between the values. Point color corresponds to sample treatment, and point shape corresponds to trial number.

At the end of trial 3, we streaked colonies from the B+P1 populations to determine whether any colonies were phage resistant. None of the isolated colonies (total n=44) were resistant, in line with previous observations from adult plants (Hernandez and Koskella 2019).

Discussion

In this work, we tested a seedling-based method for screening phage-mediated reduction of disease symptoms and bacterial densities *in vivo*. In two of three trials, prophylactic application of a *P. syringae* phage reduced disease symptoms and endpoint bacterial densities. Phages replicated in all trials and final phage density positively correlated with bacterial density. We propose that this method could be used to screen for biocontrol candidates prior to large scale trials in agricultural settings.

Although we did not explicitly test the impact of applied MOI within a single trial, the different outcomes across trials offer some suggestion that dosing is important. Phage P1 replicated in all trials, but only reduced disease progression and pathogen densities in trials 2 and 3. In the first trial, we inoculated seedlings with a higher dose of bacteria and lower MOI than in the other two trials. The second and third trials were done with the same starting bacterial densities, but trial 3 had a much higher applied MOI (455:1 compared to ~8:1). Interestingly, we expected that this higher MOI would lead to greater bacterial reduction, but we instead found the opposite. Phages reduced bacterial densities in both trials, but in trial 2 there were some seedlings in which we recovered no live bacterial cells, which we did not observe in trial 3. One possible explanation is that the high concentration of phage in trial 3 could have resulted in some non-productive adsorption events (as in the phenomenon "lysis from without"), in which binding of multiple phages leads to cellular bursting without productive replication and with loss of adsorbed phages (Delbrück 1940; Abedon 2011). It is also possible that the high MOI imposed strong selection for phage resistance, but results from our streaking assays suggest that if any resistant mutants did evolve, they did not reach a high frequency. Optimal dosing for phage therapy is a non-trivial challenge, and the results from our third trial suggest that more phage is not necessarily better for this pathosystem.

Despite the active phage replication observed in the first trial, endpoint bacterial densities were not different from seedlings that had been inoculated with bacteria alone. This is not unexpected given that we sampled for bacterial density at a single time point. It is possible that phage replication and bacterial lysis occurred early after inoculation, and bacterial densities had sufficient time to rebound and reach carrying capacity in the seedlings. This pathogen first grows as an epiphyte on the leaf surface, and then grows in the internal spaces of leaves causing disease symptoms (Xin and He 2013). During the internal phase, *P. syringae* forms biofilms which may be limiting bacteria-phage contact rates (Ude et al. 2006; Hosseinidoust et al. 2013; Vidakovic et al. 2018). If true, phage replication may be occurring largely in the initial stages of growth on the leaf surface. Additionally, it is possible that *P. syringae* evolved resistance to the phage as we did not assay for resistance at the end of this first trial. However, the MOI (and essentially

strength of selection for resistance) in the first trial was orders of magnitude lower than in trial 3, in which we did not identify resistant colonies. Prior work in this system also found that rates of phage resistance evolution were extremely low during experimental evolution *in vivo* (Hernandez and Koskella 2019). Nevertheless, both limited internal replication and resistance evolution could be occurring in this system, and future work could test this by combining time series sampling for bacteria and phage densities with assays for phage resistance.

By quantifying both disease scores and bacterial density, we also investigated whether virulence (defined as severity of disease) had any qualitative relationship with endpoint pathogen density. The two trials where phages reduced pathogen density also had reduced AUDPC values compared to "B only" seedlings, which suggests that disease scores alone could be used to identify effective phages. This would eliminate the need for endpoint sampling, and further reduce the resources needed to screen for phage therapy candidates (although the relationship between disease progression and pathogen density should first be experimentally tested in any system of interest).

This is a resource-efficient screening method for testing phage therapy candidates *in vivo*. Greenhouse and incubator space can limit the number of replicates in plant experiments, particularly when working with older plants. Using this highly controlled method, each replicate requires the incubation space of a single 15 ml conical tube, and phage effectiveness can be determined in under two weeks. This method also minimizes the likelihood of bacteria-phage interactions occurring on off-target surfaces such as the water agar surface (which is more likely in studies using water agar plates). Importantly, however, field and greenhouse trials of phage effectiveness are critical components of effective therapy development. Age-related changes in plant immunity and phyllosphere tissue structures can impact bacteria-phage interactions, and seedling-based methods should act in concert with, but not replace, more agriculturally-relevant studies (Panter and Jones 2002). We propose a model in which researchers first screen for possible phage therapy candidates on seedlings, and then test the impact of phage treatment on improving crop yield in greenhouse and field trials.

Transition

Using this seedling-based method, I found that when both bacteria and phage were inoculated via flooding, phages reached densities that were about one to two orders of magnitude higher than their densities in the absence of bacteria. This is in contrast to my prior chapter, in which I observed that there was not even an order of magnitude difference between these same treatments when the organisms were syringe-infiltrated into the leaf apoplast. While not a direct test, this does suggest that the inoculation method (and plant age) can lead to different phage replication rates. In my final chapter, I follow this work by testing how biofilm formation might play a role in this difference. The bacterial biofilm matrix is composed of extracellular polymeric substances that can impact diffusion, and phages rely on diffusion (or bacterial movement) to come into contact with hosts. I hypothesized that *P. syringae* exopolysaccharide formation might be limiting phage replication, which I tested by studying the impacts of phage application on biofilm biomass *in vitro*, the evolutionary responses of bacteria to combined biofilm and phage selection pressures, and finally the relationship between phage resistance, biofilm formation, and virulence in the evolved mutants.

Chapter 4. Experimental manipulation and evolution of biofilm formation demonstrates its role in *Pseudomonas syringae*-phage interactions

Introduction

Bacteria can grow as part of surface-attached structures called biofilms, which are composed of microbial cells and extracellular polymeric substances (EPS; Flemming and Wingender 2010). Biofilm formation proceeds after freely suspended planktonic cells attach to a surface (or other cells) and begin to produce various polysaccharides and other biopolymers that form a hydrated extracellular matrix (Jones et al. 1969; Christensen 1989; Whitchurch et al. 2002). The transition between planktonic and biofilm growth is accompanied by changes in gene expression and cellular physiology (Prigent-Combaret et al. 1999; Becker et al. 2001; Resch et al. 2006; Park et al. 2014). Biofilm formation occurs as a sort of developmental process that starts with reversible attachment to the surface and is followed by irreversible attachment, maturation, and finally dispersal (Sauer et al. 2002; Kierek-Pearson and Karatan 2005). Both abiotic and biotic surfaces can support biofilm formation, and many pathogens form biofilms as an important virulence strategy (Hall-Stoodley and Stoodley 2005; Danhorn and Fuqua 2007; Feazel et al. 2009; Percival et al. 2015). This poses a challenge for infectious disease treatment, as biofilm-associated cells are generally more protected from environmental stressors (such as antibiotics) and removal processes (due to both the physical barrier of the biofilm and changes in cell physiology; Characklis 1973; Lewis 2001; Coenye et al. 2007). One possible mechanism for biofilm removal involves the use of bacteriophages (phages; viruses that infect bacteria), but our understanding of biofilm-phage interactions is still limited.

Biofilm-phage interactions can have a diverse range of outcomes, ranging from biofilm reduction or elimination to an increase in biofilm biomass (Sutherland et al. 2004; Hosseinidoust et al. 2013). Compared to antibiotics, the ability of phages to replicate and concentrate locally may make them more efficient at removing biofilm-associated bacteria (Abedon 2015). In addition, some phages have enzymes that specifically break down EPSs (EPS depolymerases) or bacterial cell walls (endolysins) that can cause biofilm degradation (Hughes et al. 1998; Gutiérrez et al. 2014; Chan and Abedon 2015). However, since phages rely on diffusion to contact their hosts, the physical structure of the biofilm may also act as a barrier that reduces bacteria-phage contact rates (Doolittle et al. 1996; Hu et al. 2010; González et al. 2018). Specific biofilm components can also be responsible for blocking phage infection. For example, in one study of *Escherichia coli* biofilms and T7 phage, protection from phage was due specifically to the production of curli fibers in the biofilm matrix (Vidakovic et al. 2018). In this case, the protection mechanism was two-fold; curli fibers reduced phage movement in the biofilms and prevented access to cell-surface receptors by coating individual cells.

Given the varied impacts of phages on biofilm-associated bacteria, we sought to test how biofilms of the bacterial plant pathogen *Pseudomonas syringae* (pathovar *tomato*, strain DC3000) impact phage interactions on both ecological and evolutionary timescales. This pathogen first grows epiphytically on the surface of leaves and relies on motility to reach entry points (such as stomata) into the interior intercellular space of the leaf (Haefele and Lindow 1987). While growing in this internal space (called the apoplast), bacterial cells produce various exopolysaccharides including alginate, levan, and cellulose (Laue et al. 2006; Ude et al. 2006). We hypothesized that EPS production might impact phage contact rates with bacterial cells in the apoplast, and might be one factor that contributed to previously observed low rates of phage replication in this environment (Hernandez and Koskella 2019). We first tested how *P. syringae*

biofilm biomass is impacted by different lytic phages on relatively short timescales (throughout the course of a week) under different experimental conditions. Next, we experimentally evolved DC3000 in a factorial experiment varying selection on biofilm formation and phage selection pressure. We then measured biofilm formation and phage resistance at both the population and individual level for all evolved lines, which was followed by sequencing of individual isolates. Finally, we selected a subset of isolates for *in vivo* virulence assays on tomato seedlings in the presence and absence of phage. These results have implications for the understanding of biofilm-phage interactions in both environmental contexts and in agricultural biocontrol.

Methods

Biofilm-phage interactions on ecological timescales

We performed a series of *in vitro* experiments to first test how biofilm production is impacted by phage presence on ecological timescales. We varied the phage application timing (age of biofilm at phage addition), phage concentration, media type, and phage identity in separate experiments (see Table 1). In all experiments, we first grew an overnight culture of DC3000 in 10 mL King's B (KB) broth (shaken at 150 rpm, incubated 28°C). We then diluted the culture to ~.05-0.1 OD600 in KB and set up a randomized "source" 96-well plate with 100 µL of diluted bacterial culture in each well or an equivalent volume of negative control (culture media only). We did not use the outer rows and columns in order to avoid edge effects. Next, we prepared "sink" 96-well plate(s) using a plate type that allows cell adhesion (BrandTech® Catalog #781660, polystyrene non-treated plates), and added 200 µL of defined minimal media to each well. We used a modified Mannitol-Glutamate recipe that substituted fructose (1% wt/vol) for mannitol, and included 2 mM $CaCl_2$ (as used in Chakravarthy et al. 2017). This minimal media recipe was previously optimized for DC3000 biofilm assays *in vitro*, and we chose fructose as an added carbon source based on low variation across replicates in preliminary assays (data not shown) and its relevance as an available sugar on plant leaves (Mercier and Lindow 2000). Approximately 1 µL from each well of the source plate was then transferred to each corresponding well of the sink plate(s) using a flame-sterilized 96-well metal pin replicator. The plates were then statically incubated at 28°C for differing lengths of time prior to phage addition and crystal violet staining for biofilm densities. Phages were typically prepared as co-cultures with DC3000 in KB and filter sterilized (0.45 µm) after 24 hours of growth at 28°C, except for the "media" experiment in which we co-cultured the phages and host in minimal media for the minimal media wells. For phage-treated biofilms, we first grew the biofilms in the absence of phage for a pre-determined length of time (72 hours in all experiments except the time series). After biofilm incubation, we removed the minimal media in each well, rinsed the wells once with sterile water, and finally added phage at the appropriate concentration. Non-phage treated controls had spent KB added in the same volume as the phage in phage-treated wells. Both phage and non-phage treated control wells also had fresh media added in the same volume as the phage. Plates were incubated with phage for 24 hours, static, at 28°C.

Table 1. List of biofilm-phage interaction experiments. PFUs: plaque forming units; MM: minimal media; KB: King's B (rich media).

Experiment	Variable of interest	Media	Phages	PFUs per well	Biofilm age when phage added
Time series	Biofilm age at phage addition	MM	FRS, SHL	10^6	24, 48, 72, 168 hrs
Concentration	Phage concentration	MM	FRS, SHL	High (10^7), low (10^1)	72 hrs
Media	Impact of phage in media that does/does not promote biofilm formation	MM, KB	FRS, SHL	10^5	72 hrs
Screen	Phage identity	MM	Panel	10^6	72 hrs

After incubation, we used a crystal violet staining method to quantify biofilm formation in each well, modified from O'Toole (O'Toole 2011). We first removed the planktonic portion (liquid in each well) and washed the wells with 300 µL of MilliQ water to remove any residual planktonic cells. After removing the water, we added 225 µL of 0.1% crystal violet and stained for 10 minutes. Next, we removed the crystal violet, washed the wells twice with 300 µL MilliQ water, removed the water, and allowed the wells to dry completely. The crystal violet stain was then solubilized using 250 µL of 30% acetic acid for 10 minutes, and 150 µL of the resulting crystal violet/acetic acid solution was transferred to a flat-bottom 96-well plate for OD570 quantification. All plates included negative control wells, and the average OD value of the control wells were subtracted from all samples on each plate. All crystal violet assays were performed with a minimum of 5 replicates per sample on each plate.

Experimental evolution

We next tested how selection on biofilm formation in the presence and absence of two different phages (FRS and SHL) impacts DC3000 evolution. We began with a bacterial culture generated from a single colony of DC3000 and filter-sterile (0.45 µm) phage lysates generated from DC3000 co-cultures with a single plaque of phages FRS and SHL, all grown in minimal media. We had a fully-factorial design where we altered biofilm selection regime ("B" = biofilm-selected, "P" = planktonic-selected, "M" = mixed, "C" = control) and phage treatment ("NP" = no phage, "F" = FRS, "S" = SHL) for a total of 12 treatments. We used 12-well plates and replicated at the plate level, with a single replicate of each treatment on each of six plates. Plates were initially prepared with a starting bacterial OD of .013 (approximately $6.5*10^6$ CFU/mL) in a total volume of 1500 µL minimal media with either $9.75*10^2$ PFU of phage (for a multiplicity of infection of ~1 phage:10000 bacteria) or an equivalent volume of spent minimal media (filtered media after bacterial growth) depending on the treatment. All wells had a single

sterilized borosilicate glass bead (6 mm) except for the C treatments. Treatment positions were randomized on each plate, and all plates were incubated statically at 28°C for 72 hours.

At each subsequent passage, we transferred bacteria from the prior passage depending on the biofilm selection regime. Biofilm passaging methods were adapted from the work of Turner et al. (Turner et al. 2018). The old bead from the B treatments was transferred to a new well that also contained a sterile bead with fresh minimal media (with alternating marks to distinguish between new and old beads). Beads were discarded from P treatments, and instead we transferred 75 µL of liquid (as we determined that this volume was similar in bacterial density to the CFUs on a bead after 72 hours of growth). M treatments had both the bead and 75 µL of liquid transferred into wells with a sterile bead and fresh media, while C treatments had 75 µL of liquid transferred into a well with fresh media and no bead. For phage-selected treatments, we added an equivalent concentration of non-evolved phage at each transfer to maintain some level of phage selection pressure throughout the experiment. Non-phage selected treatments got an equal volume of spent minimal media. After six passages, we sampled the wells according to their biofilm selection regime. We placed the new bead from each B treatment into a microcentrifuge tube with 1 mL minimal media. 1 mL of liquid was sampled from the P and C treatments, while both the bead and 1 mL of liquid were sampled from the M treatments (into a single tube). All tubes were sonicated for 10 minutes in a sonicating water bath (Branson M5800) to dislodge any surface-attached cells. We then froze three sets of each sample in 25% glycerol at -80°C.

Population-level phage resistance and biofilm assays

At the end of experimental evolution, we quantified the population-level biofilm formation of all lines using two different methods - one using the 96-well crystal violet stain method as used in the ecological experiments, and the second measuring the relative amount of bacterial growth on beads to planktonic liquid. For all assays, we prepared a 72 hour culture of ancestral DC3000 in minimal media to compare to the evolved lines. All assays were blocked by the same blocks used in passaging (i.e. lines on the same plate were assayed on the same day). We thawed one set of samples for each line. For the first block of samples, we plated serial dilutions directly from the thawed homogenate. For the other five blocks, we centrifuged the bacterial cells (4000 rcf for 10 minutes) to remove the glycerol, and resuspended the cells in minimal media without glycerol prior to plating. Duplicate serial dilutions for all blocks were spotted on three types of KB hard agar plates: one without any added phage, one with high titer FRS lysate spread on the plate, and one with high titer SHL lysate. Plates were incubated for 48 hours at 28°C. We then compared the CFUs that formed on the phage plates to those on the non-phage plates to determine the frequency of resistant mutants in each population. Next, using the CFUs from the non-phage plates as a metric of bacterial density in each sample, we diluted all samples in minimal media to match the lowest concentration sample in the block. We then added 200 µL of each sample to a 96-well plate for crystal violet assays, and 1500 µL of each sample to a 12-well plate for the bead assay (both assays to assess biofilm formation). The culture of ancestral DC3000 was included at the same density as the other samples in each block. After 72 hours of static incubation at 28°C, we stained the 96-well plate using the same crystal violet assay as described previously, with an additional step where we measured the OD600 of the planktonic liquid. For the 12-well plates, we sampled both beads into a single tube with 1 mL minimal media, as well as 1 mL of planktonic liquid into a separate tube (for all wells). We sonicated the tubes for 10 minutes to dislodge cells, and then plated duplicate serial dilutions of each sample on KB hard agar. We recorded CFUs after 48 hours of incubation at 28°C. For

analysis, we calculated the ratio of CFUs formed on the beads to the total amount of CFUs (bead+planktonic), as a measure of relative investment in biofilm production. A few populations were not recoverable after thawing and were excluded from phenotypic assays.

Colony isolation and whole genome resequencing

After measuring biofilm formation and phage resistance at the population-level, we then isolated a single random colony from each recoverable population for individual-level assays. We first sequenced the whole genomes of each isolate to determine any genetic changes relative to the ancestral strain. DNA was extracted from overnight cultures of each evolved colony and the ancestor using the Qiagen DNeasy Blood and Tissue Kit (Catalog #69504) with all recommended steps as listed, and was sequenced at the Microbial Genome Sequencing Center (MiGS, PA, USA) using the Illumina NextSeq 2000 platform. For variant calling, we used the Burrows-Wheeler aligner (bwa-mem) to align our reads to the DC3000 reference genome (NCBI assembly accession GCF_000007805.1; Buell et al. 2003; Li 2013). We then used SAMtools to convert the sam files to sorted bam files, which were then run through SAMtools/bcftools to call variants (Li et al. 2009). Next, we filtered the variants based on a minimum read depth of 10 and minimum RMS mapping quality of 20 (using varFilter). We then merged all vcf (variant) files and used the annotated genome to identify the associated genes at each variant position (or if intergenic). For each variant site, we plotted the listed "product description" found in the annotation file.

Individual-level phage resistance and biofilm assays

We next assayed each isolate for phage resistance and biofilm formation. For the phage resistance assay, we performed cross-streak assays using high-titer lysates of FRS and SHL. In these assays, a small volume of overnight bacterial culture is streaked perpendicularly across a dried line of high-titer phage on a hard agar plate. We performed these streaks in duplicate for each colony, incubated the plates at 28°C for 48 hours, and then scored the plates for resistance. If the growth of the culture was not inhibited by the phage line, it was scored as resistant. Cultures unable to grow over any portion of the phage line were scored as sensitive, and cultures that were only slightly inhibited were scored as moderately resistant (we included this phenotype as somewhat resistant given that it visually differed from the ancestor). We then performed crystal violet assays to quantify biofilm formation. We grew cultures of each isolate in 8 mL KB broth for 48 hours (28°C shaken), diluted all to 0.05 OD600, and prepared a randomized source plate with 100 µL of the diluted cultures. We then transferred 1 µL from the source wells to a 96-well sink plate containing 200 µL minimal media per well, which was then incubated for 72 hours, static, at 28°C. After 72 hours, we performed the biofilm assay as described previously, with the additional planktonic liquid quantification step. There were four replicates per isolate on each plate, and positions were assigned randomly.

Bacteria-phage interactions in tomato seedlings

To test how the evolved isolates interact with phage *in vivo*, we performed a seedling inoculation experiment with a subset of isolates (chosen based on having motility/biofilm-related mutations or having high/low biofilm formation in the crystal violet assays). Seedling germination and inoculation methods were adapted from prior work (Hernandez et al. 2020). Briefly, tomato seeds (*Solanum lycopersicum* cultivar Moneymaker, from Eden Brothers, NC, USA) were surface-sterilized using 70% ethanol for 1 minute, soaked in a sterilization solution

(three parts 0.2% Tween 20, one part 8.25% bleach) for 20 minutes, then rinsed three times in sterile MilliQ water. We germinated the seeds individually in sterile 15 mL conical tubes with 7 mL water agar (1% agar) which were placed in a dark growth chamber set to 21°C. After we observed signs of germination, the tubes were moved to a 28°C chamber with a 15h day:9h night light cycle. When the seedlings were 1 week post-seed sterilization, we inoculated the seedlings with treatments (assigned randomly) composed of either bacteria, bacteria with phage (FRS or SHL), or various controls (magnesium chloride only, magnesium chloride with spent KB, FRS in magnesium chloride, SHL in magnesium chloride). We also included the ancestral bacterial strain with and without added Silwet L-77 (0.015%; a surfactant used to enhance spreading/reduce aggregation) to test whether Silwet impacts bacteria-phage interactions *in vivo*. Bacterial cultures were grown from freezer stocks in 10 mL KB broth for 72 hours, centrifuged at 3500 rcf for 10 minutes twice to remove the media, then resuspended in sterile 10 mM MgCl2 and diluted to 0.0002 OD600 (approximately 10^5 CFU per mL). Phage lysates of FRS and SHL were prepared by filtering (0.45 µm) 24 hr co-cultures of the phage grown with DC3000 in KB broth. We then plated triplicate independent dilution series of the lysates on soft agar overlays with DC3000 to determine the PFUs. For inoculations, the lysates were then diluted to 10^6 PFU per mL using 10 mM MgCl2. We added equal amounts of phage and bacteria suspensions to the final inocula, which corresponds to a 10:1 (phage:bacteria) MOI. In order to minimize bacteria-phage interactions occurring on off-target (i.e. non-seedling) surfaces, inoculations were done in two rounds. Seedlings were first inoculated with the phage suspension or appropriate control (spent KB diluted in MgCl2), shaken for 4 minutes at room temperature, and then the suspensions were removed and tubes were dried. Seedlings were inoculated with bacteria or appropriate controls in the second round using the same methods, and there were three replicate seedlings for each treatment. Seedling tubes were incubated in the 28°C chamber with a 15h day:9h night light cycle and scored daily for disease symptoms according to the scale used by Morella et al. (Morella et al. 2019).

Statistics and figures

We used R version 4.0.2 for statistical analysis and figure generation, and compiled figure panels in Adobe Illustrator (R Core Team 2017). For most analyses, we fit linear models or linear mixed models (to incorporate random effects) and determined significance of factors using analysis of variance. Experimental blocks were always included in statistical models where necessary. For experiments with factorial designs, we first tested for an interaction between the factors, and if not significant we dropped the interaction term from the models. We performed posthoc analyses through pairwise comparisons of estimated marginal means (emmeans package in R; Lenth 2020) with a Tukey adjustment for multiple comparisons. For the population-level bead assay and resistance plating, proportion data were logit-transformed to improve the distribution of model residuals. Analyses of the relationship between phage resistance and area under the disease progress curve (AUDPC; estimated using the trapezoidal integration method; Jeger and Viljanen-Rollinson 2001; Madden et al. 2007) in the seedling assay were performed using Wilcoxon tests. All other analyses were performed using linear or linear mixed models as stated previously. Model fits were assessed using visual inspection of residuals.

Results

Ecological biofilm-phage interactions

Time series experiment

In this experiment, we tested whether the effect of phage (FRS and SHL) on biofilm formation depended on age of the biofilm at time of phage application. We found that the effect of phage did not differ across time ($F_{6, 45}$=0.95, p=0.4724; Fig. 1A), and that phage treatment did not have a significant effect on biofilm formation either ($F_{2, 15}$=0.70, p=0.5115). However, biofilm formation did change across time ($F_{3, 51}$=331.90, p<0.001), with increases between all time points up to 72 hours, after which there was a decrease (all comparisons p<0.04).

Concentration experiment

We first tested for an interaction between concentration and phage type (excluding the bacteria only/no phage added wells), and found no interaction effect on biofilm formation ($F_{1, 16}$=0.001, p=0.9752; Fig. 1B). We then tested for an effect of phage type including all samples, and found that phage treatment did significantly impact biofilm formation ($F_{2, 22}$=14.87, p<0.001). Samples with SHL applied were higher than samples without phage or with FRS (all p<0.002).

Media experiment

We tested for an effect of phage treatment on biofilm formation in each media type (KB or minimal media) separately. We found that there was no effect of phage on biofilm formation in minimal media ($F_{2, 24}$=0.90, p=0.42; Fig. 1C), but that phage significantly reduced the low level of biofilm production in KB ($F_{2, 24}$=31.79, p<0.001).

Phage screen experiment

We found that phage identity significantly impacted biofilm formation ($F_{14, 94}$=29.12, p<0.001; Fig. 1D). Phages either increased (QAC, RE_1, SHB, SHL, and VCFD; all p<0.001) or had no effect on biofilm formation compared to bacteria grown in the absence of phage.

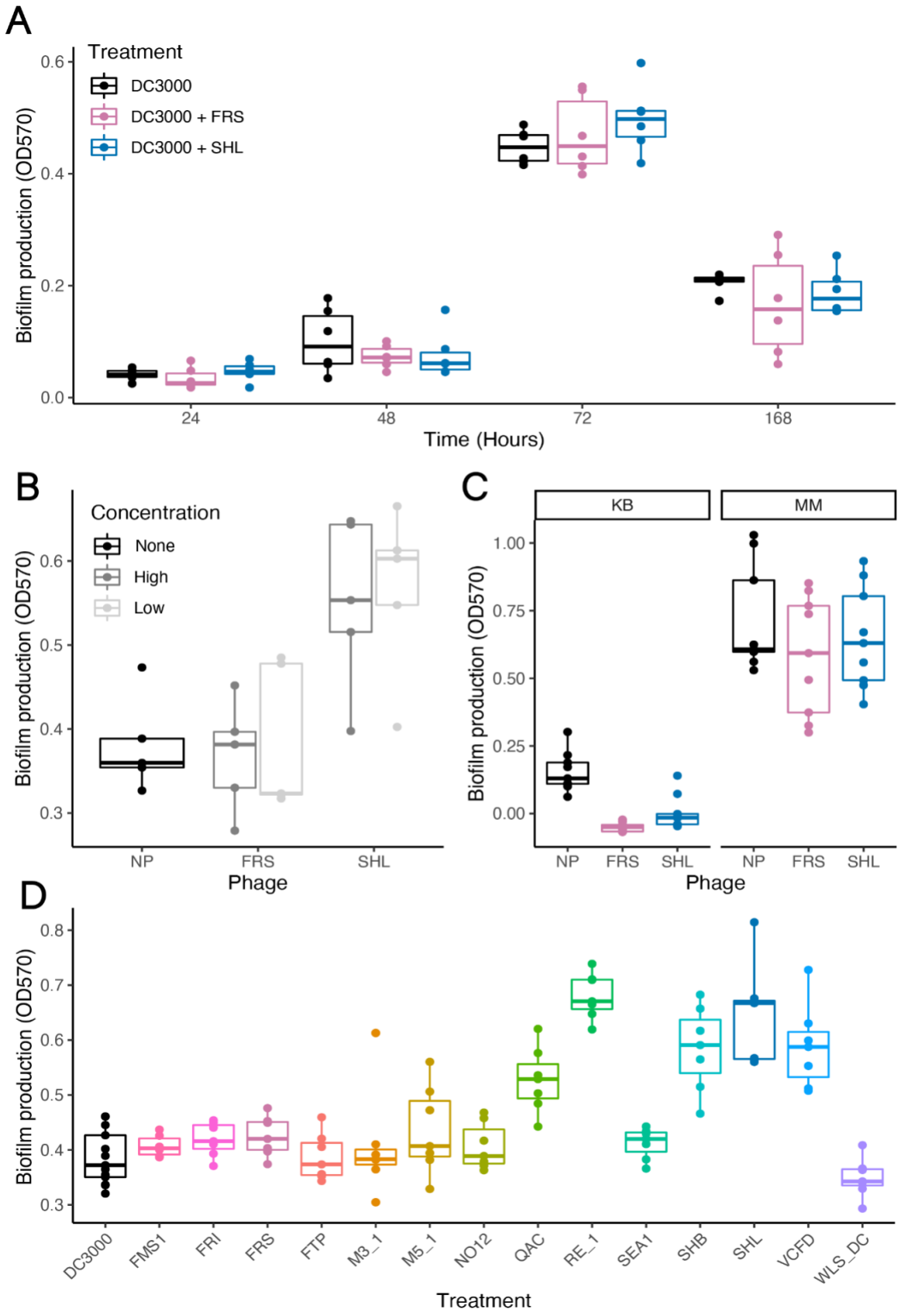
A
Treatment
DC3000
DC3000 + FRS
DC3000 + SHL
Biofilm production (OD570)
0.0
0.2
0.4
0.6
24
48
72
168
Time (Hours)
B
Concentration
None
High
Low
Biofilm production (OD570)
0.3
0.4
0.5
0.6
NP
FRS
SHL
Phage
C
KB
MM
Biofilm production (OD570)
0.00
0.25
0.50
0.75
1.00
NP
FRS
SHL
NP
FRS
SHL
Phage
D
Biofilm production (OD570)
0.3
0.4
0.5
0.6
0.7
0.8
DC3000
FMS1
FRI
FRS
FTP
M3_1
M5_1
NO12
QAC
RE_1
SEA1
SHB
SHL
VCFD
WLS_DC
Treatment

Figure 1. The impacts of biofilm age, phage concentration, media type, and phage type on DC3000 biofilm formation. (A) Boxplots of biofilm formation (OD570: optical density at 570 nm) over time in the absence (black) or presence of phages FRS (pink) and SHL (dark blue), as determined via a crystal violet staining assay. Biofilms were first grown for differing lengths of time prior to phage addition, and the listed time on the x-axis is the age of the biofilm at time of phage addition. Biofilm quantification was performed 24 hours after phage was added. **(B)** Biofilm formation in the absence ("NP": no phage) or presence of phage (FRS or SHL) at two different concentrations (high: 10^7 PFU per well, low: 10^1 PFU per well). **(C)** Biofilm formation in rich media (KB: King's B) or in minimal media (MM) in the absence (NP) or presence of phages FRS and SHL. **(D)** Biofilm formation in the absence of phage (DC3000, first box) or presence of a panel of lytic phages (individually). For panels B-D, biofilms were grown for 72 hours prior to phage addition, and biofilm quantification was performed 24 hours after phage addition. There were 10^6 PFUs per well in panels A and D, and in panel C there were 10^5 PFUs per well.

Experimental evolution

Population-level biofilm formation

Biofilm selection regime and phage selection regime significantly impacted population-level biofilm formation in the bead assay (biofilm: $F_{3, 55}$=2.30, p=0.0385; phage: $F_{2, 55}$=4.15, p=0.0209; Fig. 2A), but there was no interaction between these terms ($F_{6, 49}$=0.80, p=0.5743). After adjustment for multiple comparisons, none of the biofilm selection treatments were significantly different from one another, but the B-P comparison was closest to significance (p=0.0910). SHL-selected lines had higher biofilm levels than lines selected without phage (p=0.0160), but no other phage treatment pairwise comparisons were significant (all p>0.25).

In the crystal violet assay, we found that the biofilm and planktonic OD measurements had very different ranges. In order to get a relative metric of biofilm investment, we therefore calculated the biofilm and planktonic Z-scores for each sample's average OD (across replicate wells in the plate) compared to all other samples on the same plate. We then used the difference between the biofilm and planktonic scores as a relative measure of how much that sample invested in biofilm formation. Essentially, high values of this metric indicate that the sample produced much more biofilm than expected given its planktonic density (relative to the others on that plate). As in the bead assay, we found no interaction between biofilm and phage selection regimes ($F_{6, 49}$=1.27, p=0.2891; Fig. 2B), but biofilm selection regime had a main effect on this metric ($F_{3, 55}$=10.27, p<0.001), and phage selection regime neared significance ($F_{2, 55}$=3.03, p=0.0566). B populations had increased biofilm formation compared to P and C lines (both p<0.001), while all other comparisons were non-significant (all p>0.1).

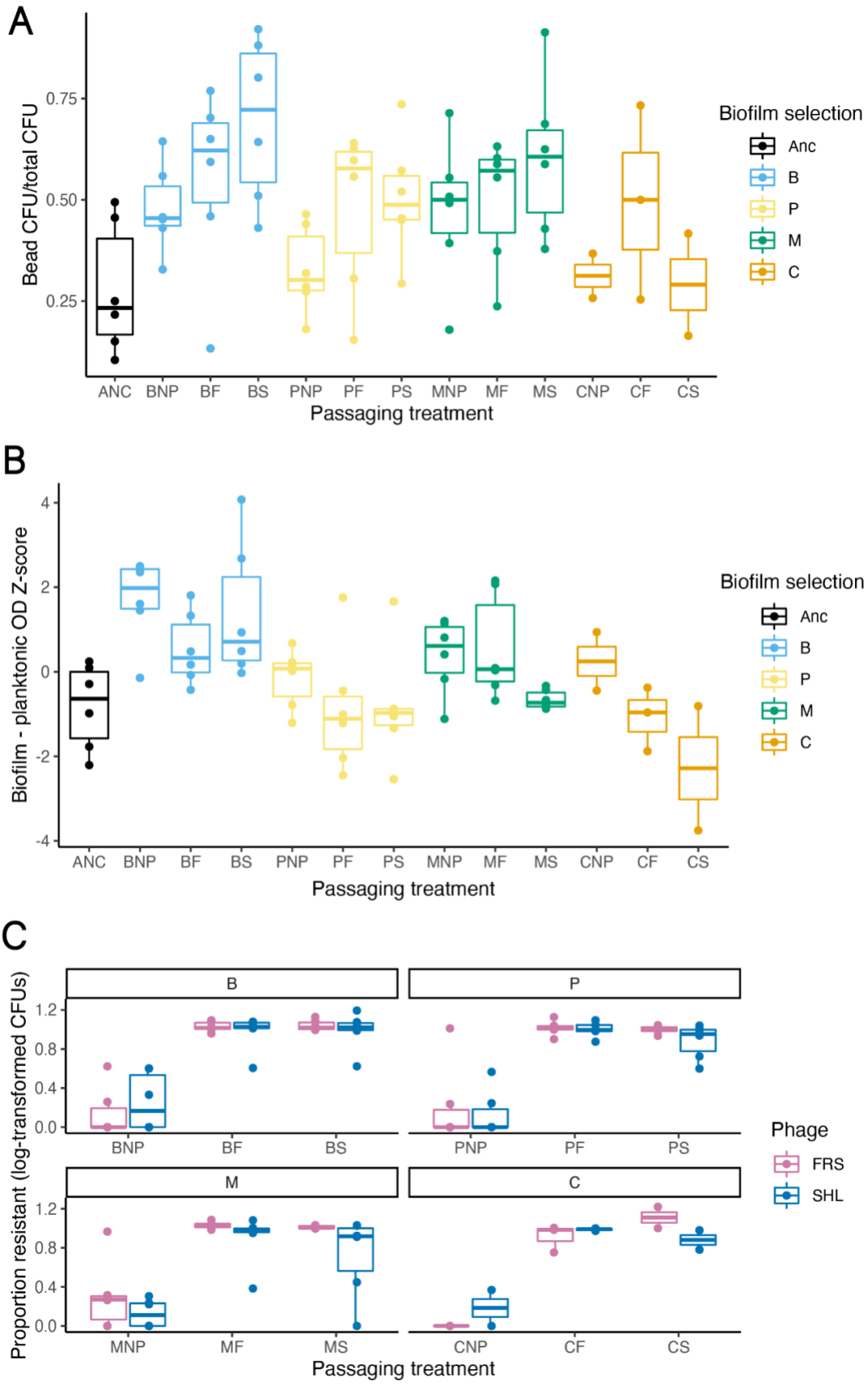
A
Bead CFU/total CFU
0.75
0.50
0.25
ANC BNP BF BS PNP PF PS MNP MF MS CNP CF CS
Passaging treatment
Biofilm selection
Anc
B
P
M
C
B
Biofilm - planktonic OD Z-score
4
2
0
-2
-4
ANC BNP BF BS PNP PF PS MNP MF MS CNP CF CS
Passaging treatment
Biofilm selection
Anc
B
P
M
C
C
B
P
M
C
Proportion resistant (log-transformed CFUs)
1.2
0.8
0.4
0.0
BNP BF BS
PNP PF PS
MNP MF MS
CNP CF CS
Passaging treatment
Phage
FRS
SHL

Figure 2. Population-level biofilm formation and phage resistance after experimental evolution. (A) Boxplots of relative investment in biofilm formation (bacterial growth on a glass bead divided by total growth in the well) for experimentally evolved populations and the bacterial ancestor ("Anc"). **(B)** The difference between biofilm formation Z-score and planktonic Z-score for each population, calculated per block. Z-scores were calculated based on OD values in a crystal violet staining assay (biofilms) or in the planktonic liquid from those same plates. **(C)** Proportion of phage-resistant colonies per population, calculated by determining the CFU per mL (log-transformed) on agar plates with high titer phage, and dividing by the CFU per mL (log-transformed) on agar plates with no phage. Facets are split by biofilm passaging regime, and the two colored boxes indicate the phage that was spread on the agar plate (pink: FRS, blue: SHL). For all panels, the first letter of each population indicates the biofilm selection regime ("B" = biofilm-selected, "P" = planktonic-selected, "M" = mixed biofilm and planktonic, "C" = control/no bead in well). The last letter(s) indicate the phage selection regime ("NP" = no phage, "F" = FRS, "S" = SHL). Points in each panel correspond to individual, independent populations within a selection regime.

Population-level phage resistance

We generated linear mixed models to test for a three-way interaction between biofilm passaging treatment, phage passaging treatment, and phage used in the streaking assay (with a random effect of block) on proportion resistant of log-transformed CFUs (log transformed CFUs, then divided value on phage plate by value on non-phage plate). We sequentially dropped the least significant interactions from the model, which led to all interactions being dropped. In the final model with only main effects, phage passaging treatment and streaking phage were significant, but biofilm passaging treatment was not (phage passaging treatment: $F_{2,109.35}$=197.97, p<0.001; streaking phage: $F_{1,109.11}$=4.15, p=0.0439; biofilm passaging treatment: $F_{3,110.52}$=0.46, p=0.7111; Fig. 2C). FRS and SHL-selected treatments were more phage-resistant than the treatments passaged without phage (all p<0.001), and resistance to FRS was greater than resistance to SHL (p=0.0440).

Whole genome resequencing (isolates)

Isolates ranged from having 0-4 variant sites, with a median of 1 mutation. The two genes that most commonly had mutations across all isolates were a membrane transport protein (in the major facilitator superfamily: MFS; PSPTO_RS10895) and a glycosyltransferase (PSPTO_RS07000). Mutations in the MFS transporter were found in isolates from all passaging treatments, while glycosyltransferase mutations were only found in isolates that came from populations passaged with phage. There were only two unique mutations in the MFS transporter; including a single base pair insertion that was found in 21 of the 23 isolates with MFS transporter mutations. In contrast, there were 13 unique glycosyltransferase mutations found across 23 isolates with identified glycosyltransferase mutations. Four isolates that had been passaged in the presence of SHL had mutations in an acetyltransferase (adjacent to the glycosyltransferase; PSPTO_RS07005), and no mutations in the glycosyltransferase. Other than these mutations, most other identified variant positions were unique to each isolate. Many of these mutations were in genes with impacts on motility or biofilm formation, including a twitching motility protein, the flagellar transcriptional regulator fleQ, flagella-associated proteins (flaG, fliC, and flgI), and a diguanylate cyclase (an enzyme involved in the formation of cyclic-

di-GMP, an important signaling molecule in the transition between planktonic and biofilm growth; Cotter and Stibitz 2007).

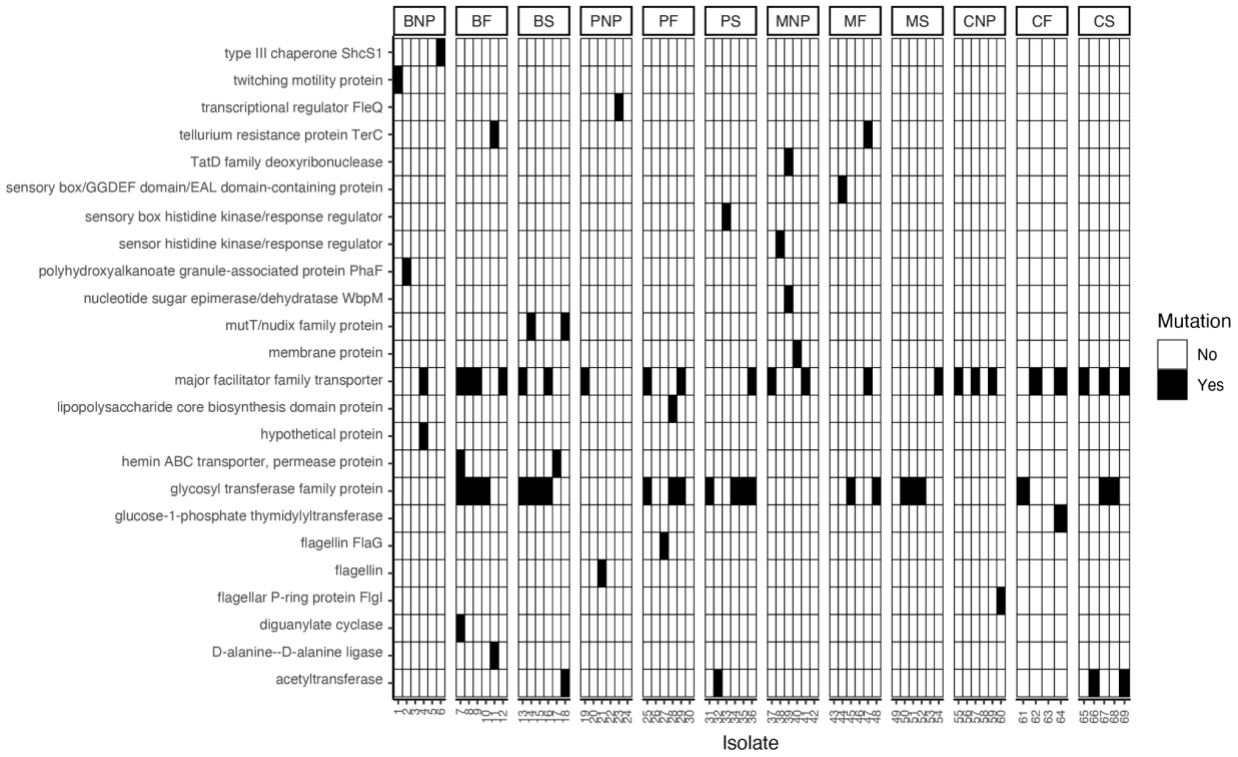

Figure 3. Mutations found in isolates from experimentally evolved populations. Identified variant sites in each sequenced isolate relative to the ancestral DC3000 strain used to begin experimental evolution. Each row corresponds to the gene found at the identified variant position, and each column is an individual isolate from a single experimentally evolved population. The facets at the top of the plot indicate which passaging regime the isolate came from. The first letter of each facet indicates the biofilm selection regime ("B" = biofilm-selected, "P" = planktonic-selected, "M" = mixed biofilm and planktonic, "C" = control/no bead in well). The last letter(s) indicate the phage selection regime ("NP" = no phage, "F" = FRS, "S" = SHL). White cells indicate absence of a variant in that protein, while black cells indicate presence of a variant. Mutations found in intergenic positions were excluded from this plot. Note that the exact type/position of mutation within a single row may differ between isolates.

Isolate biofilm formation and phage resistance

As in the population-level biofilm formation assay using crystal violet staining, we compared the biofilm and planktonic Z-scores for the isolates from each population. Similar to the populations, there was a marginal but non-significant interaction between biofilm and phage selection regimes ($F_{6,57}$=2.21, p=0.0555), but there were significant main effects of both (biofilm: $F_{3,63}$=3.48, p=0.0210; phage: $F_{2,63}$=6.43, p=0.0029). No biofilm comparisons were significant after correction for multiple testing, but M treatments were marginally higher than C treatments (p=0.0553). FRS-selected isolates had higher biofilm formation than isolates selected in the presence of SHL or in the absence of phage (both p<0.04). Isolates from FRS and SHL-selected lines were all resistant to SHL, and almost all resistant to FRS. Only a few isolates from

a single treatment passaged in the absence of phage (MNP) were phage-resistant. We next tested whether phage-resistant and sensitive isolates differed in biofilm formation (after accounting for experimental design factors), and found that phage-resistant isolates had increased biofilm formation ($F_{1,62}$=8.94, p=0.0040).

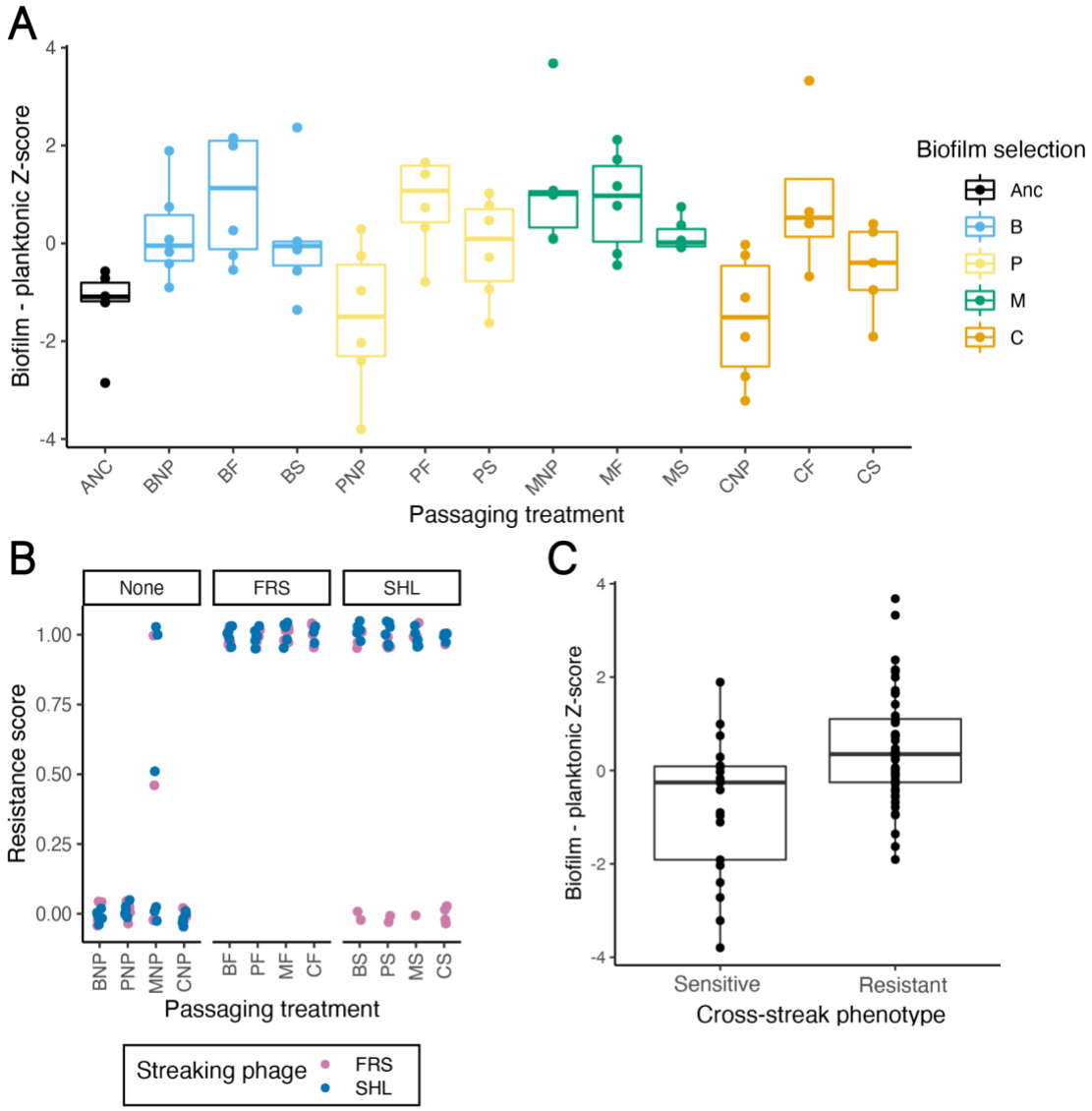

Figure 4. Isolate biofilm formation and phage resistance. (A) Boxplots of the difference between biofilm formation Z-score and planktonic Z-score for each population, calculated per block for experimentally evolved isolates and the ancestor ("ANC"). Z-scores were calculated based on OD values in a crystal violet staining assay (biofilms) or in the planktonic liquid from those same plates. **(B)** Phage resistance scores for each isolate as determined by a cross-streaking assay. Facets indicate whether the isolate came from a population passaged in the absence ("none") or presence of phage (FRS or SHL). The color of the point indicates the phage used in the streaking assay (pink: FRS, blue: SHL). Resistance scores of 0 = sensitive, 0.5 = moderately resistant, and 1 = fully resistant. **(C)** The difference between biofilm and planktonic Z-scores for each isolate, split by whether the isolate was sensitive to both phages or resistant to either phage. For this analysis, colonies that were moderately resistant (0.5) were treated as resistant. For

panels A and B, the first letter of each population indicates the biofilm selection regime ("B" = biofilm-selected, "P" = planktonic-selected, "M" = mixed biofilm and planktonic, "C" = control/no bead in well). The last letter(s) indicate the phage selection regime ("NP" = no phage, "F" = FRS, "S" = SHL). Points in these panels correspond to individual, independent isolates within a selection regime (one per experimentally evolved population).

Seedling assay

After inoculating seedlings with each isolate in the presence and absence of added phage (FRS/SHL), we scored disease symptoms daily for one week (Fig. 5) and used those scores to calculate the mean area under the disease progress curve (AUDPC) for all replicate seedlings within each treatment. We then used Wilcoxon tests to determine how AUDPC in the absence of phage and the proportion of AUDPC reduction in the presence of each phage differed for phage-sensitive and resistant isolates. Phage-resistant isolates had reduced AUDPC in the absence of phage compared to phage-sensitive isolates (W=78.5, p=0.015; Fig. 6A), but there was no difference in the impact of phage (proportion reduction of AUDPC) when comparing the sensitive and resistant isolates (FRS: W=102, p=0.1277; SHL: W=96, p=0.2486; Fig. 6B, 6C). However, for all phage-sensitive isolates, the proportion of AUDPC reduction by phage ranged from 0-1, while for phage-resistant isolates there were many that had negative proportion reduction values (which indicates increased AUDPC in the presence of phage). In addition, we tested for the effects of Silwet and phage treatment (NP/F/S) on AUDPC for the ancestral bacteria, and found that there was no significant interaction or main effects (all p>0.15).

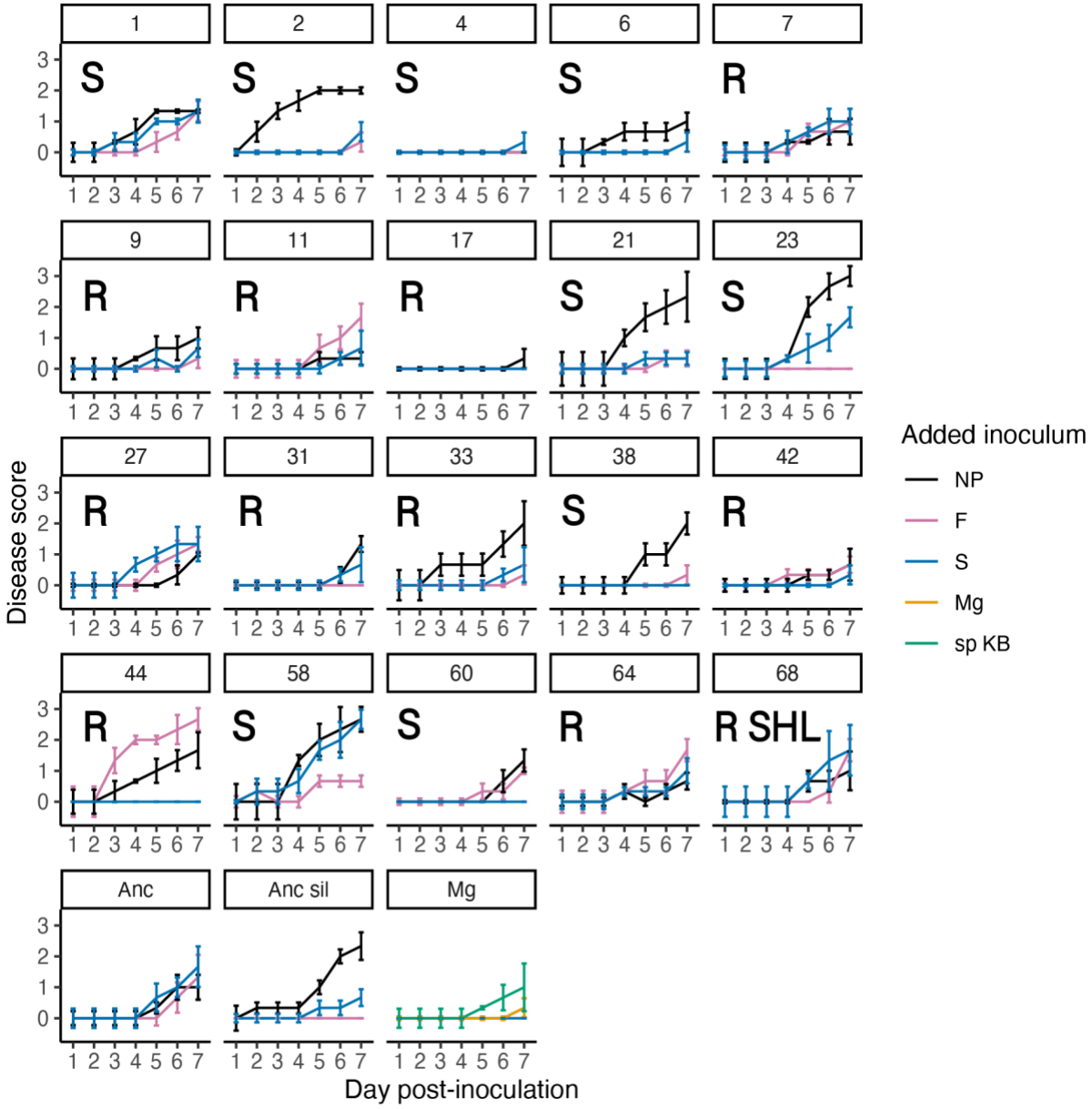

Figure 5. Seedling disease progress curves for experimentally evolved bacterial isolates in the absence and presence of added phage. Each facet corresponds to an individual bacterial isolate that was experimentally evolved *in vitro* (numbered facets) or experimental controls. The x-axis indicates the day at which we scored the seedlings, and the y-axis indicates the disease score. Lines and error bars represent the mean ± 1 standard error for three replicate seedlings within each treatment, and within each panel the letter specifies whether that isolate was sensitive or resistant to phage in the cross-streaking assay (S: sensitive to both phages, R: resistant to both phages, R SHL: resistant to SHL only). Each isolate was grown in the absence of phage ("NP", black) or presence of FRS ("F", pink) or SHL ("S", blue). Additional controls include the facets "Anc" (ancestral bacterial strain), "Anc sil" (ancestor grown in presence of 0.015% Silwet), and "Mg" (magnesium chloride buffer control). The ancestor was also grown in the presence or absence of phage to compare to the evolved isolates. The Mg control was

inoculated with a second round of magnesium chloride buffer ("Mg", orange) or added spent KB ("sp KB", green), since all seedlings were inoculated in two rounds.

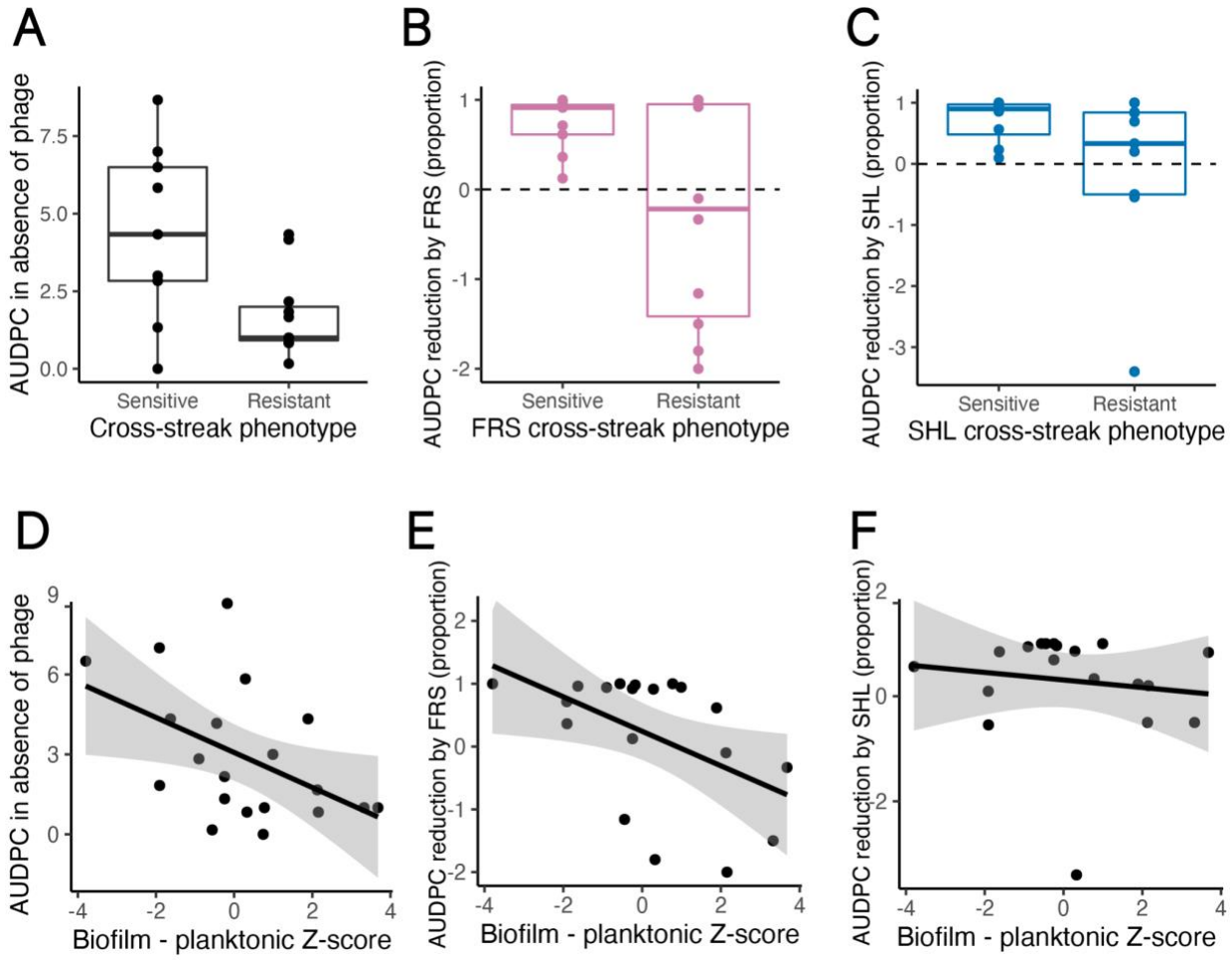

Figure 6. The relationships between phage resistance and biofilm formation on the area under the disease progress curve (AUDPC). (A) Boxplots of AUDPC in the absence of phage for phage-sensitive and resistant isolates. **(B)** Proportion of AUDPC reduced by phage FRS for FRS-sensitive and resistant isolates. Values of 1 indicate that the phage completely eliminated the disease symptoms, while values close to 0 indicate that the phage did not impact disease scores. Values below 0 represent increased AUDPC values in the presence of phage. **(C)** Proportion of AUDPC reduced by phage SHL for SHL-sensitive and resistant isolates. **(D)** The relationship between the difference between biofilm and planktonic Z-scores for each isolate, and their corresponding AUDPC in the absence of phage. **(E)** The relationship between the difference between biofilm and planktonic Z-scores for each isolate, and their corresponding proportion of AUDPC reduction in the presence of phage FRS. **(F)** The relationship between the difference between biofilm and planktonic Z-scores for each isolate, and their corresponding proportion of AUDPC reduction in the presence of phage SHL. For panels D-F, the plotted black line is a linear regression, and the shaded gray regions indicate the 95% confidence interval.

Next, we tested how our biofilm formation Z-score metric correlated with AUDPC in the absence and presence of phage. High values of the biofilm formation Z-score metric correlated with reduced AUDPC values in the absence of phage ($F_{1, 18}$=5.55, p=0.0301; Fig. 6D). High biofilm formers were less impacted by FRS than low biofilm formers ($F_{1, 17}$=5.56, p=0.0306; Fig. 6E), but there was no relationship between biofilm formation and impact of SHL on AUDPC ($F_{1, 17}$=0.29, p=0.5958; Fig. 6F).

Discussion

Biofilm biomass is increased or not impacted by phage in vitro*, depending on experimental conditions*

We first tested whether DC3000 biofilm biomass *in vitro* is impacted by phage presence under varying experimental conditions. In all experiments, we grew biofilms until a certain time point, incubated the biofilms with phage for 24 hours, and then quantified biofilm biomass using a crystal violet staining assay. We first found that under our setup conditions, biofilm biomass increased over 72 hours but decreased between 72 hours and 1 week (Fig. 1A), suggesting biofilm dispersal by 1 week post-inoculation. With this result, we chose the 72 hour time point for phage application in all subsequent experiments. In addition, the two tested lytic phages (FRS and SHL) had no impact on biomass when applied at any of these time points. We next tested whether phage concentration had any impact on biomass, and found no difference between low (10^1 PFU per well) and high (10^7 PFU per well) concentration phage stocks on biomass (Fig. 1B). However, SHL application increased biomass at both tested concentrations. We hypothesized that the biofilm increase could be due to phage-lysed (but not biofilm-associated cells) that were being stained by crystal violet. To determine whether phage-lysed cells were staining in our assay, we grew DC3000 in the presence and absence of phage in both rich media (KB; which allows for high levels of active phage replication and reduced levels of biofilm formation) and compared that to the impact of phage in biofilm-promoting minimal media (MM). We found that biofilm biomass was much lower in KB than in MM, as expected, and that phage reduced the amount of stained biomass only in KB (Fig. 1C). This suggests that the phage-lysed cells are not contributing substantially to the stained biomass, although it does not preclude some level of phage lysis occurring in the biofilms in minimal media. Finally, we tested a panel of lytic phages at a single concentration (10^6 PFU per well) and found that the phages either did not impact or increased biofilm biomass (Fig. 1D). Interestingly, across the four experiments, FRS consistently had no impact on biomass, but SHL increased biofilm biomass in two of the four experiments. There is no obvious experimental link to explain these results, except that the phage lysates were freshly prepared for each experiment. It is possible that SHL may have accumulated different mutations within each co-culture that altered its phenotype and interactions with biofilms. Together, these results show that this set of lytic phages does not reduce DC3000 biofilm biomass in minimal media, suggesting that biofilm formation could be an effective mechanism of reducing phage contact rates for this pathogen.

Experimental selection led to population-level phenotypic differences in biofilm formation and phage resistance

We next experimentally selected on biofilm formation in the presence and absence of phage selection pressure. We hypothesized that phage selection would accelerate adaptation towards higher biofilm formation or better planktonic growth, depending on the passaging treatment. Instead, we found that at the population-level, our experimental lines often had higher

biofilm formation than the ancestor (Fig. 2A, 2B). In our bead-based growth assay, we found that SHL selection actually led to higher proportions of growth on beads across all passaging treatments (Fig. 2A), and that our biofilm selection regime only weakly separated phenotypes across treatments (significant main effect of biofilm passaging regime, but only the B-P comparison was marginally significant in posthoc tests and no others were significantly different). In the crystal violet assay, B populations had higher biofilm investment than P and C treatments, while phage selection treatment was only marginally significant (Fig. 2B). In contrast to the bead assay, phage-selected lines typically had lower biofilm formation than their corresponding no-phage treatment (although this was not significant). This suggests that the populations passaged in the absence of phage are likely producing more extracellular mass given their number of live cells, when compared to the populations passaged with phage. Overall, selection in our statically incubated wells with minimal media often led to increases in biofilm biomass production, and our planktonic selection regime did not lead to a reduction in biofilm formation relative to the ancestor.

In addition to changes in biofilm formation, our selection experiment led to differences in the frequency of phage-resistant mutants across populations. Populations passaged in the presence of phage generally had high proportions of colonies resistant to both phages (i.e. high levels of cross-resistance; 2C), while populations passaged in the absence of phage had relatively fewer resistant colonies, as expected. In addition, the frequency of resistance to FRS was generally higher than resistance to SHL. Our biofilm selection regimes did not alter the frequency of phage resistant mutants across treatments, although we note that this assay was done at a single time point. It is possible that the evolutionary dynamics prior to the near-fixation of resistant mutants could have differed across treatments, as a similar experiment performed with antibiotics (instead of phage) found that biofilm-selected populations experienced more clonal interference/fewer selective sweeps than planktonic-selected populations (Santos-Lopez et al. 2019). Future work should determine whether the evolutionary dynamics of phage resistance differ in a similar manner by sampling populations over time.

Phage selection, but not biofilm selection, led to treatment-specific mutations

We isolated a single random colony from each population for whole genome resequencing, hypothesizing that planktonic-selected populations under phage selection would have more cell surface receptor-based mutations than biofilm-selected populations. First, we found that there were typically few mutations per evolved isolate (Fig. 3). This is unsurprising given the relatively short passaging length (and number of bacterial generations, accordingly) compared to other experimental evolution studies. Two genes most often had mutations across all colonies: a single major facilitator superfamily (MFS) transporter and a single glycosyltransferase (group 2). Mutations in the MFS transporter appeared in isolates from all passaging treatments, suggesting that changes to this protein may be involved in adaptation to the minimal media. Glycosyltransferase mutations appeared solely in isolates from phage-selected populations (both FRS and SHL), and in some cases were the only mutations in those isolates, indicating that these mutations likely confer phage resistance. Based on protein domain similarity, this protein may be involved in cellulose biosynthesis (COG1215: BcsA; Lu et al. 2020), although DC3000 has a separate bcsA gene. Cellulose is an important biofilm-associated EPS for *Pseudomonas syringae* and many other microbes, including the plant pathogen *Erwinia amylovora* (Ude et al. 2006; Arrebola et al. 2015; Castiblanco and Sundin 2018; Farias et al. 2019). BlastP comparisons also revealed that this protein has similarity to the gene migA, which

is involved in lipopolysaccharide (LPS) modifications in *Pseudomonas aeruginosa* (Yang et al. 2000; Poon et al. 2008). Prior work on phages FRS and SHL found that phage resistance in DC3000 arose due to changes in genes involved in LPS synthesis, although in different genes from the glycosyltransferase identified here, suggesting that LPS is a possible receptor for these phages (Meaden et al. 2015). A few phage-selected isolates in our experiment had no mutations in the glycosyltransferase but instead had mutations in an acetyltransferase (with domain similarity to CatB-related O-acetyltransferases) that is adjacent to the glycosyltransferase, indicating that this may be an alternative mechanism leading to phage resistance. In addition, we identified mutations in other motility and biofilm-related genes, but these were typically unique to a single isolate. We did not find evidence that our biofilm selection regimes led to divergent phage resistance strategies; instead, we saw that all treatments (but not all populations) under phage selection led to mutations in a glycosyltransferase with unknown substrate. In future work, we plan to further classify the mutations present in each isolate to determine whether they are likely to impact protein structure.

Biofilm formation and phage resistance in evolved isolates

We next measured biofilm formation and phage resistance in our sequenced isolates. While both biofilm and phage selection had significant impacts on biofilm formation, the pattern differed from results at the population-level. In the isolates, no pairwise comparisons between biofilm passaging treatments were significant, and FRS-selected isolates had higher biofilm formation than those selected in the absence of phage or presence of SHL (Fig. 4A). Differences between isolates and populations are expected, as it has been previously shown that biofilm productivity can differ between clonal and mixed experimentally evolved biofilms (Poltak and Cooper 2011). All phage-selected isolates were resistant to at least one phage, while only a few non-phage selected isolates were resistant (Fig. 4B). Again unlike the population results, interestingly some SHL-selected isolates were only resistant to SHL and not to FRS. Finally, we compared the biofilm formation of phage-sensitive and resistant isolates, and found that resistance was associated with higher biofilm formation (Fig. 4C). Given the identified mutations in our isolates, it is possible that alterations to cellulose synthesis or LPS had pleiotropic effects that conferred both phage resistance and increased biofilm formation. While to our knowledge cellulose has not been previously implicated in phage resistance, other extracellular polysaccharides have been shown to impact phage interactions. For instance, prior work in *Pseudomonas fluorescens* found that bacterial coevolution with phage can lead to mucoid phenotypes that overproduce alginate, a trait which was shown to be costly in the absence of phage but conferred partial resistance (Scanlan and Buckling 2012). Alginate is produced by *P. syringae* strains during plant infections, so modifications to alginate production could also possibly have pleiotropic impacts on phage resistance and biofilm formation in this pathogen (Fett and Dunn 1989; Keith et al. 2003). Since LPS is the likely receptor for the phages used in our experimental passaging, modifications to LPS that alter biofilm formation could also certainly impact phage resistance. It has been suggested that LPS may play an accessory role that interacts with cellulose in Pseudomonad biofilms (Spiers and Rainey 2005; Mann and Wozniak 2012).

The relationship between biofilm formation, phage resistance, and virulence in seedlings

Finally, we selected a subset of evolved isolates and inoculated them onto tomato seedlings in the presence and absence of phage. We scored disease symptoms daily for a week

and found a wide range of disease progression patterns over time (Fig. 5). In particular, we found that isolates resistant to either phage had reduced AUDPC compared to phage-sensitive isolates (Fig. 6A), suggesting a cost of virulence associated with phage resistance. Using our inoculation method (seedling flooding), bacterial motility is important for reaching entry points to the leaf interior where the pathogen then causes disease symptoms (Haefele and Lindow 1987). Given that phage resistance was associated with increased biofilm formation across all isolates, we hypothesize that our phage resistant mutants may have reduced motility causing a delay/reduction in disease progression. High biofilm formation Z-scores relative to planktonic Z-scores correlated with a reduction of AUDPC in the absence of phage (Fig. 6D). Although we do not know whether these isolates differ in their level of cellulose production, interestingly, one prior study found that cellulose-overproducing strains of *P. syringae* also suffered a cost of virulence (Arrebola et al. 2015). Together, our results suggest that both phage resistance and high relative investment in biofilm formation are associated with a cost of virulence on seedlings.

We next calculated the proportion of AUDPC that was reduced by phage for each isolate (a measure of how well the phages reduced disease progression) and tested whether phage-resistant isolates were less impacted by phage (lower proportion reduction). We found that for both phages, proportion of AUDPC reduction did not differ between phage-sensitive and resistant isolates, but that for FRS in particular there were numerous phage-resistant isolates whose AUDPC was increased in the presence of FRS (Fig 6B, 6C). The mechanism that caused this increase is unknown, but given that these isolates are already phage resistant, this suggests that the mechanism is likely non-evolutionary. High biofilm formation Z-scores also correlated with a reduced impact of FRS on AUDPC (Fig. 6E), but did not correlate with the impact of SHL (Fig. 6F). These results suggest that biofilm formation and phage resistance may modulate the effectiveness of phage biocontrol on disease progression. To determine whether bacterial densities and phage replication differed across isolates, future work will involve bacteria and phage quantification in frozen seedling homogenates from the end of this experiment.

Conclusions

Together, this body of work suggests that *P. syringae* biofilm formation can impact phage interactions both *in vitro* and *in planta*. We found that experimental evolution with phage in static minimal media often led to mutations in a glycosyltransferase with unknown substrate. Phage-resistant mutants had higher biofilm formation than phage-sensitive strains, and this was associated with reduced virulence in seedlings in the absence of phage (and sometimes increased virulence in the presence of phage). This suggests that if phage resistance does arise during agricultural biocontrol, continued application of phage could both continue to select for phage resistance and exacerbate disease symptoms. However, these results also offer the opportunity to design improved biocontrol strategies. If, for example, altered cellulose production is a mechanism of phage resistance and increased biofilm formation, natural or engineered phages with the ability to bind or degrade cellulose could be selected for therapeutic use (Lu and Collins 2007). This approach of finding phages that target therapy-inhibiting compounds has recently been successfully employed in a mammalian system using a phage with enhanced activity in mucin (Green et al. 2021).

Conclusion

Phages are important drivers of bacterial evolution, including in environmental and host-associated microbial communities, yet our understanding of bacteria-phage interactions in ecologically-relevant contexts remains limited. While large-scale sequencing efforts have revealed interesting patterns in bacteria and phage communities across time, it remains difficult to link those patterns to particular processes. In part, this is due to the challenge of identifying a phage's host or hosts using only sequencing data, but perhaps more importantly, this is also due to the difficulty of defining a phage's ecological role in a given environment. Even if a phage can infect a certain host, how often do those two organisms actually come into contact in that environment? Does the host's physiology in that environment support robust phage replication? How do the other organisms nearby impact the outcome of a bacteria-phage interaction? Are the fitness effects of mutations that arise in either partner dependent on environmental conditions? These are only a few of the many open questions that remain for understanding bacteria-phage interactions outside of a laboratory context. In my dissertation, I attempt to partly bridge the gap between the lab and nature by studying how a bacterial plant pathogen (*Pseudomonas syringae* pathovar *tomato*) interacts with phages while associated with its plant host.

Throughout this dissertation, I have demonstrated that context is critical for the outcome of interactions between *P. syringae* and lytic phages. In chapter 1, when a single phage was either coevolved with its host or adapted to the ancestral *P. syringae* repeatedly, I observed that both the genotypic and phenotypic evolution of the virus differed. Specifically, coevolved phages appeared to have accelerated evolution in terms of mutations in structural genes, which allowed them to better reduce coevolved bacterial population growth. This is promising for the use of phages as agricultural biocontrol, because it suggests that if bacteria evolve resistance throughout the course of treatment, these phages could potentially counteradapt in response. However, while these results indicate that the biotic (bacterial host) environment is important for *P. syringae* and phage interactions, this work was done entirely under laboratory conditions. The results from my second chapter extend this work to demonstrate that the dynamics of resistance evolution in this bacteria-phage system are fundamentally different in the leaf environment. I found that phage resistance essentially had no fitness benefit *in planta* due to low phage replication rates and a slight cost of resistance, which meant that phage resistance was unlikely to be positively selected for and reach high frequencies in that environment. Nevertheless, this is only one step towards realism as these experiments were done using semi-sterile plants grown in a growth chamber. It is likely that in a natural infection, bacterial evolution in response to phage would be impacted in ways beyond just the pace of evolution. For example, when infecting a host in nature, the pathogen would have to invade a resident microbiome to reach high densities and cause disease. The resident microbiome could include other bacteria with phage defense mechanisms that may be horizontally transferred to the pathogen, leading to an entirely different mechanism of resistance that would not be possible without the community context. In addition, there are likely other phages within the microbiome that could alter the phage-mediated selection being imposed on the pathogen. Thus, while my work is one step towards understanding how bacterial plant pathogens interact with phages on plants, it remains unknown whether this step towards realism is sufficient for predicting the outcome of interactions in nature.

The work in my final two chapters provides some additional support that the plant environment impacts *P. syringae*-phage interactions. In my third chapter, I observed that phage replication rates were higher on seedlings than I had observed in my second chapter using older

plants. These experiments were also done using different inoculation methods; seedlings were flooded (allowing the pathogen and phage to interact first on the leaf surface), while older plants were syringe-infiltrated directly into the apoplast. This indicates that bacteria-phage interactions on the leaf surface of younger plants differ from those within leaves of older plants. While unsurprising, it indicates that even being "plant-associated" may be too general for understanding these interactions, and that the specific habitat on or within the plant may be important to consider. Next, I hypothesized that one factor that might have led to the low phage replication rates observed in the apoplast could be bacterial biofilm formation. Biofilms are commonly produced by pathogenic microbes as they can protect against external stressors. In doing so, they may also limit phage access to bacterial cells (although this depends on the phage type, as some phages have enzymes that can break down biofilm components). In my work, I found that *P. syringae* pathovar *tomato* strain DC3000 produces significantly more biofilm biomass in minimal media compared to the high-nutrient rich media used in my prior work. In addition, phages had more of an impact on biofilm biomass in rich media than in minimal media. In minimal media, phage application either did not impact or increased biomass. After experimental evolution focused on selecting for both biofilm formation and phage resistance in a factorial design, I found that phage-resistant strains generally had increased biofilm formation relative to phage-sensitive strains. This was coupled with a cost of virulence on seedlings for phage-resistant isolates. Together, this suggests that biofilm formation in this pathogen does impact phage interactions, with important implications for pathogen virulence. Given that biofilm formation is minimal under standard laboratory growth conditions (high-nutrient media) for this pathogen, it seems likely that this did play a role in the difference between the *in vitro* and *in planta* findings in my second chapter. Additional approaches (e.g. microscopy-based) should be explored in order to further determine how bacterial biofilm formation in and on leaves impacts phage contact and replication rates.

This dissertation demonstrates that the ecological and coevolutionary consequences of interactions between a plant pathogenic bacterium and lytic phages are context-dependent. In this work, I have tested a few elements of "context", including the available bacterial hosts (for the phages), the external environment (laboratory media vs. plant leaves), the age of plants and inoculation method, and finally the physiological state of the bacterium (promoting biofilm formation). While laboratory studies are a useful model for understanding the hypothetically possible outcomes of bacteria-phage interactions, my results support the idea that recreating relevant environmental features (e.g. resource availability, spatial structure) may improve predictive power for understanding environmental and host-associated microbes. As it is intractable in many systems to perform experiments in a fully natural context, studies with increasing steps towards realism should help us determine the boundary between insufficient and sufficient model conditions.

References

Abedon, S. T. 2015. Ecology of Anti-Biofilm Agents I: Antibiotics versus Bacteriophages. Pharmaceuticals 8:525–558.

Abedon, S. T. 2011. Lysis from without. Bacteriophage 1:46–49.

Abramovitch, R. B., J. C. Anderson, and G. B. Martin. 2006. Bacterial elicitation and evasion of plant innate immunity. Nat. Rev. Mol. Cell Biol. 7:601–611.

Afgan, E., D. Baker, B. Batut, M. van den Beek, D. Bouvier, M. Čech, J. Chilton, D. Clements, N. Coraor, B. A. Grüning, A. Guerler, J. Hillman-Jackson, S. Hiltemann, V. Jalili, H. Rasche, N. Soranzo, J. Goecks, J. Taylor, A. Nekrutenko, and D. Blankenberg. 2018. The Galaxy platform for accessible, reproducible and collaborative biomedical analyses: 2018 update. Nucleic Acids Res. 46:W537–W544.

Agrawal, A., and C. M. Lively. 2002. Infection genetics: gene-for-gene versus matching- alleles models and all points in between. Evol. Ecol. Res. 4:79–90.

Anderson, R. M., and R. M. May. 1982. Coevolution of hosts and parasites. Parasitology 85:411–426.

Antonovics, J., and P. H. Thrall. 1994. The Cost of Resistance and the Maintenance of Genetic Polymorphism in Host-Pathogen Systems. Proc. R. Soc. Lond. B. Biol. Sci. 257:105–110.

Arrebola, E., V. J. Carrión, J. A. Gutiérrez-Barranquero, A. Pérez-García, P. Rodríguez-Palenzuela, F. M. Cazorla, and A. de Vicente. 2015. Cellulose production in Pseudomonas syringae pv. syringae: a compromise between epiphytic and pathogenic lifestyles. FEMS Microbiol. Ecol. 91:71.

Balogh, B. 2006. Characterization and use of bacteriophages associated with citrus bacterial pathogens for disease control. Doctoral Dissertation, University of Florida.

Balogh, B., N. T. T. Nga, and J. B. Jones. 2018. Relative level of bacteriophage multiplication in vitro or in phyllosphere may not predict in planta efficacy for controlling bacterial leaf spot on tomato caused by Xanthomonas perforans. Front. Microbiol. 9:2176.

Barrangou, R., C. Fremaux, H. Deveau, M. Richards, P. Boyaval, S. Moineau, D. A. Romero, and P. Horvath. 2007. CRISPR Provides Acquired Resistance Against Viruses in Prokaryotes. Science 315:1709–1712.

Bassanezi, R. B., L. H. Montesino, and E. S. Stuchi. 2009. Effects of huanglongbing on fruit quality of sweet orange cultivars in Brazil. Eur. J. Plant Pathol. 125:565–572.

Bates, D., M. Mächler, B. M. Bolker, and S. C. Walker. 2015. Fitting linear mixed-effects models using lme4. J. Stat. Softw. 67:1–48.

Becker, P., W. Hufnagle, G. Peters, and M. Herrmann. 2001. Detection of differential gene expression in biofilm-forming versus planktonic populations of Staphylococcus aureus using micro-representational-difference analysis. Appl. Environ. Microbiol. 67:2958–2965.

Bender, C. L., and D. A. Cooksey. 1986. Indigenous Plasmids in Pseudomonas syringae pv. tomato: Conjugative Transfer and Role in Copper Resistance. J. Bacteriol. 165:534–541.

Bérénos, C., P. Schmid-Hempel, and K. M. Wegner. 2009. Evolution of host resistance and trade-offs between virulence and transmission potential in an obligately killing parasite. J. Evol. Biol. 22:2049–2056.

Bergelson, J., and C. B. Purrington. 1996. Surveying Patterns in the Cost of Resistance in Plants. Am. Nat. 148:536–558.

Bertozzi Silva, J., Z. Storms, and D. Sauvageau. 2016. Host receptors for bacteriophage adsorption. FEMS Microbiol. Lett. 363:fnw002.

Best, A., A. White, and M. Boots. 2014. The coevolutionary implications of host tolerance. Evolution 68:1426–1435.
Blazanin, M., and P. E. Turner. 2021. Community context matters for bacteria-phage ecology and evolution. ISME J. 1–10.
Bohannan, B. J. M., M. Travisano, and R. E. Lenski. 1999. Epistatic interactions can lower the cost of resistance to multiple consumers. Evolution 53:292–295.
Boots, M., and Y. Haraguchi. 1999. The Evolution of Costly Resistance in Host-Parasite Systems. Am. Nat. 153:359–370.
Boots, M., P. J. Hudson, and A. Sasaki. 2004. Large Shifts in Pathogen Virulence Relate to Host Population Structure. Science 303:842–844.
Boratyn, G. M., A. A. Schäffer, R. Agarwala, S. F. Altschul, D. J. Lipman, and T. L. Madden. 2012. Domain enhanced lookup time accelerated BLAST. Biol. Direct 7:12.
Brockhurst, M. A., and B. Koskella. 2013. Experimental coevolution of species interactions. Trends Ecol. Evol. 28:367–375.
Brockhurst, M. A., A. D. Morgan, A. Fenton, and A. Buckling. 2007. Experimental coevolution with bacteria and phage. The Pseudomonas fluorescens--Phi2 model system. Infect. Genet. Evol. 7:547–552.
Brockhurst, M. A., A. D. Morgan, P. B. Rainey, and A. Buckling. 2003. Population mixing accelerates coevolution. Ecol. Lett. 6:975–979.
Brown, J. K. M. 2015. Durable Resistance of Crops to Disease: A Darwinian Perspective. Annu. Rev. Phytopathol. 53:513–539.
Bryan, D., A. El-Shibiny, Z. Z. Hobbs, J. Porter, and E. M. Kutter. 2016. Bacteriophage T4 Infection of Stationary Phase E. coli: Life after Log from a Phage Perspective. Front. Microbiol. 7:1391.
Buckling, A., and P. B. . Rainey. 2002. Antagonistic coevolution between a bacterium and a bacteriophage. Proc. R. Soc. Lond. B. Biol. Sci. 269:931–936.
Buell, C. R., V. Joardar, M. Lindeberg, J. Selengut, I. T. Paulsen, M. L. Gwinn, R. J. Dodson, R. T. Deboy, A. S. Durkin, J. F. Kolonay, R. Madupu, S. Daugherty, L. Brinkac, M. J. Beanan, D. H. Haft, W. C. Nelson, T. Davidsen, N. Zafar, L. Zhou, J. Liu, Q. Yuan, H. Khouri, N. Fedorova, B. Tran, D. Russell, K. Berry, T. Utterback, S. E. Van Aken, T. V. Feldblyum, M. D'Ascenzo, W.-L. Deng, A. R. Ramos, J. R. Alfano, S. Cartinhour, A. K. Chatterjee, T. P. Delaney, S. G. Lazarowitz, G. B. Martin, D. J. Schneider, X. Tang, C. L. Bender, O. White, C. M. Fraser, and A. Collmer. 2003. The complete genome sequence of the Arabidopsis and tomato pathogen Pseudomonas syringae pv. tomato DC3000. Proc. Natl. Acad. Sci. 100:10181–10186.
Bull, J. J., C. S. Vegge, M. Schmerer, W. N. Chaudhry, and B. R. Levin. 2014. Phenotypic Resistance and the Dynamics of Bacterial Escape from Phage Control. PLoS One 9:e94690.
Burmeister, A. R., R. E. Lenski, and J. R. Meyer. 2016. Host coevolution alters the adaptive landscape of a virus. Proc. R. Soc. Lond. B. Biol. Sci. 283:20161528.
Buttimer, C., O. McAuliffe, R. P. Ross, C. Hill, J. O'Mahony, and A. Coffey. 2017. Bacteriophages and Bacterial Plant Diseases. Front. Microbiol. 8:34.
Capparelli, R., I. Ventimiglia, S. Roperto, D. Fenizia, and D. Iannelli. 2006. Selection of an Escherichia coli O157:H7 bacteriophage for persistence in the circulatory system of mice infected experimentally. Clin. Microbiol. Infect. 12:248–253.
Castiblanco, L. F., and G. W. Sundin. 2018. Cellulose production, activated by cyclic di-GMP through BcsA and BcsZ, is a virulence factor and an essential determinant of the three-

dimensional architectures of biofilms formed by Erwinia amylovora Ea1189. Mol. Plant Pathol. 19:90–103.
Cenens, W., A. Makumi, S. K. Govers, R. Lavigne, and A. Aertsen. 2015. Viral Transmission Dynamics at Single-Cell Resolution Reveal Transiently Immune Subpopulations Caused by a Carrier State Association. PLoS Genet. 11:1–19.
Chakravarthy, S., B. G. Butcher, Y. Liu, K. D'Amico, M. Coster, and M. J. Filiatrault. 2017. Virulence of Pseudomonas syringae pv. tomato DC3000 Is Influenced by the Catabolite Repression Control Protein Crc. Mol. Plant-Microbe Interact. 30:283–294.
Chan, B. K., and S. T. Abedon. 2015. Bacteriophages and their Enzymes in Biofilm Control. Curr. Pharm. Des. 21:85–99.
Characklis, W. G. 1973. Attached microbial growths-II. Frictional resistance due to microbial slimes. Water Res. 7:1249–1258.
Christensen, B. E. 1989. The role of extracellular polysaccharides in biofilms. J. Biotechnol. 10:181–202.
Coates, L., and G. Johnson. 1997. Postharvest diseases of fruit and vegetables. Pp. 533–548 *in* Plant pathogens and plant diseases.
Coenye, T., E. Peeters, and H. J. Nelis. 2007. Biofilm formation by Propionibacterium acnes is associated with increased resistance to antimicrobial agents and increased production of putative virulence factors. Res. Microbiol. 158:386–392.
Constantinidou, H. A., S. S. Hirano, L. S. Baker, and C. D. Upper. 1990. Atmospheric Dispersal of Ice Nucleation-Active Bacteria: The Role of Rain. Phytopathology 80:934–937.
Cooksey, D. A. 1987. Characterization of a Copper Resistance Plasmid Conserved in Copper-Resistant Strains of Pseudomonas syringae pv. tomato. Appl. Environ. Microbiol. 53:454–456.
Cooksey, D. A. 1994. Molecular mechanisms of copper resistance and accumulation in bacteria. FEMS Microbiol. Rev. 14:381–386.
Cotter, P. A., and S. Stibitz. 2007. c-di-GMP-mediated regulation of virulence and biofilm formation. Curr. Opin. Microbiol. 10:17–23.
Danhorn, T., and C. Fuqua. 2007. Biofilm Formation by Plant-Associated Bacteria. Annu. Rev. Microbiol. 61:401–422.
de Jonge, P. A., F. L. Nobrega, S. J. J. Brouns, and B. E. Dutilh. 2019. Molecular and Evolutionary Determinants of Bacteriophage Host Range. Trends Microbiol. 27:51–63.
De Sordi, L., V. Khanna, and L. Debarbieux. 2017. The Gut Microbiota Facilitates Drifts in the Genetic Diversity and Infectivity of Bacterial Viruses. Cell Host Microbe 22:1–8.
De Sordi, L., M. Lourenço, and L. Debarbieux. 2018. Gut Microbes "I will survive": A tale of bacteriophage-bacteria coevolution in the gut. Cell Host Microbe 22:801–808.
Delbrück, M. 1940. The growth of bacteriophage and lysis of the host. J. Gen. Physiol. 23:643–660.
Delcher, A. L., D. Harmon, S. Kasif, O. White, and S. L. Salzberg. 1999. Improved microbial gene identification with GLIMMER. Nucleic Acids Res. 27:4636–4641.
Deutsch, C. A., J. J. Tewksbury, M. Tigchelaar, D. S. Battisti, S. C. Merrill, R. B. Huey, and R. L. Naylor. 2018. Increase in crop losses to insect pests in a warming climate. Science 361:916–919.
Dietrich, R., K. Ploss, and M. Heil. 2005. Growth responses and fitness costs after induction of pathogen resistance depend on environmental conditions. Plant Cell Environ. 28:211–222.
Dinno, A. 2017. dunn.test: Dunn's Test of Multiple Comparisons Using Rank Sums. R Package

version 1.3.5 https://CRAN.R-project.org/package=dunn.test.
Dobson, A., K. D. Lafferty, A. M. Kuris, R. F. Hechinger, and W. Jetz. 2008. Colloquium paper: homage to Linnaeus: how many parasites? How many hosts? Proc. Natl. Acad. Sci. 105:11482–11489.
Doolittle, M. M., J. J. Cooney, and D. E. Caldwell. 1996. Tracing the interaction of bacteriophage with bacterial biofilms using fluorescent and chromogenic probes. J. Ind. Microbiol. 16:331–341.
Ekstrøm, C. T. 2020. MESS: Miscellaneous Esoteric Statistical Scripts. R Package version 0.5.7 https://CRAN.R-project.org/package=MESS.
Everett, K. R., R. K. Taylor, M. K. Romberg, J. Rees-George, R. A. Fullerton, J. L. Vanneste, and M. A. Manning. 2011. First report of Pseudomonas syringae pv. actinidiae causing kiwifruit bacterial canker in New Zealand. Australas. Plant Dis. Notes 6:67–71.
Farias, G. A., A. Olmedilla, and M. T. Gallegos. 2019. Visualization and characterization of Pseudomonas syringae pv. tomato DC3000 pellicles. Microb. Biotechnol. 12:688–702.
Faruque, S. M., I. Bin Naser, M. J. Islam, A. S. G. Faruque, A. N. Ghosh, G. B. Nair, D. A. Sack, and J. J. Mekalanos. 2005. Seasonal epidemics of cholera inversely correlate with the prevalence of environmental cholera phages. Proc. Natl. Acad. Sci. 102:1702–1707.
Feazel, L. M., L. K. Baumgartner, K. L. Peterson, D. N. Frank, J. K. Harris, and N. R. Pace. 2009. Opportunistic pathogens enriched in showerhead biofilms. Proc. Natl. Acad. Sci. 106:16393–16399.
Ferrari, J., C. B. Müller, A. R. Kraaijeveld, and H. C. J. Godfray. 2001. Clonal variation and covariation in aphid resistance to parasitoids and a pathogen. Evolution 55:1805–1814.
Fett, W. F., and M. F. Dunn. 1989. Exopolysaccharides Produced by Phytopathogenic Pseudomonas syringae Pathovars in Infected Leaves of Susceptible Hosts. Plant Physiol. 89:5–9.
Flemming, H.-C., and J. Wingender. 2010. The biofilm matrix. Nat. Rev. Microbiol. 8:623–633.
Frampton, R. A., A. R. Pitman, and P. C. Fineran. 2012. Advances in bacteriophage-mediated control of plant pathogens. Int. J. Microbiol. 2012.
Frank, S. A. 1994. Coevolutionary genetics of hosts and parasites with quantitative inheritance. Evol. Ecol. 8:74–94.
Funk, C. C., and M. E. Brown. 2009. Declining global per capita agricultural production and warming oceans threaten food security. Food Secur. 1:271–289.
Gandon, S., and Y. Michalakis. 2000. Evolution of parasite virulence against qualitative or quantitative host resistance. Proc. R. Soc. Lond. B. Biol. Sci. 267:985–990.
Garneau, J. R., F. Depardieu, L.-C. Fortier, D. Bikard, and M. Monot. 2017. PhageTerm: a tool for fast and accurate determination of phage termini and packaging mechanism using next-generation sequencing data. Sci. Rep. 7:1–10.
Gibson, A. K., H. Baffoe-Bonnie, M. J. Penley, J. Lin, R. Owens, A. Khalid, and L. T. Morran. 2020. The evolution of parasite host range in heterogeneous host populations. J. Evol. Biol. 33:773–782.
Gómez, P., J. Bennie, K. J. Gaston, and A. Buckling. 2015. The Impact of Resource Availability on Bacterial Resistance to Phages in Soil. PLoS One 10:e0123752.
Gómez, P., and A. Buckling. 2011. Bacteria-Phage Antagonistic Coevolution in Soil. Science 332:106–109.
González, S., L. Fernández, D. Gutiérrez, A. B. Campelo, A. Rodríguez, and P. García. 2018. Analysis of Different Parameters Affecting Diffusion, Propagation and Survival of

Staphylophages in Bacterial Biofilms. Front. Microbiol. 9:2348.
Goode, M. J., and M. Sasser. 1980. Prevention- the Key to Controlling Bacterial Spot and Bacterial Speck of Tomato. Plant Dis. 64:831–834.
Gordillo Altamirano, F. L., and J. J. Barr. 2019. Phage therapy in the postantibiotic era. Clin. Microbiol. Rev. 32:e00066-18.
Gordon, D., and P. Green. 2013. Consed: a graphical editor for next-generation sequencing. Bioinformatics 29:2936–2937.
Gornall, J., R. Betts, E. Burke, R. Clark, J. Camp, K. Willett, and A. Wiltshire. 2010. Implications of climate change for agricultural productivity in the early twenty-first century. Philos. Trans. R. Soc. B Biol. Sci. 365:2973–2989.
Gottwald, T. R., X. Sun, T. Riley, J. H. Graham, F. Ferrandino, and E. L. Taylor. 2002. Geo-referenced spatiotemporal analysis of the urban citrus canker epidemic in Florida. Phytopathology 92:361–377.
Green, S. I., C. G. Liu, X. Yu, S. Gibson, W. Salmen, A. Rajan, H. E. Carter, J. R. Clark, X. Song, R. F. Ramig, B. W. Trautner, H. B. Kaplan, and A. W. Maresso. 2021. Targeting of mammalian glycans enhances phage predation in the gastrointestinal tract. MBio 12:1–18.
Gupta, A., L. Zaman, H. M. Strobel, J. Gallie, A. R. Burmeister, B. Kerr, E. S. Tamar, R. Kishony, and J. R. Meyer. 2021. Host-parasite coevolution promotes innovation through deformations in fitness landscapes. bioRxiv 2021.06.25.449783.
Gurney, J., L. Aldakak, A. Betts, C. Gougat-Barbera, T. Poisot, O. Kaltz, and M. E. Hochberg. 2017. Network structure and local adaptation in co-evolving bacteria-phage interactions. Mol. Ecol. 26:1764–1777.
Gutiérrez, D., P. Ruas-Madiedo, B. Martínez, A. Rodríguez, and P. García. 2014. Effective Removal of Staphylococcal Biofilms by the Endolysin LysH5. PLoS One 9:e107307.
Guttman, D. S., B. A. Vinatzer, S. F. Sarkar, M. V Ranall, G. Kettler, and J. T. Greenberg. 2002. A Functional Screen for the Type III (Hrp) Secretome of the Plant Pathogen Pseudomonas syringae. Science 295:1722–1726.
Haapalainen, M. 2014. Biology and epidemics of *Candidatus* Liberibacter species, psyllid-transmitted plant-pathogenic bacteria. Ann. Appl. Biol. 165:172–198.
Hadas, H., M. Einav, I. Fishov, and A. Zaritsky. 1997. Bacteriophage T4 development depends on the physiology of its host Escherichia coli. Microbiology 143:179–185.
Haefele, D. M., and S. E. Lindow. 1987. Flagellar Motility Confers Epiphytic Fitness Advantages upon Pseudomonas syringae. Appl. Environ. Microbiol. 53:2528–2533.
Hall-Stoodley, L., and P. Stoodley. 2005. Biofilm formation and dispersal and the transmission of human pathogens. Trends Microbiol. 13:7–10.
Hall, A. R., P. D. Scanlan, and A. Buckling. 2011a. Bacteria-phage coevolution and the emergence of generalist pathogens. Am. Nat. 177:44–53.
Hall, A. R., P. D. Scanlan, A. D. Morgan, and A. Buckling. 2011b. Host-parasite coevolutionary arms races give way to fluctuating selection. Ecol. Lett. 14:635–642.
Hammad, A. M. M. 1998. Evaluation of alginate-encapsulated Azotobacter chroococcum as a phage-resistant and an effective inoculum. J. Basic Microbiol. 38:9–16.
Hauck, P., R. Thilmony, and S. Y. He. 2003. A Pseudomonas syringae type III effector suppresses cell wall-based extracellular defense in susceptible Arabidopsis plants. Proc. Natl. Acad. Sci. 100:8577–8582.
Heinze, G., and M. Schemper. 2002. A solution to the problem of separation in logistic regression. Stat. Med. 21:2409–2419.

Hernandez, C. A., and B. Koskella. 2019. Phage resistance evolution in vitro is not reflective of in vivo outcome in a plant-bacteria-phage system. Evolution 73:2461–2475.
Hernandez, C. A., A. J. Salazar, and B. Koskella. 2020. Bacteriophage-Mediated Reduction of Bacterial Speck on Tomato Seedlings. PHAGE Ther. Appl. Res. 1:205–212.
Hodyra-Stefaniak, K., P. Miernikiewicz, J. Drapała, M. Drab, E. Jonczyk-Matysiak, D. Lecion, Z. Kazmierczak, W. Beta, J. Majewska, M. Harhala, B. Bubak, A. Kłopot, A. Górski, and K. Dabrowska. 2015. Mammalian Host-Versus-Phage immune response determines phage fate in vivo. Sci. Rep. 5:1–13.
Hopkins, D. L., and A. H. Purcell. 2002. Xylella fastidiosa: Cause of Pierce's disease of grapevine and other emergent diseases. Plant Dis. 86:1056–1066.
Hosseinidoust, Z., N. Tufenkji, and T. G. M. van de Ven. 2013. Formation of biofilms under phage predation: considerations concerning a biofilm increase. Biofouling 29:457–468.
Hu, J., K. Miyanaga, and Y. Tanji. 2010. Diffusion properties of bacteriophages through agarose gel membrane. Biotechnol. Prog. 26:1213–1221.
Hughes, K. A., I. W. Sutherland, and M. V. Jones. 1998. Biofilm susceptibility to bacteriophage attack: the role of phage-borne polysaccharide depolymerase. Microbiology 144:3039–3047.
Hyman, P., and S. T. Abedon. 2010. Bacteriophage host range and bacterial resistance. Adv. Appl. Microbiol. 70:217–248.
Iriarte, F. B., B. Balogh, M. T. Momol, L. M. Smith, M. Wilson, and J. B. Jones. 2007. Factors affecting survival of bacteriophage on tomato leaf surfaces. Appl. Environ. Microbiol. 73:1704–1711.
Ishiga, Y., S. R. Uppalapati, T. Ishiga, S. Elavarthi, B. Martin, and C. L. Bender. 2009. The phytotoxin coronatine induces light-dependent reactive oxygen species in tomato seedlings. New Phytol. 181:147–160.
Jacobsen, B. J. 1997. Role of plant pathology in integrated pest management. Annu. Rev. Phytopathol. 35:373–391.
Jeger, M. J., and S. L. H. Viljanen-Rollinson. 2001. The use of the area under the disease-progress curve (AUDPC) to assess quantitative disease resistance in crop cultivars. Theor. Appl. Genet. 102:32–40.
Jończyk, E., M. Kłak, R. Międzybrodzki, and A. Górski. 2011. The influence of external factors on bacteriophages—review. Folia Microbiol. (Praha). 56:191–200.
Jones, H. C., I. L. Roth, and W. M. Sanders. 1969. Electron microscopic study of a slime layer. J. Bacteriol. 99:316–325.
Jones, J. B., G. E. Vallad, F. B. Iriarte, A. Obradović, M. H. Wernsing, L. E. Jackson, B. Balogh, J. C. Hong, and M. T. Momol. 2012. Considerations for using bacteriophages for plant disease control. Bacteriophage 2:208–214.
Kashiwagi, A., and T. Yomo. 2011. Ongoing Phenotypic and Genomic Changes in Experimental Coevolution of RNA Bacteriophage Qβ and Escherichia coli. PLoS Genet. 7:e1002188.
Katagiri, F., R. Thilmony, and S. Y. He. 2002. The Arabidopsis thaliana-Pseudomonas syringae interaction. P. e0039 *in* C. R. Somerville and E. M. Meyerowitz, eds. The Arabidopsis Book.
Kearney, B., P. C. Ronald, D. Dahlbeck, and B. J. Staskawicz. 1988. Molecular basis for evasion of plant host defence in bacterial spot disease of pepper. Nature 332:541–543.
Keith, R. C., L. M. W. Keith, G. Hernández-Guzmán, S. R. Uppalapati, and C. L. Bender. 2003. Alginate gene expression by Pseudomonas syringae pv. tomato DC3000 in host and non-

host plants. Microbiology 149:1127–1138.
Kering, K. K., X. Zhang, R. Nyaruaba, J. Yu, and H. Wei. 2020. Application of Adaptive Evolution to Improve the Stability of Bacteriophages during Storage. Viruses 12:423.
Kierek-Pearson, K., and E. Karatan. 2005. Biofilm Development in Bacteria. Adv. Appl. Microbiol. 57:79–111.
Kim, H.-S., D. Desveaux, A. U. Singer, P. Patel, J. Sondek, and J. L. Dangl. 2005. The Pseudomonas syringae effector AvrRpt2 cleaves its C-terminally acylated target, RIN4, from Arabidopsis membranes to block RPM1 activation. Proc. Natl. Acad. Sci. 102:6496–6501.
Koskella, B. 2013. Phage-mediated selection on microbiota of a long-lived host. Curr. Biol. 23:1256–1260.
Koskella, B. 2018. Resistance gained, resistance lost: An explanation for host–parasite coexistence. PLoS Biol. 16:e3000013.
Koskella, B., and N. Parr. 2015. The evolution of bacterial resistance against bacteriophages in the horse chestnut phyllosphere is general across both space and time. Phil Trans R Soc B 370:20140297.
Koskella, B., J. N. Thompson, G. M. Preston, and A. Buckling. 2011. Local biotic environment shapes the spatial scale of bacteriophage adaptation to bacteria. Am. Nat. 177:440–451.
Kraaijeveld, A. R., and H. C. J. Godfray. 1997. Trade-off between parasitoid resistance and larval competitive ability in Drosophila melanogaster. Nature 389:278–280.
Krut, O., and I. Bekeredjian-Ding. 2018. Contribution of the Immune Response to Phage Therapy. J. Immunol. 200:3037–3044.
Kumar, S., G. Stecher, M. Li, C. Knyaz, and K. Tamura. 2018. MEGA X: Molecular Evolutionary Genetics Analysis across Computing Platforms. Mol. Biol. Evol. 35:1547–1549.
Kunkeaw, S., S. Tan, and G. Coaker. 2010. Molecular and Evolutionary Analyses of Pseudomonas syringae pv. tomato Race 1. Mol. Plant-Microbe Interact. 23:415–424.
Kuznetsova, A., P. B. Brockhoff, and R. H. B. Christensen. 2017. lmerTest Package: Tests in Linear Mixed Effects Models. J. Stat. Softw. 82:1–26.
Laanto, E., V. Hoikkala, J. Ravantti, and L.-R. Sundberg. 2017. Long-term genomic coevolution of host-parasite interaction in the natural environment. Nat. Commun. 8:111.
Labrie, S. J., J. E. Samson, and S. Moineau. 2010. Bacteriophage resistance mechanisms. Nat. Rev. Microbiol. 8:317–327.
Lal, R. 2015. Restoring Soil Quality to Mitigate Soil Degradation. Sustainability 7:5875–5895.
Lamichhane, J. R., A. Messéan, and C. E. Morris. 2015. Insights into epidemiology and control of diseases of annual plants caused by the Pseudomonas syringae species complex. J. Gen. Plant Pathol. 81:331–350.
Lamichhane, J. R., L. Varvaro, L. Parisi, J.-M. Audergon, and C. E. Morris. 2014. Disease and Frost Damage of Woody Plants Caused by Pseudomonas syringae: Seeing the Forest for the Trees. Pp. 235–295 *in* Advances in Agronomy.
Laue, H., A. Schenk, H. Li, L. Lambertsen, T. R. Neu, S. Molin, and M. S. Ullrich. 2006. Contribution of alginate and levan production to biofilm formation by Pseudomonas syringae. Microbiology 152:2909–2918.
Lebeis, S. L., S. Herrera Paredes, D. S. Lundberg, N. Breakfield, J. Gehring, M. McDonald, S. Malfatti, T. Glavina del Rio, C. D. Jones, S. G. Tringe, and J. L. Dangl. 2015. Salicylic acid modulates colonization of the root microbiome by specific bacterial taxa. Science

1681:1678–1681.
Lederberg, J., and E. M. Lederberg. 1952. Replica plating and indirect selection of bacterial mutants. J. Bacteriol. 63:399–406.
Lennon, J. T., S. A. M. Khatana, M. F. Marston, and J. B. H. Martiny. 2007. Is there a cost of virus resistance in marine cyanobacteria? ISME J. 1:300–312.
Lenski, R. E. 1984. Coevolution of bacteria and phage: Are there endless cycles of bacterial defenses and phage counterdefenses? J. Theor. Biol. 108:319–325.
Lenski, R. E., and B. R. Levin. 1985. Constraints on the Coevolution of Bacteria and Virulent Phage: A Model, Some Experiments, and Predictions for Natural Communities. Am. Nat. 125:585–602.
Lenth, R. 2020. emmeans: Estimated Marginal Means, aka Least-Squares Means. R Package version 1.6.2-1 https://CRAN.R-project.org/package=emmeans.
Lewis, K. 2001. Riddle of biofilm resistance. Antimicrob. Agents Chemother. 45:999–1007.
Li, H. 2013. Aligning sequence reads, clone sequences and assembly contigs with BWA-MEM. arXiv:1303.3997.
Li, H., B. Handsaker, A. Wysoker, T. Fennell, J. Ruan, N. Homer, G. Marth, G. Abecasis, R. Durbin, and 1000 Genome Project Data Processing Subgroup. 2009. The Sequence Alignment/Map format and SAMtools. Bioinformatics 25:2078–2079.
Lindemann, J., H. A. Constantinidou, W. R. Barchet, and C. D. Upper. 1982. Plants as sources of airborne bacteria, including ice nucleation-active bacteria. Appl. Environ. Microbiol. 44:1059–1063.
Lindow, S. E., and M. T. Brandl. 2003. Microbiology of the phyllosphere. Appl. Environ. Microbiol. 69:1875–1883.
Loc-Carrillo, C., and S. T. Abedon. 2011. Pros and cons of phage therapy. Bacteriophage 1:111–114.
Lochmiller, R. L., and C. Deerenberg. 2000. Trade-offs in evolutionary immunology: just what is the cost of immunity? Oikos 88:87–98.
Lopatina, A., N. Tal, and R. Sorek. 2020. Abortive Infection: Bacterial Suicide as an Antiviral Immune Strategy. Annu. Rev. Virol. 7:371–384.
Lopez-Pascua, L. D. C., and A. Buckling. 2008. Increasing productivity accelerates host–parasite coevolution. J. Evol. Biol. 21:853–860.
Louis, P., and C. P. O'Byrne. 2010. Life in the gut: microbial responses to stress in the gastrointestinal tract. Sci. Prog. 93:7–36.
Lu, S., J. Wang, F. Chitsaz, M. K. Derbyshire, R. C. Geer, N. R. Gonzales, M. Gwadz, D. I. Hurwitz, G. H. Marchler, J. S. Song, N. Thanki, R. A. Yamashita, M. Yang, D. Zhang, C. Zheng, C. J. Lanczycki, and A. Marchler-Bauer. 2020. CDD/SPARCLE: the conserved domain database in 2020. Nucleic Acids Res. 48:D265–D268.
Lu, T. K., and J. J. Collins. 2007. Dispersing biofilms with engineered enzymatic bacteriophage. Proc. Natl. Acad. Sci. 104:11197–11202.
Lukashin, A. V., and M. Borodovsky. 1998. GeneMark.hmm: new solutions for gene finding. Nucleic Acids Res. 26:1107–1115.
Luong, L. T., and M. Polak. 2007. Costs of resistance in the Drosophila-Macrocheles system: a negative genetic correlation between ectoparasite resistance and reproduction. Evolution 61:1391–1402.
Mackinnon, M. J., S. Gandon, and A. F. Read. 2008. Virulence evolution in response to vaccination: The case of malaria. Vaccine 26:C42-52.

Madden, L. V., G. Hughes, and F. van den Bosch. 2007. The Study of Plant Disease Epidemics.
Mann, E. E., and D. J. Wozniak. 2012. Pseudomonas biofilm matrix composition and niche biology. FEMS Microbiol. Rev. 36:893–916.
Maura, D., M. Galtier, C. Le Bouguénec, and L. Debarbieux. 2012. Virulent bacteriophages can target O104:H4 enteroaggregative Escherichia coli in the mouse intestine. Antimicrob. Agents Chemother. 56:6235–6242.
McCarter, S. M., J. B. Jones, R. D. Gitaitis, and D. R. Smitley. 1983. Survival of Pseudomonas syringae pv. tomato in Association with Tomato Seed, Soil, Host Tissue, and Epiphytic Weed Hosts in Georgia. Phytopathology 73:1393–1398.
Meaden, S., and B. Koskella. 2017. Adaptation of the pathogen, Pseudomonas syringae, during experimental evolution on a native vs. alternative host plant. Mol. Ecol. 26:1790–1801.
Meaden, S., K. Paszkiewicz, and B. Koskella. 2015. The cost of phage resistance in a plant pathogenic bacterium is context-dependent. Evolution 69:1321–1328.
Mercier, J., and S. E. Lindow. 2000. Role of leaf surface sugars in colonization of plants by bacterial epiphytes. Appl. Environ. Microbiol. 66:369–374.
Miller, R. V. 1998. Methods for enumeration and characterization of bacteriophages from environmental samples. Pp. 218–235 *in* Techniques in microbial ecology.
Misas-Villamil, J. C., I. Kolodziejek, E. Crabill, F. Kaschani, S. Niessen, T. Shindo, M. Kaiser, J. R. Alfano, and R. A. L. van der Hoorn. 2013. Pseudomonas syringae pv. syringae Uses Proteasome Inhibitor Syringolin A to Colonize from Wound Infection Sites. PLoS Pathog. 9:e1003281.
Morella, N. M., S. C. Yang, C. A. Hernandez, and B. Koskella. 2018. Rapid quantification of bacteriophages and their bacterial hosts in vitro and in vivo using droplet digital PCR. J. Virol. Methods 259:18–24.
Morella, N. M., X. Zhang, and B. Koskella. 2019. Tomato Seed-Associated Bacteria Confer Protection of Seedlings Against Foliar Disease Caused by *Pseudomonas syringae*. Phytobiomes J. 3:177–190.
Moret, Y., and P. Schmid-Hempel. 2000. Survival for immunity: the price of immune system activation for bumblebee workers. Science 290:1166–1168.
Morris, C. E., J. R. Lamichhane, I. Nikolić, S. Stanković, and B. Moury. 2019. The overlapping continuum of host range among strains in the Pseudomonas syringae complex. Phytopathol. Res. 1:4.
Morris, C. E., D. C. Sands, B. A. Vinatzer, C. Glaux, C. Guilbaud, A. Buffière, S. Yan, H. Dominguez, and B. M. Thompson. 2008. The life history of the plant pathogen Pseudomonas syringae is linked to the water cycle. ISME J. 2:321–334.
Nilsson, A. S. 2014. Phage therapy-constraints and possibilities. Ups. J. Med. Sci. 119:192–198.
O'Toole, G. A. 2011. Microtiter Dish Biofilm Formation Assay. J. Vis. Exp., doi: 10.3791/2437.
Ofir, G., S. Melamed, H. Sberro, Z. Mukamel, S. Silverman, G. Yaakov, S. Doron, and R. Sorek. 2017. DISARM is a widespread bacterial defence system with broad anti-phage activities. Nat. Microbiol. 2017 31 3:90–98.
Omnilytics, Inc. 2018. Agriphage. EPA Reg. No. 67986-1.
Panter, S. N., and D. A. Jones. 2002. Age-related resistance to plant pathogens. Adv. Bot. Res. 38:251–280.
Park, A. J., K. Murphy, J. R. Krieger, D. Brewer, P. Taylor, M. Habash, and C. M. Khursigara. 2014. A Temporal Examination of the Planktonic and Biofilm Proteome of Whole Cell Pseudomonas aeruginosa PAO1 Using Quantitative Mass Spectrometry. Mol. Cell.

Proteomics 13:1095–1105.
Paterson, S., T. Vogwill, A. Buckling, R. Benmayor, A. J. Spiers, N. R. Thomson, M. Quail, F. Smith, D. Walker, B. Libberton, A. Fenton, N. Hall, and M. A. Brockhurst. 2010. Antagonistic coevolution accelerates molecular evolution. Nature 464:275–278.
Pedley, K. F., and G. B. Martin. 2003. Molecular Basis of Pto-Mediated Resistance to Bacterial Speck Disease in Tomato. Annu. Rev. Phytopathol. 41:215–243.
Percival, S. L., L. Suleman, C. Vuotto, and G. Donelli. 2015. Healthcare-associated infections, medical devices and biofilms: risk, tolerance and control. J. Med. Microbiol. 64:323–334.
Perry, E. B., J. E. Barrick, and B. J. M. Bohannan. 2015. The Molecular and Genetic Basis of Repeatable Coevolution between Escherichia coli and Bacteriophage T3 in a Laboratory Microcosm. PLoS One 10:e0130639.
Pitblado, R. E., and E. A. Kerr. 1979. A source of resistance to bacterial speck-Pseudomonas tomato. Tomato Genet Coop Rep 29:30.
Pitblado, R. E., and B. H. MacNeill. 1983. Genetic basis of resistance to Pseudomonas syringae pv. tomato in field tomatoes. Can. J. Plant Pathol. 5:251–255.
Pohlert, T. 2018. The Pairwise Multiple Comparison of Mean Ranks Package (PMCMR). R Package version 4.3 https://CRAN.R-project.org/package=PMCMR.
Poltak, S. R., and V. S. Cooper. 2011. Ecological succession in long-term experimentally evolved biofilms produces synergistic communities. ISME J. 5:369–378.
Poon, K. K. H., E. L. Westman, E. Vinogradov, S. Jin, and J. S. Lam. 2008. Functional characterization of MigA and WapR: putative rhamnosyltransferases involved in outer core oligosaccharide biosynthesis of Pseudomonas aeruginosa. J. Bacteriol. 190:1857–1865.
Poullain, V., S. Gandon, M. A. Brockhurst, A. Buckling, and M. E. Hochberg. 2008. The evolution of specificity in evolving and coevolving antagonistic interactions between a bacteria and its phage. Evolution 62:1–11.
Prigent-Combaret, C., O. Vidal, C. Dorel, and P. Lejeune. 1999. Abiotic surface sensing and biofilm-dependent regulation of gene expression in Escherichia coli. J. Bacteriol. 181:5993–6002.
Quiñones, B., G. Dulla, and S. E. Lindow. 2005. Quorum Sensing Regulates Exopolysaccharide Production, Motility, and Virulence in Pseudomonas syringae. Mol. Plant-Microbe Interact. 18:682–693.
R Core Team. 2017. R: A language and environment for statistical computing. Vienna, Austria. URL https://www.R-project.org/.
Ray, D. K., N. D. Mueller, P. C. West, and J. A. Foley. 2013. Yield Trends Are Insufficient to Double Global Crop Production by 2050. PLoS One 8:e66428.
Resch, A., S. Leicht, M. Saric, L. Pásztor, A. Jakob, F. Götz, and A. Nordheim. 2006. Comparative proteome analysis of Staphylococcus aureus biofilm and planktonic cells and correlation with transcriptome profiling. Proteomics 6:1867–1877.
Romantschuk, M., and D. H. Bamford. 1986. The causal agent of halo blight in bean, Pseudomonas syringae pv. phaseolicola, attaches to stomata via its pili. Microb. Pathog. 1:139–48.
Romantschuk, M., E.-L. Nurmiaho-Lassila, E. Roine, and A. Suoniemi. 1993. Pilus-mediated adsorption of Pseudomonas syringae to the surface of host and non-host plant leaves. J. Gen. Microbiol. 139:2251–2260.
Russell, D. A. 2018. Sequencing, Assembling, and Finishing Complete Bacteriophage Genomes. Pp. 109–125 *in* M. R. J. Clokie, A. M. Kropinski, and R. Lavigne, eds. Bacteriophages:

methods and protocols.
Sabouri, S., Z. Sepehrizadeh, S. Amirpour-Rostami, and M. Skurnik. 2017. A minireview on the in vitro and in vivo experiments with anti-Escherichia coli O157:H7 phages as potential biocontrol and phage therapy agents. Int. J. Food Microbiol. 243:52–57.
Santos-Lopez, A., C. W. Marshall, M. R. Scribner, D. J. Snyder, and V. S. Cooper. 2019. Evolutionary pathways to antibiotic resistance are dependent upon environmental structure and bacterial lifestyle. Elife 8:e47612.
Sarkar, S. F., and D. S. Guttman. 2004. Evolution of the core genome of Pseudomonas syringae, a highly clonal, endemic plant pathogen. Appl. Environ. Microbiol. 70:1999–2012.
Sauer, K., A. K. Camper, G. D. Ehrlich, J. W. Costerton, and D. G. Davies. 2002. Pseudomonas aeruginosa displays multiple phenotypes during development as a biofilm. J. Bacteriol. 184:1140–1154.
Savary, S., L. Willocquet, S. J. Pethybridge, P. Esker, N. McRoberts, and A. Nelson. 2019. The global burden of pathogens and pests on major food crops. Nat. Ecol. Evol. 3:430–439.
Scanlan, J. G., A. R. Hall, and P. D. Scanlan. 2019. Impact of bile salts on coevolutionary dynamics between the gut bacterium Escherichia coli and its lytic phage PP01. Infect. Genet. Evol. 73:425–432.
Scanlan, P. D., and A. Buckling. 2012. Co-evolution with lytic phage selects for the mucoid phenotype of Pseudomonas fluorescens SBW25. ISME J. 6:1148–1158.
Scanlan, P. D., A. R. Hall, and A. Buckling. 2017. Parasite genetic distance and local adaptation in co-evolving bacteria-bacteriophage populations. Mol. Ecol. 26:1747–1755.
Scanlan, P. D., A. R. Hall, L. D. C. Lopez-Pascua, and A. Buckling. 2011. Genetic basis of infectivity evolution in a bacteriophage. Mol. Ecol. 20:981–989.
Schneider, D. S., and J. S. Ayres. 2008. Two ways to survive infection: what resistance and tolerance can teach us about treating infectious diseases. Nat. Rev. Immunol. 8:889–895.
Sheldon, B. C., and S. Verhulst. 1996. Ecological immunology: costly parasite defences and trade-offs in evolutionary ecology. Trends Ecol. Evol. 11:317–321.
Silva-Valenzuela, C. A., and A. Camilli. 2019. Niche adaptation limits bacteriophage predation of Vibrio cholerae in a nutrient-poor aquatic environment. Proc. Natl. Acad. Sci. 116:1627–1632.
Söding, J., A. Biegert, and A. N. Lupas. 2005. The HHpred interactive server for protein homology detection and structure prediction. Nucleic Acids Res. 33:W244–W248.
Spiers, A. J., and P. B. Rainey. 2005. The Pseudomonas fluorescens SBW25 wrinkly spreader biofilm requires attachment factor, cellulose fibre and LPS interactions to maintain strength and integrity. Microbiology 151:2829–2839.
Stahl, E. A., G. Dwyer, R. Mauricio, M. Kreitman, and J. Bergelson. 1999. Dynamics of disease resistance polymorphism at the Rpm1 locus of Arabidopsis. Nature 400:667–671.
Sundin, G. W., L. F. Castiblanco, X. Yuan, Q. Zeng, and C.-H. Yang. 2016. Bacterial disease management: challenges, experience, innovation and future prospects. Mol. Plant Pathol. 17:1506–1518.
Sundin, G. W., and N. Wang. 2018. Antibiotic Resistance in Plant-Pathogenic Bacteria. Annu. Rev. Phytopathol. 56:161–180.
Sutherland, I. W., K. A. Hughes, L. C. Skillman, and K. Tait. 2004. The interaction of phage and biofilms. FEMS Microbiol. Lett. 232:1–6.
Thirion, J. P., and M. Hofnung. 1972. On some genetic aspects of phage lambda resistance in E. coli K12. Genetics 71:207–216.

Tian, D., M. B. Traw, J. Q. Chen, M. Kreitman, and J. Bergelson. 2003. Fitness costs of R-gene-mediated resistance in Arabidopsis thaliana. Nature 423:74–77.
Tilman, D., C. Balzer, J. Hill, and B. L. Befort. 2011. Global food demand and the sustainable intensification of agriculture. Proc. Natl. Acad. Sci. 108:20260–20264.
Tock, M. R., and D. T. F. Dryden. 2005. The biology of restriction and anti-restriction. Curr. Opin. Microbiol. 8:466–472.
Turner, C. B., C. W. Marshall, and V. S. Cooper. 2018. Parallel genetic adaptation across environments differing in mode of growth or resource availability. Evol. Lett. 2:355–367.
Turner, P. E., J. A. Draghi, and R. Wilpiszeski. 2012. High-throughput analysis of growth differences among phage strains. J. Microbiol. Methods 88:117–121.
Ude, S., D. L. Arnold, C. D. Moon, T. Timms-Wilson, and A. J. Spiers. 2006. Biofilm formation and cellulose expression among diverse environmental Pseudomonas isolates. Environ. Microbiol. 8:1997–2011.
Vale, P. F., G. Lafforgue, F. Gatchitch, R. Gardan, S. Moineau, and S. Gandon. 2015. Costs of CRISPR-Cas-mediated resistance in Streptococcus thermophilus. Proc. R. Soc. Lond. B. Biol. Sci. 282:20151270.
Vidakovic, L., P. K. Singh, R. Hartmann, C. D. Nadell, and K. Drescher. 2018. Dynamic biofilm architecture confers individual and collective mechanisms of viral protection. Nat. Microbiol. 3:26–31.
Vieira, A. R., S. Wu, L. B. Jensen, A. Dalsgaard, H. Houe, H. C. Wegener, D. M. A. Lo, F. Wong, and H.-D. Emborg. 2008. Using data on resistance prevalence per sample in the surveillance of antimicrobial resistance. J. Antimicrob. Chemother. 62:535–538.
Wandro, S., A. Oliver, T. Gallagher, C. Weihe, W. England, J. B. H. Martiny, and K. Whiteson. 2019. Predictable Molecular Adaptation of Coevolving Enterococcus faecium and Lytic Phage EfV12-phi1. Front. Microbiol. 9:3192.
Wang, X., Z. Wei, M. Li, X. Wang, A. Shan, X. Mei, A. Jousset, Q. Shen, Y. Xu, and V.-P. Friman. 2017. Parasites and competitors suppress bacterial pathogen synergistically due to evolutionary trade-offs. Evolution 71:733–746.
Whitchurch, C., T. Tolker-Nielsen, P. C. Ragas, and J. S. Mattick. 2002. Extracellular DNA Required for Bacterial Biofilm Formation. Science 295:1487.
Xin, X.-F., and S. Y. He. 2013. Pseudomonas syringae pv. tomato DC3000: A Model Pathogen for Probing Disease Susceptibility and Hormone Signaling in Plants. Annu. Rev. Phytopathol. 51:473–498.
Xin, X.-F., K. Nomura, K. Aung, A. C. Velásquez, J. Yao, F. Boutrot, J. H. Chang, C. Zipfel, and S. Y. He. 2016. Bacteria establish an aqueous living space in plants crucial for virulence. Nature 539:524–529.
Yang, H., M. Matewish, I. Loubens, D. G. Storey, J. S. Lam, and S. Jin. 2000. migA, a quorum-responsive gene of Pseudomonas aeruginosa, is highly expressed in the cystic fibrosis lung environment and modifies low-molecular-mass lipopolysaccharide. Microbiology 146:2509–2519.
Yu, X., S. P. Lund, R. A. Scott, J. W. Greenwald, A. H. Records, D. Nettleton, S. E. Lindow, D. C. Gross, and G. A. Beattie. 2013. Transcriptional responses of Pseudomonas syringae to growth in epiphytic versus apoplastic leaf sites. Proc. Natl. Acad. Sci. 110:E425–E434.
Zhang, J., F. Shao, Y. Li, H. Cui, L. Chen, H. Li, Y. Zou, C. Long, L. Lan, J. Chai, S. Chen, X. Tang, and J.-M. Zhou. 2007. A Pseudomonas syringae Effector Inactivates MAPKs to Suppress PAMP-Induced Immunity in Plants. Cell Host Microbe 1:175–185.